

AMATO

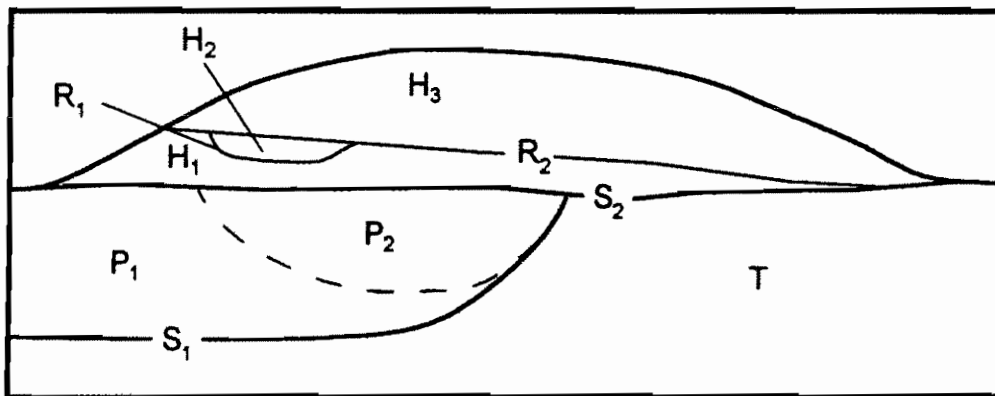
NEARSHORE RIDGES AND UNDERLYING UPPER
PLEISTOCENE SEDIMENTS ON THE INNER CONTINENTAL
SHELF OF NEW JERSEY

PETER C. SMITH

MSc. Thesis 1996

Geological Sciences, Rutgers University

Supervised by:
Gail M. Ashley
Robert E. Sheridan



Report prepared as part of New Jersey
Geological Survey's Co-operative Agreements
#14-35-0001-30666 and #14-35-0001-30751
with Minerals Management Service,
U.S. Department of Interior

NEARSHORE RIDGES AND UNDERLYING UPPER PLEISTOCENE
SEDIMENTS ON THE INNER CONTINENTAL SHELF OF NEW JERSEY

by

Peter C. Smith²

MSc. Thesis - Dept. of Geological Sciences
Rutgers University - Oct. 1996
Supervised by: Gail M. Ashley² and Robert E. Sheridan²

Supported through New Jersey Geological Survey's
Cooperative Agreements #14-35-0001-30666 and
#14-35-0001-30751 with Minerals Management Service,
U.S. Department of the Interior, to investigate
sources of beach replenishment sand in Federal
waters offshore of New Jersey

Contracting Officer's Technical Representative (COTR):
Roger V. Amato
Minerals Management Service
U.S. Dept. of the Interior

New Brunswick, New Jersey 08903
October, 1996

ABSTRACT OF THE THESIS

Nearshore ridges and underlying upper Pleistocene
sediments on the inner continental shelf of New Jersey

by PETER C. SMITH

Thesis Co-Directors: Professors

Gail M. Ashley and Robert E. Sheridan

Recent, severe and persistent erosion along the New Jersey coastline has led to the development of shoreline remediation plans which require the emplacement of large volumes of beach quality sand at the shoreface. To meet the enormous demand for beach quality sediment, nearshore detached sand ridges are investigated to characterize their physical suitability for beach remediation. Analysis of 303 km of seismic reflection (GEOPULSE™) profiles and twenty Vibracores™ (1-6 m) on the inner shelf off of Avalon, New Jersey documents five distinct lithologies which comprise two unconformity bounded units. The lithologies, in relative temporal order, are interpreted as: 1) Pleistocene lake and estuarine facies; 2) Pleistocene fluvial channel facies; 3) Holocene estuarine facies; 4) tidal ravinement channel facies; and 5) inner shelf sand ridge facies.

The two unconformity bounded sequences are separated from one another in seismic section by a regional unconformity. The inner shelf sand ridge facies is part of the upper sequence and forms the topographic linear ridge systems. Three large sand ridges are identified through seismic analysis, two of which are considered to be of potential economic importance based upon their location, sediment characteristics and volume estimates. The Inner Sand Ridge contains an estimated 48 million cubic meters of usable sediment; Avalon Shoal contains an estimated 37 million cubic meters of usable sediment. Wood fragments dated at greater than 42 ka were recovered from the lower sequence below the regional unconformity.

ACKNOWLEDGMENTS

The writer wishes to thank his co-advisors, Gail Ashley and Robert Sheridan, for their advice and expert opinions which they provided during this research. I would also like to thank Kenneth Miller for his critical review and comments concerning this thesis.

Funding for this research was provided through the United States Mineral Management Service Cooperative Agreements 14-35-0001-30666 and 14-35-0001-30751 in conjunction with the New Jersey Geological Survey and Rutgers University. I offer special thanks to the staff of the New Jersey Geological Survey, including Jane Uptegrove (Program Coordinator), Jeffery Waldner and David Hall (Geophysics), Rich Henney (Computational Support), James Gilroy (Laboratory Assistance), and Lloyd Mulliken, all of whom provided invaluable support to this project.

I thank the New Jersey Department of Environmental Protection for providing the vessel R/V James Howard, Captain Joseph Rommel and crew which enabled the seismic data to be collected with minimal problems. I would also like to thank the Rutgers University Field Station, Tuckerton, New Jersey, for providing lodging support during the seismic cruise.

Special thanks also go to Matthew Goss for his help in the field collection of cores and their processing. I would like to thank Robert Baldy for providing valuable equipment support, and am most appreciative of the staff and faculty of the Rutgers Department of Geological Sciences, and my friends who have provided support in numerous ways.

Finally, the author would like to thank his family and especially his wife, Lisa, for their loving support and encouragement in every part of my life.

TABLE OF CONTENTS

Abstract	ii
Acknowledgments	iii
Table of contents	iv
List of figures	vi
List of tables	viii
Appendices	viii
INTRODUCTION	1
GEOLOGICAL SETTING	6
Regional Setting	6
New Jersey Coastline	7
Study Area	11
PREVIOUS INVESTIGATIONS	15
Sand Ridge Development	15
Regional Seismic and Coring Studies	20
METHODS	28
Seismic Data Collection	28
Field Instrumentation	28
<u><i>ORE Geopulse™ Seismic System</i></u>	28
<u><i>Navigational Equipment</i></u>	30
<u><i>Vibrational Coring System</i></u>	31
<u><i>Jetting</i></u>	34

Vibracore™ Data Collection and Processing	35
<u><i>Vibracore™ Data Collection</i></u>	35
<u><i>Core Processing</i></u>	37
<u><i>Laboratory Procedures</i></u>	39
Seismic Reflection Profiling	40
<u><i>Reflectivity and Attenuation</i></u>	41
<u><i>Vertical Resolution</i></u>	43
<u><i>Seismic Analysis</i></u>	45
RESULTS	49
Bathymetry	49
Regional Seismic Stratigraphy	54
Unconformity Surfaces	57
<u><i>S₁ Boundary</i></u>	57
<u><i>S₂ Boundary</i></u>	57
<u><i>Ravinement Unconformity</i></u>	65
Depositional Units	65
<u><i>Depositional Unit (T)</i></u>	68
<u><i>Depositional Units P₁, P₂</i></u>	69
<u><i>Depositional Units H₁, H₂, and H₃</i></u>	78
Sand Ridge Characterization	87
Oil	90
INTERPRETATION AND DISCUSSION	91
Geophysical Interpretation	91

Depositional Units	95
<u><i>Tertiary Succession</i></u>	96
<u><i>Pleistocene Succession</i></u>	97
<u><i>Holocene Succession</i></u>	99
Sand Ridge Development	99
CONCLUSIONS AND SUMMARY	107
Stratigraphy	107
Sand Ridge Evolution	107
Remediation Potential	108
Summary	110
REFERENCES CITED	111

LIST OF FIGURES

1. Region of Severe Erosion.	2
2. Regional Location Map.	8
3. Gains and Losses of Beach Sand.	10
4. Study Area and Seismic Lines.	12
5. Shelf Topography.	13
6. Previous Seismic Investigations.	21
7. Study Area/Vibracore Location.	38
8. Multiple Reflections (TI-13N).	44
9. Seismic Reflection Pattern Sedimentary Relationships.	47

10. Sediment Thickness Above the S ₂ Unconformity.	50
11. Avalon Shoal Sediment Thickness	51
12. Inner Sand Ridge Sediment Thickness.	53
13. Average Bathymetric Slope.	55
14. Composite Regional Stratigraphy and Generalized Cross-Section	56
15. S ₁ and Incised Valley (TI-4N).	58
16. Termination of Reflections along the S ₂ Regional Unconformity (TI-12N).	59
17. Erosion at the Periphery of Sand Ridges (TI-12N)	60
18. S ₂ Merges with the Sea-Floor (TI-13N).	61
19. S ₂ Unconformity Underlies all Sand Ridges (TI-9N).	63
20. Average Slope of S ₂ .	64
21. R ₂ Ravinement Unconformity Within Sand Ridges (TI-12N).	66
22. Photo and Lithologic Log of R ₂ (Ravinement Unconformity), AV-09, 4.4 m.	67
23. Arcuate Reflections Underlying S ₂ (TI-1.8E).	70
24. Reflections Terminate Against S ₁ at Depth (TI-14N).	71
25. Photo and Lithologic Log of P ₁ Upper Surface, AV-06, 1.05 m.	72
26. Photo and Lithologic Log of Yellow Clay, AV-09, 4.4 m.	73
27. Sub-Parallel, Steeply Dipping Lateral Clinofolds (TI-12N).	74
28. Location of 40,000 + b.p. Wood Fragments Recovered at AV-18 (TI-1N).	76
29. Paleochannel (TI-1N).	77
30. Deeply Incised and Buried Pleistocene Valley (TI-12N).	79
31. Channel Path.	80

32. Seismic Reflection Pattern In Sand Ridges (TI-8N).	83
33. Seismic Reflection Patterns in Shelf Sediments (TI-13N).	84
34. Calculation of Sand Ridge Sediment (TI-13N).	88
35. Oxygen Isotope Curve.	92

List of Tables

1. Allowable Horizontal Positioning Criteria.	32
2. Average Strike and Dip of the Two Mapped Surfaces.	62
3. Summary Statistics of the Upper Four Depositional Units.	86
4. Sand Ridge Summary Statistics.	90

Appendices

A. Core Logs	118
B. Navigation and Isopach Data	140
C. Summary Sediment Statistics	154

INTRODUCTION

New Jersey beaches are an economic and recreational resource which are vital to the interests of the State of New Jersey. In 1981, the New Jersey Department of Environmental Protection (NJDEP) completed the Shore Protection Master Plan as designed to assist in the management of coastal regions by regulating development along the New Jersey shoreline and by designing a cooperative policy with Federal agencies to address the problem of coastal erosion (U. S. Army Corps of Engineers General Design Memorandum, 1989). In response to increasingly severe coastal erosion which occurred along the New Jersey coastline during the 1980's, the NJDEP developed the New Jersey Coastal Management Program to assess the rate of New Jersey beach erosion and to develop a strategy for implementing realistic solutions to combat the destruction of coastal land area and property.

The New Jersey Shore Protection Study was initiated in 1989 to document the extent of beach erosion and property damage along the entire New Jersey coast from Sandy Hook to Cape May. At its completion in September of 1990, the study identified six coastal regions with high erosional rates which necessitated further study, including the coastal region from Townsends Inlet to Cold Spring (Cape May) Inlet. The study of this smaller region was completed in January of 1992 (New Jersey Shore Protection Update, June 1994) and identified severe erosion along portions of Sea Isle City, Avalon Township, Stone Harbor, and North Wildwood (figure 1). The New Jersey Shore Management Program estimates that approximately 1.5 million cubic yards of fill will be needed to initially stabilize the beaches between Townsends Inlet and Cold Spring Inlet.

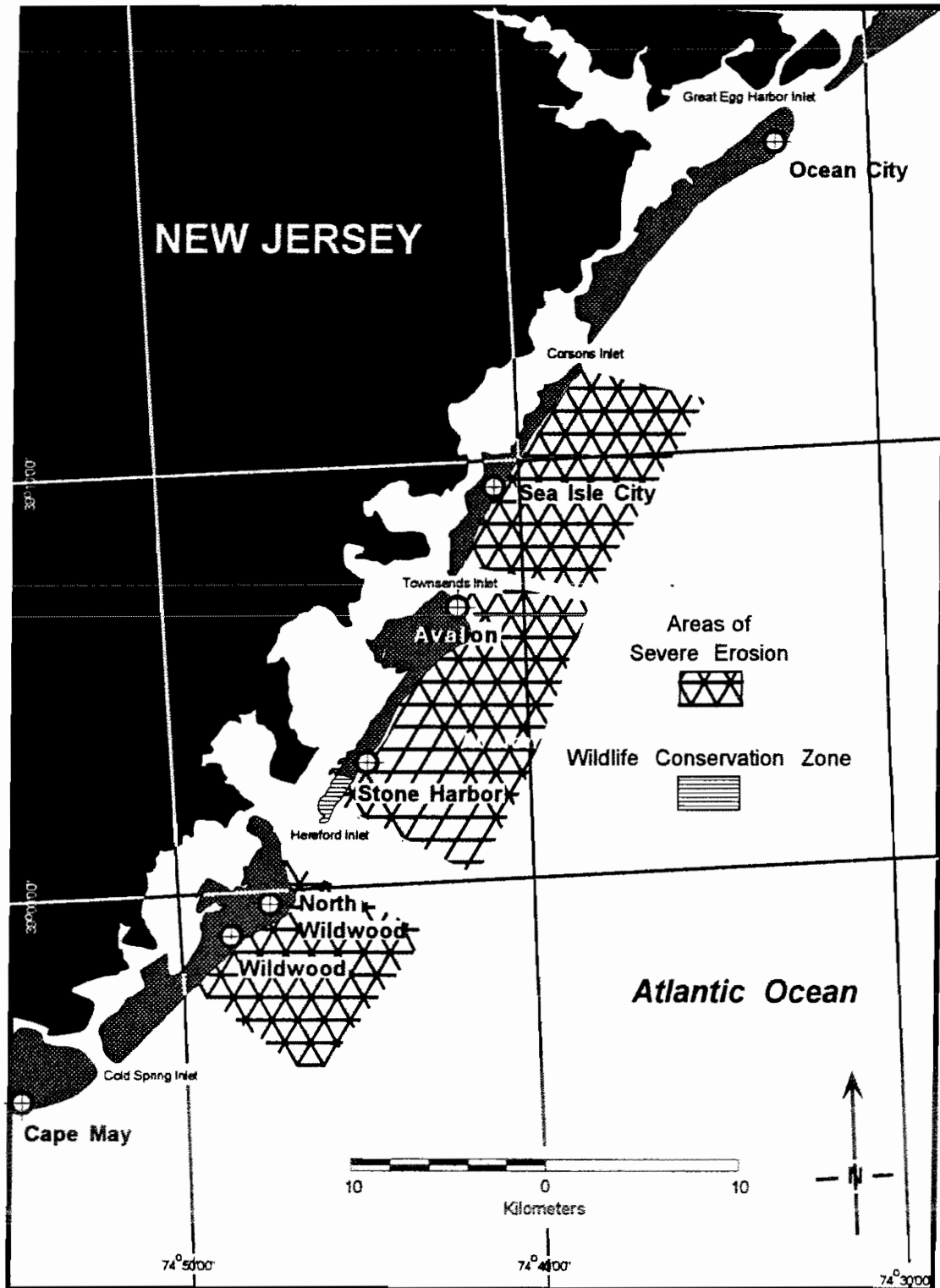


Figure 1. Many shore communities in southern New Jersey suffer from severe erosional problems. Offshore mining of sand resources could help provide a stable source of remediation sand for the most severely affected areas.

9.5 million cubic yards of fill will be needed to stabilize beaches between Great Egg Harbor Inlet and Brigantine Inlet, while millions more cubic yards of sediment will be needed for periodic beach maintenance (unpublished data, New Jersey Geological Survey).

The demand for very large volumes of beach-quality sand along the New Jersey coastline has resulted in an intense search for borrow areas. Borrow areas on land are increasingly scarce due to a shortage of suitable beach-grade sand and stringent environmental regulations governing excavation of sediments. Transportation of the material also poses logistical and environmental problems on crowded New Jersey roadways. If roadways were utilized to transport beach remediation sediment, 56,000 truckloads would have to be moved between the borrow sites and beaches for every 1,000,000 m³ of needed material (based upon standard 18-yd vehicle loads). In addition, access to many coastal sites by vehicular traffic is very limited or non-existent, especially in wildlife or wetland protection zones such as the wildlife conservation area along the southern end of Stone Harbor near Hereford Inlet (figure 1) (New Jersey Shore Protection Update Bulletin, June 1994). In such cases, roadways would have to be built for vehicles to reach the remediation area, adding greatly to the cost, complexity and environmental impact of remediation projects. Within environmentally protected and wildlife conservation areas, infrastructure would have to be removed afterward, and in some cases may be altogether prohibited.

To mitigate environmental disruptions and reduce the cost of remediation projects, a cooperative program to locate and assess the suitability of offshore borrow areas which lie near severely eroded coastal regions was initiated among the federal Minerals Management Service, the NJDEP, and Rutgers University. Once suitable borrow areas

(James, 1975) are located, well established suction dredging technologies can be employed to recover the sediment before transporting it to nearby coastal remediation areas (Brinkhuis, 1980). This solution avoids the more environmentally disruptive land transportation and results in a cost effective remediation strategy.

The Army Corps of Engineers is currently utilizing this form of remediation in some areas along the coast of Northern New Jersey (U.S. Army Corps of Engineers General Design Memorandum, 1989) and Maryland (Conkwright and Gast, 1994), bringing sediment from borrow areas which are located in state jurisdictional waters. However, prolonged and extensive dredging activity within the three mile state jurisdictional limit could lead to local environmental, commercial and recreational disruptions close to shore, as well as a depletion of state resources similar to what has occurred along coastal Maryland (Conkwright and Gast, 1994). Access to resources in federal jurisdictional waters will provide additional sources of sediment, minimize economic and social impacts along shoreline areas, and improve the potential for successful remediation activities along the New Jersey coast (Uptegrove et al., 1995).

To address this problem, a reconnaissance level study was developed to locate and quantitatively characterize potential borrow sites near regions of high erosional activity off of southern New Jersey. The objectives of this study are:

- Delineate an investigative area between Cape May Inlet and Great Egg Harbor inlet which lies within economic distance of the coastline (maximum 25 m water depth and 20 km distance) using available bathymetric and other oceanographic data;

- Document the regional stratigraphy and interpret the regional geological history;
- Identify potentially large volume sand resources using geophysical techniques;
- Ground truth the seismic data and quantify the suitability of the resource through sediment coring and sedimentological analysis, particularly:
 - a. the physical suitability of offshore sand for beach nourishment;
 - b. the percentage of usable sediment and the percentage of unusable mud and coarse gravel;
 - c. the thickness and lateral extent of the resource.

GEOLOGICAL SETTING

Regional Setting

The continental shelf of the United States Atlantic Coast is an south-eastwardly dipping extension of the Atlantic Coastal Plain. It extends from the chain of shore-parallel barrier islands along the edge of the continental land mass to the shelf break which is at an approximate water depth of 135 m (Emery and Uchupi, 1984). Average shelf gradient is about 0.001 (Swift et al., 1981) with shelf topography characterized by obliquely convergent shore-attached and shore-detached ridges (McBride and Moslow, 1991). Present rate of sea-level rise is estimated to be 2-3 mm/yr (Braatz and Aubry, 1987) with a resulting transgression rate of 2-3 m/yr (Sheridan et al., 1974; Ashley et al., 1991).

The Atlantic shelf has recorded many variations in relative sea-level throughout its depositional history. These variations are reflected in different depositional regimes and lithofacies patterns (Miller et al., 1990). Evidence of rapidly fluctuating relative sea-level occurs in upper shelf sediments of the central Atlantic coast which date from the late Miocene period. Significant expansion of Antarctic and northern hemispheric glaciers occurred during the Pliocene, with the most intense northern glacial activity taking place during the Pleistocene. Pleistocene eustatic global sea-level fluctuations are related to expansion and contraction of the large northern ice masses (Ashley et al., 1991). Beginning approximately 18 ka, post-glacial rise in sea-level forced the coastline across the shelf to its present position and created a transgressive succession of sediments above the regional lowstand unconformity (Riggs and Belknap, 1988; Fletcher et al., 1992).

New Jersey Coastline

The New Jersey coastline is 209 km in length and forms part of the passive, slowly subsiding eastern North American continental margin. The coastline is composed of a continuous series of sandy beaches and barrier islands. Coastal sediment is derived from eroding coastal formations and from redistributed shelf deposits (figure 2). Little sediment is transported to the coast by rivers. Along the northern coastline from Long Branch to Point Pleasant, beaches have formed beneath a series of Cretaceous, Tertiary and Quaternary coastal sedimentary bluffs which rise as much as 8 m above the beaches (Uptegrove et al., 1995). These bluffs are the principle contributor of coastal sand in northern New Jersey. Longshore currents have redistributed the coastal sediment into a series of spits and barrier island complexes, the northern extent of which extends well into Raritan Bay (Sandy Hook spit).

In southern New Jersey from Point Pleasant to Cape May, a continuous chain of barrier islands range in length from 8-29 km and shield the coastal sediments from direct wave erosion. Whereas the northern islands derive much of their sediment from the eroding coastal bluffs (McMaster, 1954), the southern islands exhibit a differing sediment and mineralogical composition which is indicative of another source area, or of sediment reworking. Mean grain size of the southern beaches is generally one-half that of beaches north of Long Beach Island (Uptegrove et al., 1995).

Landward of the barrier islands, estuarine bays, salt water marshes, and tidally influenced streams form the inland coastal waterway system, a series of interconnected and navigable coastal channels. Eleven tidal inlets breach the barrier islands and allow intermixing of marine and fresh water within the back-barrier system. Complex tidal

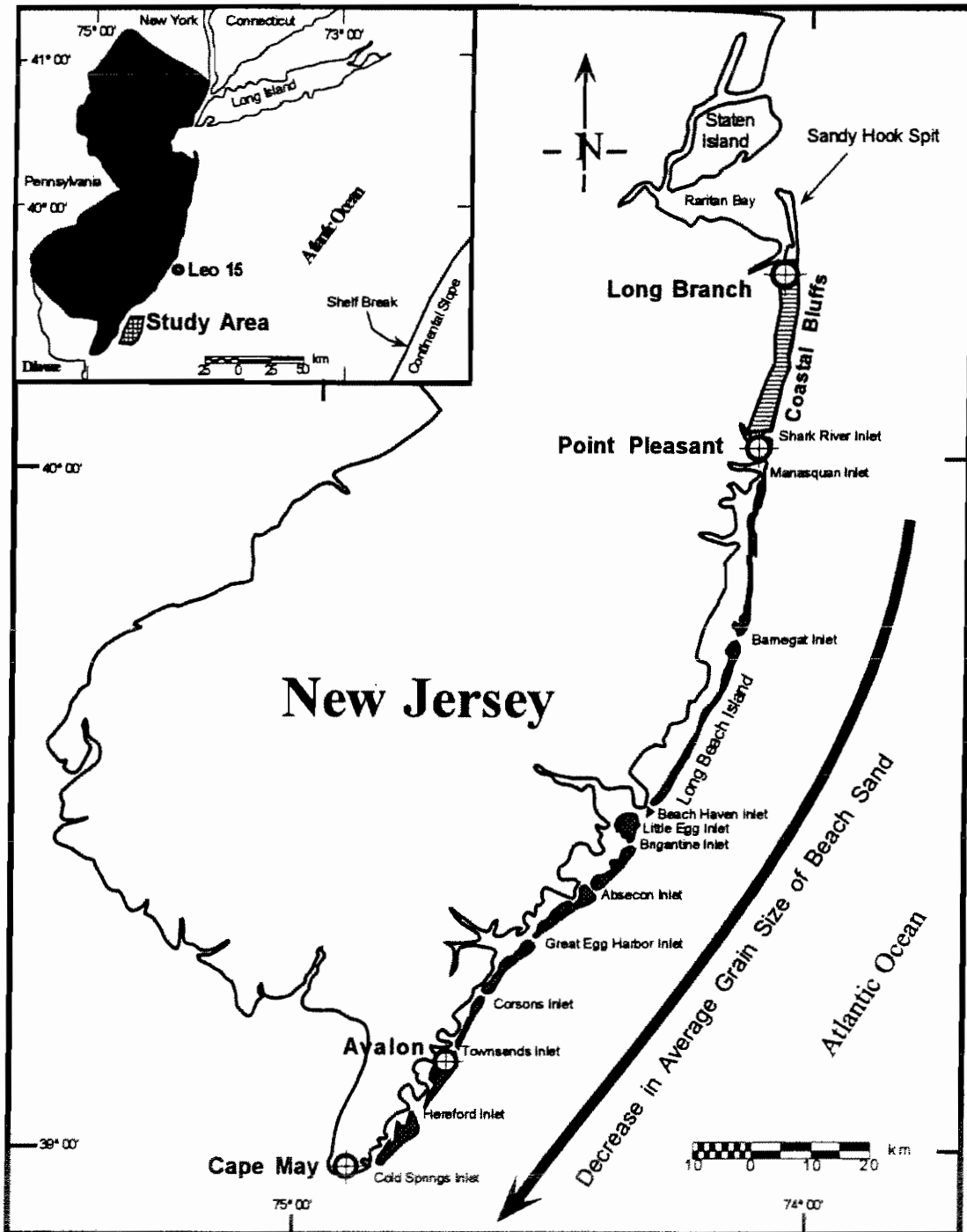


Figure 2. The New Jersey coastline is located at the landward limit of the North American Continental Shelf (inset). Sandy barrier islands (shaded) and the coastal beaches derive much of their sediment from the eroding central New Jersey coastal bluffs and re-worked shelf sediment. Average grain size of beach sand decreases to the south. The location of New Jersey inlets and other physiological features are indicated.

currents move through the inlets and cause lateral migration of many tidal channels and commensurate reworking and redistribution of sand along adjacent islands (Ashley, 1987; Dalrymple et al. 1992). To maintain inlet integrity and prevent channel migration, five inlets have been stabilized by the construction of parallel rock jetties (Shark River, Manasquan, Barnegat, Absecon, Cold Springs); three have been partially stabilized by the construction of one rock jetty or rock armoring of one shoreline (Great Egg, Townsends, Hereford); three inlets continue to migrate in an unconfined natural setting (Beach Haven/Little Egg, Brigantine, Corsons) (Uptegrove et al., 1995).

The New Jersey Geological Survey (NJDEP) maintains a program of beach monitoring and erosional assessment for the State of New Jersey. Begun in 1986, the program has divided the coastline into 13 segments (reaches) which are used to consolidate approximately 100 beach survey profiles, geophysical data, beach remediation history, and political information into discrete beach remediation assessment zones. Individual beach survey profiles which measure and quantify beach volume relative to fixed markers are compiled and analyzed to determine sediment loss or gain through time. This information is tabulated by reach by Stuart Farrell (Stockton State College) and compared to the U.S. Army Corps of Engineers estimates of New Jersey coastal beach erosion (Farrell et al., 1993).

The resulting map data show a complex pattern of net sediment gain and loss which is related to longshore drift, storm activity, sea-level change, migrating tidal channels, and on-going beach remediation projects (figure 3). Severely eroded beaches are identified along portions of Cape May and Atlantic counties adjacent to the study area. Ocean City and Sea Isle City experienced particularly severe erosional problems during the

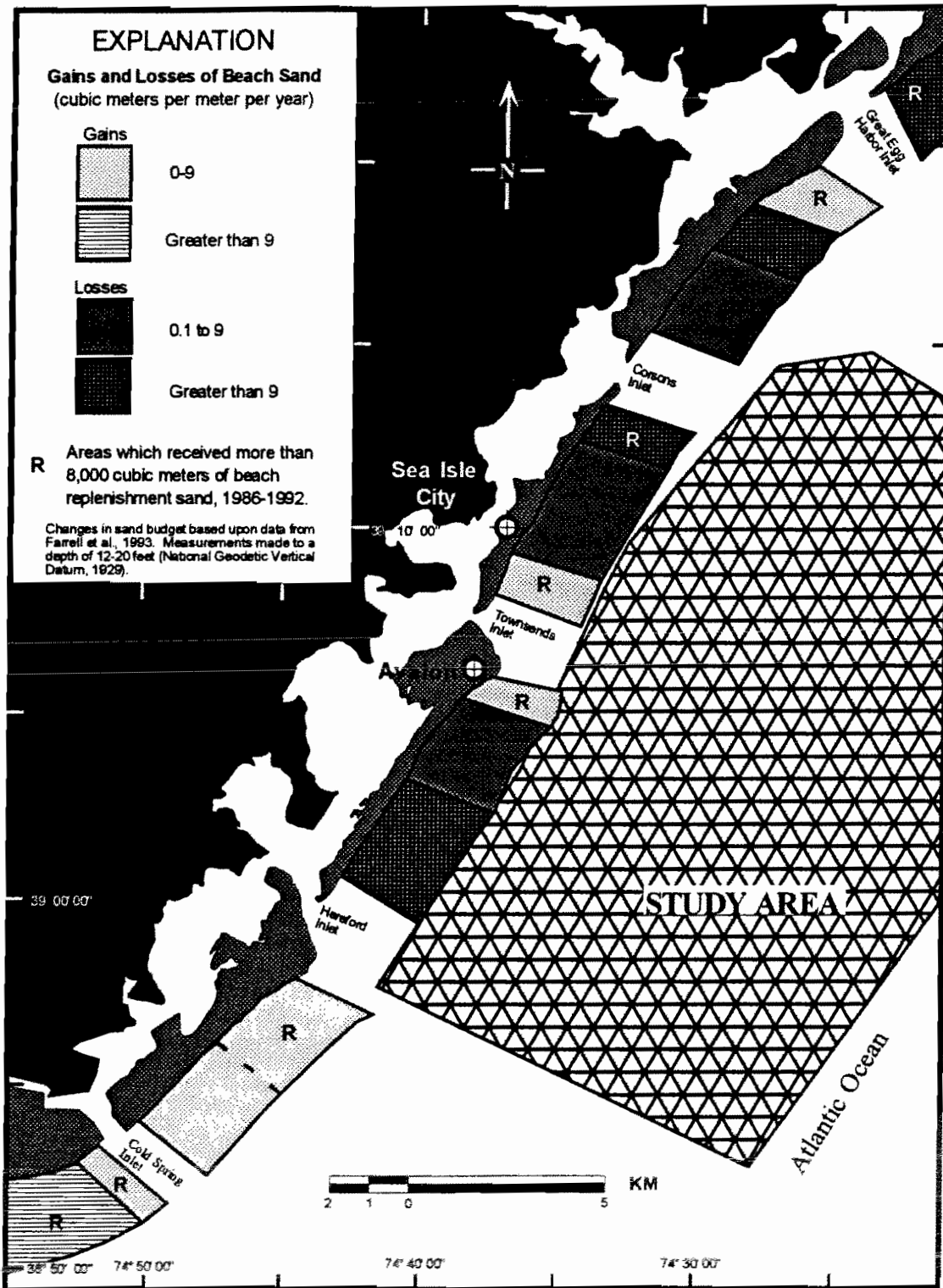


Figure 3. Gains and losses of beach sand along the southern New Jersey coastline, Atlantic and Cape May Counties, 1986-1992. Some locations which show gains are due to active beach replenishment activity. Study area is shown for reference (after Uptegrove et al., 1995).

7-year beach profile study, as well as beaches near Stone Harbor (figure 1). Selection of the survey area was designed, in part, to help meet the sediment requirements of these high priority remediation zones.

Study Area

The study area is located from 2 to 25 km (1-13 nm) offshore from Sea Isle City and Avalon Township in southern New Jersey (figure 4). The northern end of the study area is approximately 20 km (10 nm) from Atlantic City and 200 km (100 nm) from New York City. The study area is divided into northern and southern regions as defined by the seismic coverage. High resolution seismic reflection survey lines were run both parallel and perpendicular to the coastline, generally along and across the regional strike of the seafloor. Water depths in the area range from 8 m (25 ft.) near the coastline to 27 m (80 ft.) at 25 km (13 nm) distance from the shoreline. Tides are semi-diurnal with a mean tidal range of 0.94 m and a spring tidal range of 1.16 m (Ashley, 1987). Prevailing winds are from the west to northwest with a southerly onshore component during the summer (Ashley et al., 1987). Storm generated winds frequently approach from the east to northeast.

Shelf topography within the study area consists of a series of shore attached and detached ridges (figure 5) which are similar in form to sand ridges found off of the U.S. Atlantic shelf from New York to Florida (McBride and Moslow, 1991). Within the study area, the long axis of sand ridges trend approximately 15-30° with respect to the shoreline, and vary in length from 2 km to 6.5 km. Ridge widths tend to be approximately

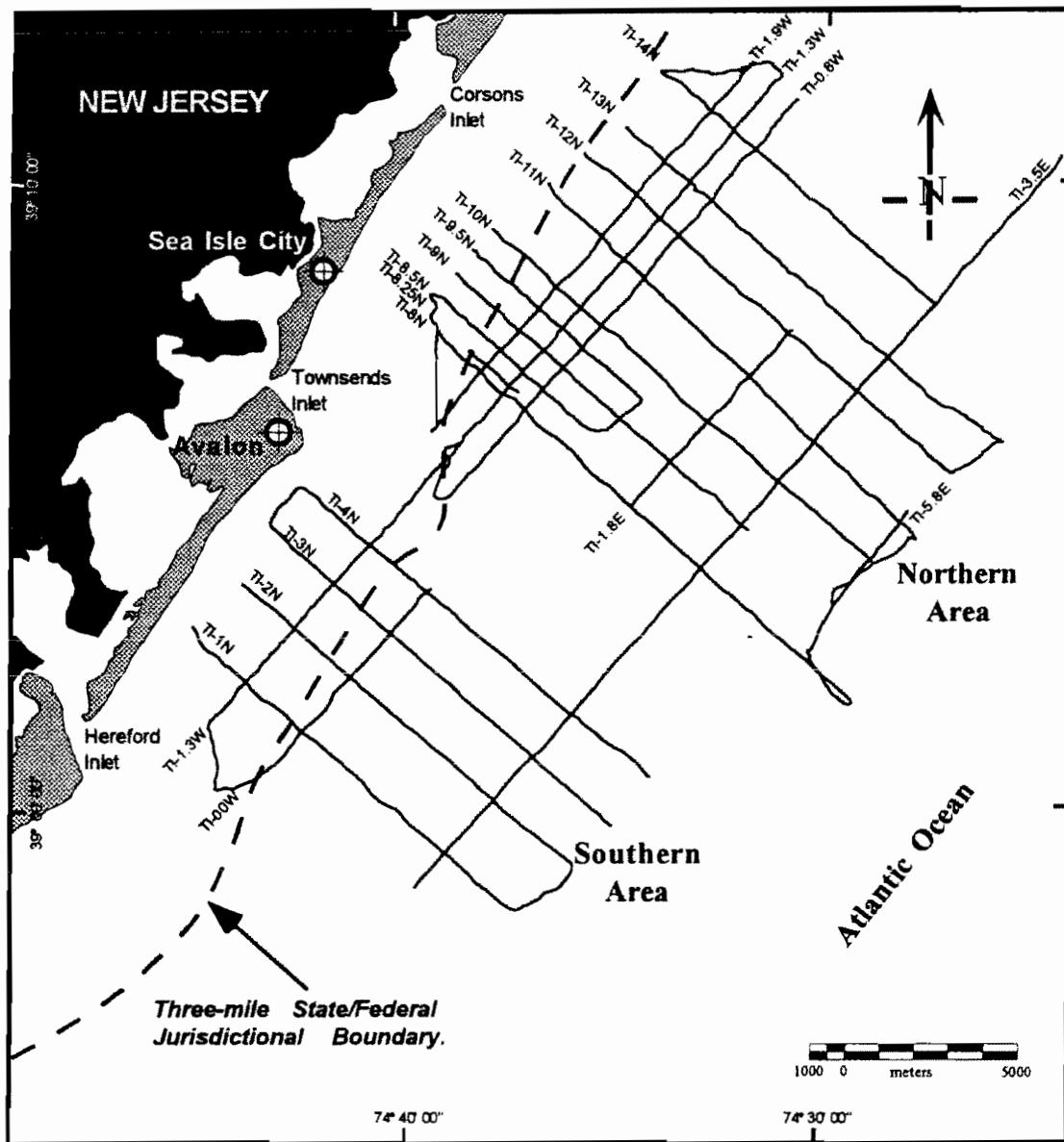


Figure 4. The study area is located off of the southern New Jersey coast between Corsons and Hereford Inlets. 303 km of high-resolution seismic lines were used to map the bathymetry and subsurface structure of the region. The study area is divided into northern and southern areas which correspond to the two concentrations of seismic line coverage. Sand ridges of interest are located on the landward portion of the study area within federal water jurisdiction.

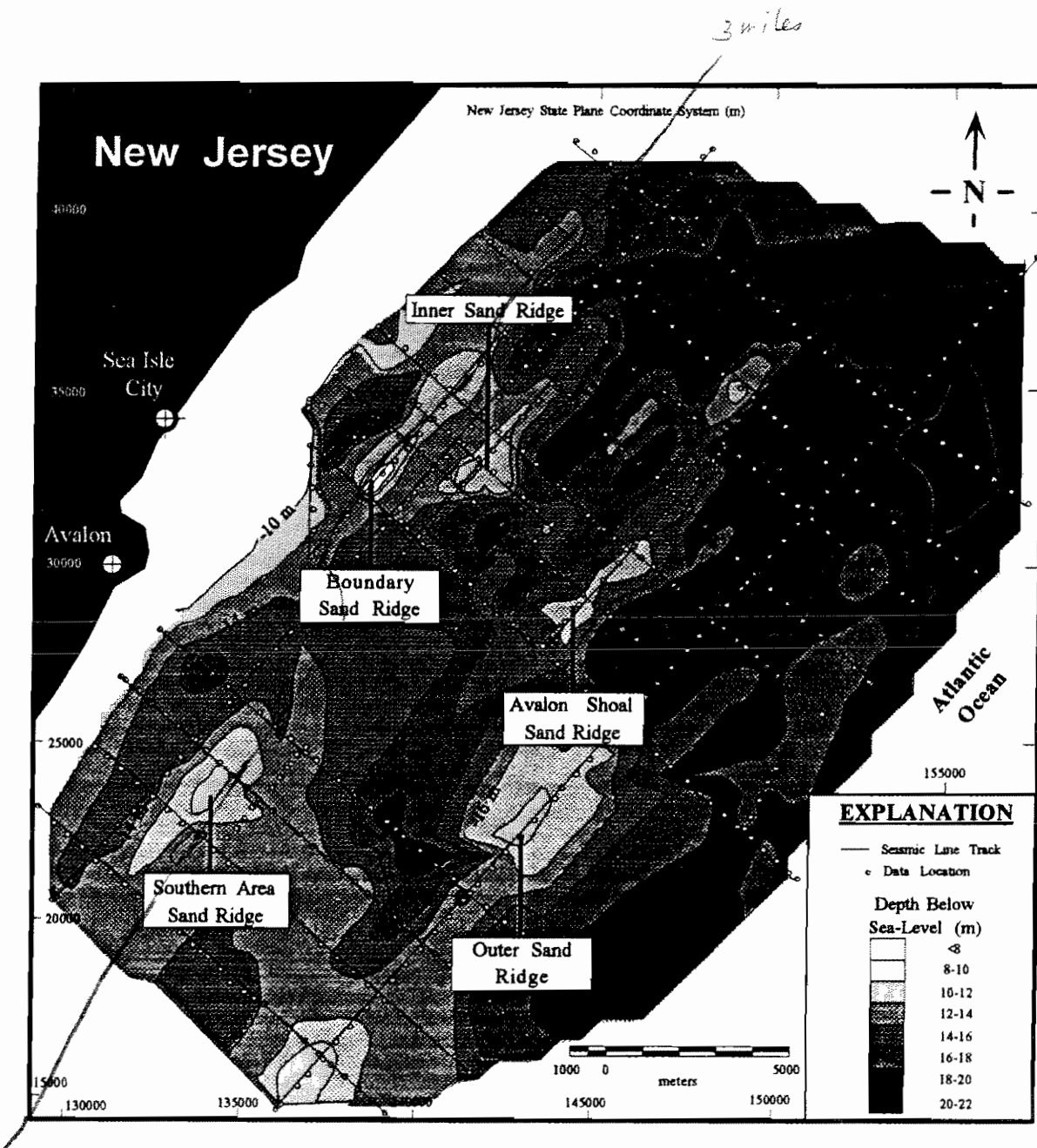


Figure 5. Shelf topography in the study area was constructed from 550 data points (dots) recorded at five minute intervals along each seismic track line. The topography is characterized by a series of shore-oblique sand ridges (lighter shades indicate shallower depths than darker shades) on a gently sloping continental shelf. Avalon Shoal and the inner ridge are the principle targets of this study.

10-25% of the length, while shape is variable. Maximum measured sediment depth from ridge crest to the underlying strong seismic reflection is 13 m.

PREVIOUS INVESTIGATIONS

Sand Ridge Development

The origin of the eastern North American continental shelf ridge system has been debated since early in the twentieth century. Shortly after the first bathymetric mapping of the Atlantic margin ridge system in the early 1930's, Van Veen (1935) suggested that large sand ridges were formed by multiple tidal current ebb flow paths which converged in the offshore. Similarly, Off (1963) and Huthnance (1973, 1982) found that alternating and obliquely converging slow and fast moving tidal currents could carry sand offshore and form linear ridge systems on the United Kingdom tidally dominated shelf. A variation of that model suggested that ridges in the North Sea were formed in a modern, dynamic process when asymmetrical sand streams converged at the ridge crest (Caston, 1972). Experimental studies later determined that tidal bottom velocities of 50-250 cm/s would be necessary to effectively transport the sediment which comprises most ridge systems, effectively eliminating tidal flow as the formative mechanism on storm-wave dominated shelves (Stubblefield et al., 1984). However, studies of sediment transport along the Atlantic shelf of the United States demonstrated that some nearshore and mid-shelf bottom currents are sufficiently strong to allow for reworking of surface materials, particularly during storm events (McClennen, 1973; Stubblefield et al., 1975; Scott and Csanady, 1976; Lavelle et al., 1976). Although ridge sediment was shown to be affected by dynamic shelf processes, the observed reworking of the sediment was limited to the upper 1 m of the ridges.

Based upon bathymetric analysis of subsurface topography and on grain size characteristics of sediment samples from sand ridge surfaces off of Long Island, New

York, McKinney and Friedman (1970) concluded that ridges are best explained as relict fluvial drainage topography which has been modified by modern day processes.

Bathymetric analysis of the New Jersey shelf by Swift et al. (1973) also identified drowned, relict, subaerial tributaries, though the link between fluvial channels and shelf ridges was uncertain. Other investigators have interpreted the shelf topography as remnant coastal structures, including Holocene transgressive stillstand deposits (Shepard, 1963), Pleistocene regressionary stillstand deposits (Kraft, 1969), overstepped beach ridges or barrier island sediments which are built upon older Pleistocene deposits (McClennen and McMaster, 1971), and in-place drowning of partially preserved barrier island sediments during Holocene rise in sea-level (Sanders and Kumar, 1975).

Sand ridges which are similar in form to those found on the eastern North American shelf are also found along the retreat path of the Holocene Mississippi River in the Gulf of Mexico. These ridges form a series of shallow shoals which cannot be adequately explained by erosional shoreface retreat and in-place drowning of barrier island or shore-attached ridge systems. The Gulf of Mexico ridge systems are better explained by transgressive submergence: former barrier shorelines integrated shoreface erosion with relative sea-level rise during a period of coastal submergence due to sediment loading (Penland et al., 1986). Depending upon the time of formation, sediment loading could have played a role in the development of eastern shelf ridge systems. However, Stubblefield et al. (1984) recognized that sand ridge morphology along the eastern seaboard varies depending upon shelf location. They suggested that the observed differences between ridges along the same portion of the Atlantic shelf can best be

explained by in-place reworking and modification of the barrier island sediments while on the continental shelf.

Various themes have been proposed regarding the effect which post-transgressive topography has had on modern sediment transport processes. Swift et al. (1973) proposed that offshore sand ridges were initiated in the shoreface, perhaps along littoral drift zones near estuary mouths, and that storm induced currents caused their migration offshore. Predominantly erosional processes on the shelf gradually produced a stable ridge and swale topography end-product toward which nearshore and shore-attached sand ridges naturally evolved. Duane et al. (1972) argued against a shoreline origin for sand ridges and suggested that storm induced helical tidal flow forms sand ridges in a dynamic offshore process. Swift and Field (1981) dismissed helical flow in favor of constructive feedbacks between shelf topography and bottom shear stress. They determined that the observed grain size distributions of sediment across individual ridges is characteristic of large scale bedforms which result from linear, dynamic processes, although their model was not able to account for the variable ridge orientations.

Relationships have also been observed between tidal inlets and some shore attached sand ridges. McBride and Moslow (1991) used a computer mapping system to plot the location of 259 shore attached and detached sand ridges along the inner Atlantic shelf between New York and Florida, along with 309 tidal inlets, both active and historical. 'Genetic relationships' between the tidal inlets and ridges were documented and used to develop a two step model of ridge formation in which sand is first deposited in ebb-tidal deltas before being reworked into shore attached ridges during transgression. Sometime during continued oceanic transgression, ridges become detached from the

shoreline. McBride and Moslow (1991) acknowledged that not all ridges can be explained by this model, and that more than one formative process is likely needed to explain all Atlantic shelf sand ridges.

Infragravity wave models of 0.5 to 5.0 minute periods were invoked by Boczar-Karakiewicz and Bona (1986) and Boczar-Karakiewicz et al. (1990) in mathematical computer models of sand ridge formation. These models showed good agreement with observed features of sand ridges along the United States Atlantic coast and accurately described increases in crest to crest distances with increasing water depth. The models indicated that crest to crest distances were directly related to the mean slope of the shelf and that the horizontal distance between ridge crests are several times the wavelength of the incident train. Computer simulations calculate that as few as 890 years are necessary to develop eastern North American shelf ridges in 40 meters of water.

Knebel and Spiker (1977) were the first to propose that sand ridges can form by two different processes during an oceanic transgression. They concluded that different ridges often have different formative histories which will necessarily result in variable internal structure between ridges. Stubblefield et al. (1984) demonstrated that the Atlantic margin contains two distinct types of sand ridges: shore attached sand ridges which are morphologically similar to ridges near the outer shelf, and mid-shelf ridges which are morphologically and orientationally dissimilar to the nearshore and outer shelf ridges. This study suggests that at least two processes must govern sand ridge formation on the eastern North American continental shelf.

Rine et al. (1986, 1991) conducted a seismic and sedimentological study of an inner, nearshore sand ridge and a middle shelf ridge off of the southern New Jersey coast.

The inner sand ridge was located in or near the present study area. Cores which were obtained on both the inner and mid-shelf ridges indicate that three lithologies were consistently present (but were not necessarily resolvable on seismic profiles): 1) a non-fossiliferous laminated sand and mud layer at the base of the sand ridge which contains only traces of microfauna; 2) a shell-rich, poorly sorted sand and mud unit which overlies the non-fossiliferous unit, and; 3) an upper ridge sand unit with some faunal elements. Based upon radiocarbon dating of shell fragments in the shell-rich portion of the sand ridge (2), the midshelf ridge appears to have formed much earlier than the upper shelf ridge (approximately 14 ka versus 3 ka). Multivariate analysis of core samples indicates that the three lithologies are sedimentologically resolvable from one another and represent three distinct environments of deposition:

- 1) The non-fossiliferous unit is composed of mud and fine grained sand which contains sparse foraminiferal assemblages. These assemblages indicate deposition in an inner shelf or estuarine environment. Abundant terrestrial plant remains suggest deposition of the sediment in proximity to the shoreline.
- 2) The shell-rich unit contains beds of sand and gravel which alternate with mud and silt. Foraminiferal and macroscopic faunal assemblages are indicative of open mid-shelf conditions. Differences in the composition of foraminiferal assemblages between core locations demonstrates that faunal heterogeneities exist and suggest that sub-facies may be present.

3) The upper sand ridge unit is composed of a coarsening upward, fine to medium sand which abruptly overlies an unconformity or period of non-deposition at all core locations. This boundary is located within the area of ridge relief due to erosion of the surrounding sediments. Intervals are heavily bioturbated and burrow traces are recognizable throughout the unit. This is the only portion of the ridge which is considered active and attributable to modern shelf processes.

Regional Seismic and Coring Studies

Eleven major high-resolution seismic reflection and/or sedimentological studies have been conducted along the New Jersey continental shelf since 1961 (figure 6):

1. ***Fray and Ewing, 1961***: Sparker survey and echosounder data were collected from two transects along the northern New Jersey coastline. The Navasink, Red Bank, Manasquan, and Kirkwood Formations were tentatively identified based upon the survey data and information from twenty piston cores.
2. ***Williams and Duane, 1974***: 445 miles of continuous seismic reflection profiles (50-200 joule Sparker) and 61 VibracoresTM were obtained from the inner New York Bight, an area encompassing approximately 250 square miles of shelf from northern New Jersey to western Long Island. Shrewsbury Rocks marks the demarcation between two distinct geomorphic provinces to the north and south. The northern region is underlain by coastal plain strata which were deeply eroded by Pleistocene glaciation and subsequently buried by glacial sand and gravel outwash. Strata within the

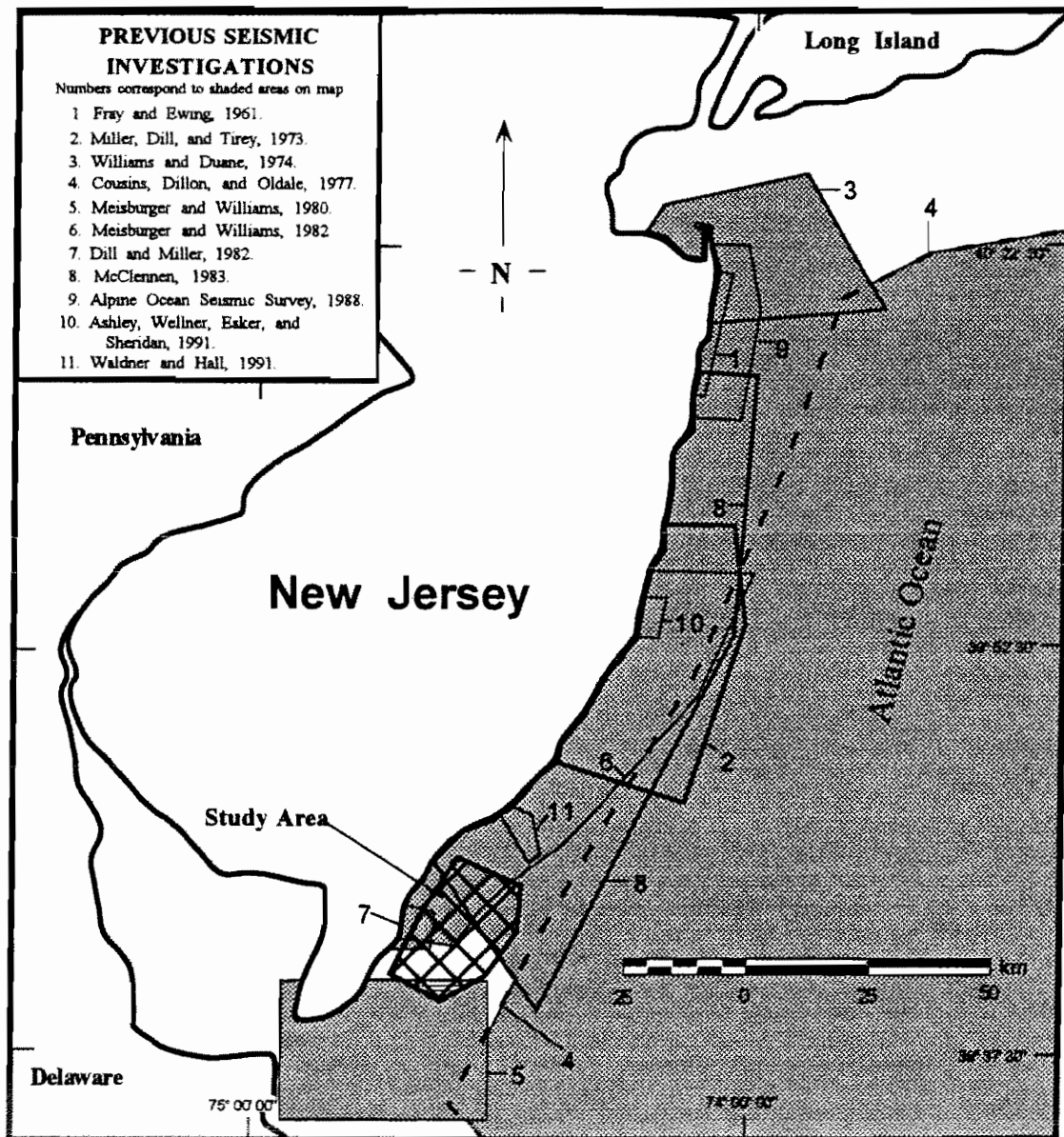


Figure 6. Location of the study area (hatchure) and previous seismic and sedimentological investigations (gray) along the New Jersey inner continental shelf (after Uptegrove et al., 1995).

southern region have been evenly truncated and covered by a veneer of sediment which differs from that in the northern region.

3. *Miller, Dill and Tirey, 1973*: High resolution seismic data (UNIBOOM™ and 3.5 kHz Sparker) were collected off of Beach Haven Ridge to assess the local geology at the proposed offshore Atlantic Generating Station nuclear power plant. Sand thickness varies from 1.5 m in the northern end to 6.0 m at the southern end of the survey area. A deep, mud-filled Holocene valley underlies the sand at depths of more than 18 m. The valley is incised into Pleistocene clay units which may have been deposited during the stage-5 regional highstand. Sparker data indicates that the older Tertiary and Pleistocene units dip southeastward to at least 150 m below the seafloor, but are shallow north of Barnegat Inlet where they crop out at the seafloor.

4. *Cousins, Dillon and Oldale, 1977*: A regional seismic study of the central Atlantic continental shelf from Long Island to Chesapeake Bay was conducted to investigate and identify potential environmental hazards by the Bureau of Land Management and the U.S. Geological Survey. The seismic survey was conducted during the months of April and May, 1975 aboard the R/V Atlantis II using UNIBOOM™ and MINI SPARKER™ systems. The investigation documented mobile sand sheets, areas of sedimentary faulting, subsurface structures and regional stratigraphy.

Seismic records reveal three principle types of bedding: coastal plain strata which exhibit a monoclinial regional southeast dip; steeply inclined crossbeds which appear to be of fluvial or deltaic origin but are restricted to an elongate basin east of Sandy

Hook; and Pleistocene-Holocene stratified fluvial sands and gravels which are regionally discontinuous and exhibit a gentle seaward dip. Other portions of the Hudson Channel have been filled with anthropogenically derived disposal material (0.76 billion m³). Vibracore™ data show that fine to medium grained sand is ubiquitous on the shelf, with coarse material being found in smaller patches off of Long Island and parts of New Jersey.

5. *Meisburger and Williams, 1980*: This study was conducted to locate bodies of sand and gravel off of Cape May, New Jersey for the purpose of beach remediation and restoration projects. 1258 km of seismic reflection profiles and 104 sediment cores of up to 3.7 m in length were collected from the inner continental shelf. 18 sites contain an estimated 1.086 billion m³ of sand, all but two sites of which are linear to arcuate sand ridges. The ridges are approximately 6 m thick, composed of clean, quartz sand, and appear to rest on a pre-Holocene fluvial surface which is composed of dense silty sand and gravel. The 6 ridges which are most proximal to Cape May beaches contain approximately 216 million m³ of sand and gravel, making them the most suitable sites for consideration within the southern region.

6. *Meisburger and Williams, 1982*: About 1800² km of the central New Jersey inner continental shelf between Avalon Township and a line 7.5 km north of Barnegat Inlet were surveyed to assess and quantify potential offshore marine sand and gravel resources. 1133 km of high-resolution seismic reflection profiles and limited sidescan-sonar images were used to identify surficial sand ridges on this portion of the

continental shelf. 97 Vibracores™ were drilled on or near sand ridges in order to gather sedimentologic and stratigraphic data which reflects the physical suitability of the resource. From the derived data, an estimated 172 million m³ of suitable sand are available in 15 areas, but require further evaluation.

The seismic data reveal a large number of linear and arcuate sand ridges within the study area. Sedimentologic data show that the ridges contain large volumes of clean quartz sand. Most of the ridges appear to be Holocene in age and overlie older pre-Holocene age sediments. The pre-Holocene deposits are typically yellowish-brown in color and contain shell and other calcareous material. The heterogeneous character, extremely poor sorting, oxidation-like color of the more coarse material, and the presence of channel-like reflections in the seismic data suggest that this sediment may have a fluvial origin.

7. ***Dill and Miller, 1982:*** Geophysical survey data were collected off Avalon, New Jersey for the proposed installation of an electric generating station outfall pipe. Detailed bathymetry of the adjacent coastal waters was conducted using a DE-719-B Echo Sounder. The ocean bottom drops to the 13 m (40 ft) contour within 1.5 km (5000 ft) of the beach and remains relatively flat seaward of that point. ORE 3.5 kHz sub-bottom profiler data was collected along 20 transects run parallel to the shoreline, and along another 13 transects run perpendicular to the shoreline. The seismic profiling penetrated to a maximum sub-bottom depth of 18 m (60 ft) and revealed a series of flat-lying reflections, the upper of which are truncated at the seafloor on their seaward edge.

Eleven Vibracores™ were drilled to a maximum depth of 9 m (30 ft) and reveal that most of the sediment is sand and gravel with some minor layers of silt. The upper unit is composed of dense, medium to fine sand which originates at the beach and thins rapidly away from the shoreline. The middle unit consists of organic silt which is mixed with gravel and is interpreted to be upper Pleistocene/lower Holocene. The lower unit is much older and contains abundant clean sand and gravel.

8. *McClennen, 1983*: Sidescan sonar and seismic profiles were used to record topological characteristics of the region as well as its subsurface geology. Megaripples with 2-3 m crestal spacing were imaged within an area of general darkening. The darkened area may represent smaller, unresolvable ripples. The megaripples were concentrated in clusters at moderate water depths (20-22 m), but were found from depths of 12 meters to 40 meters.

The seismic imagery penetrated to 42 m below seabed and revealed flat-lying reflections south of Barnegat Inlet, with incised valleys and buried channels found southeast of Great Egg, Little Egg and Barnegat Inlets. Some reflections are traceable for several miles to the north of Barnegat Inlet where they are separated by 5-12 m of sediment. A 2-km wide seismic transition zone separates sediments to the north of Barnegat Inlet from those to the south. The southern sediments average less than 1 m in thickness.

9. *Alpine Ocean Seismic Survey, Inc., 1988*: The Sea Bright Borrow Area was investigated using a UNIBOOM™ sub-bottom seismic profiler to help delineate offshore borrow material and the deep, sub-bottom strata. 30 Vibracores™ were

drilled at selected locations following analysis of the seismic data to categorize the physical parameters of the sediment and to help constrain the geophysical interpretations. This study delineated 41.4 million cubic yards of sand which is suitable for nearby beach remediation.

10. Ashley, Wellner, Esker, Sheridan, 1991: 100 km of GEOPULSE™ high resolution seismic reflection profiles and 12 Vibracores™ were taken within a 47 km² grid on the inner continental shelf just off of Barnegat Inlet. Analysis of the seismic data revealed three unconformity bounded units and three depositional systems which developed during two glacio-eustatic cycles during the past 125 ka. Non-marine, fluvial sands and gravels which were deposited during a regional lowering of sea-level separate marine sequences characterized by estuarine, tidal delta and nearshore barrier island type deposits. In addition to identifying the marine sequence boundary type unconformities, a transgressive ravinement unconformity was identified which separates the most recent Holocene transgressive sediments from older upper Pleistocene/lower Holocene nearshore sediments. The inner shelf sand ridges near Barnegat Inlet were found to exhibit shallow, offshore dipping internal bedding.

11. Waldner and Hall, 1991: Deeply penetrating seismic data off Atlantic City, New Jersey reveal that the Miocene period "800-ft aquifer" dips southeastward. The seismic reflections were tied to the U.S.G.S. offshore monitoring well to yield reliable identification. High resolution GEOPULSE™ reflection data show an incised valley higher in the stratigraphic section which trends southeast along the study area.

Several other early seismic and bathymetric studies have been conducted near this region, and include Veatch and Smith (1939), Emery (1966, 1968), Stearns (1969), Uchupi (1968, 1970), Emery and Uchupi (1972), and Schlee and Pratt (1972).

METHODS

Seismic Data Collection

303 km (164 nm) of shallow (30 m penetration), high-resolution seismic reflection profiles were collected from August 9-27, 1993 from aboard the R/V James Howard, a vessel owned and operated by the New Jersey Department of Environmental Protection. The seismic profiles cover an area of 603 km² off of the southern New Jersey coastline from Corsons Inlet in the north to Hereford Inlet in the south (figure 4). Mean water depths in the area range from 10 m (30 ft.) within 2 km of the shoreline to 25 m (90 ft.) at 20 km distance. Seismic lines run perpendicular to the coastline at an approximate spacing of 2 km. Two shore-parallel tie-lines run the length of the study area, with smaller tie lines located over high-priority targets which were identified during the cruise. Due to time and budgetary constraints, a 7 km data gap exists near the center of the study area where shore-perpendicular seismic lines were not run. This data gap divides the study area into a northern and southern region. Additional seismic lines are concentrated in the shore-proximal portion of the northern region to better delineate sand ridges found in that area.

Field Instrumentation

ORE Geopulse™ Seismic System

The seismic system is composed of an electrically driven towed acoustic source, a hydrophone reception array, and recording instrumentation. The sound source is a 30 cm diameter magnetostrictive plate which is sealed in a rubber diaphragm beneath an electroconductive coil and mounted under a 1.5 meter long catamaran (Ashley et al., 1988). The unit is towed obliquely behind a vessel by attaching a 15 m long rope to the

front side of the catamaran, thereby forcing the catamaran to the side of the towing vessel and avoiding the turbulent water within the ship wake. This configuration provides a stable platform which properly aligns the transducer with respect to the water surface (Wellner, 1990).

An acoustic pulse is generated in the water when magnetic field variations within the transducer cause the non-magnetic, metallic plate to move rapidly away from the conductive coil. The energy used to drive the transducer is provided by a 4000 volt bank of capacitors (model 5420A) which is connected to the catamaran by an insulated electrical cable and which emits 105 joule pulses every 0.64 s, with a peak frequency of about 1.0 kHz. With a speed-over-ground of approximately 6-7 km/hr (3-4 knots), the resulting shot spacing is approximately 1 m. Gating of the EPC graphic recorder enables the 80 msec sweep rate to be synchronized with the external sound source trigger (Ashley et al., 1991).

The detector is a 20 element, 6 meter long piezoelectric crystal hydrophone array which is attached to buoys floating at the water surface. This configuration helps to eliminate surface ghost reflections. The detector is towed 15 meters behind, and an equal distance to the side of the vessel as is the catamaran. The relatively small separation distance between the sound source and the detector relative to operational water depths minimizes movout effects (Wellner, 1990).

Signal processing is done on an ORE Geopulse™ receiver/pre-amplifier (model 5210A) with a bandpass filter fixed at 700 Hz lowcut and 2000 Hz highcut settings. The receiver controls the firing rate, frequency filtering and gain scaling. Time variable gain (TVG) is manually adjusted for best resolution of each profile. Positive seismic waveforms

only are printed on an EPC strip chart recorder, with positional time fixes recorded approximately every five minutes. A Hewlett Packard Model 54200A/D oscilloscope displays the incoming raw and filtered signal.

Simultaneous digital recording is made using a Bison Instruments 9024™ 24-channel engineering seismograph. Analog to digital signal conversion is 16 bit with instantaneous floating point. The signal is filtered through the analog system prior to entering the digital equipment. Shot points were saved without signal enhancement to an 80 megabyte hard disk using a 10:1 trigger divider to reduce the number of shots to a manageable quantity, given the cycling time of the engineering seismograph. 12 adjacent traces were grouped into each file using an automatic roll-along switch, with a hard drive capacity of 1000 files, sufficient for 11 hours of continuous coverage. Data is downloaded to the main processing computer from the onboard computer each evening (Uptegrove et al., 1995).

Navigational Equipment

Navigational equipment was provided by the New Jersey Geological Survey and consists of a ship-mounted Loran-C Navigational System and a mobile NAVSTAR™ Global Positioning System (GPS) trisponder with antenna. The system is hardwired to the onboard computer system for continuous navigational recording. Loran C is accurate to approximately 50 meters and is used to determine and maintain ship course or position. GPS is a satellite utilized electronic positioning system originally intended for a rapid, worldwide estimation of position. It operates by geometrical triangulation with satellites in known orbital positions. Since its original deployment, the theoretical positional resolution

has been improved to approximately ± 2.0 m when operated in differential mode to eliminate intentional signal degradation initiated by the United States Government (table 1). Positional data from GPS is recorded every 3 seconds throughout each cruise and down-loaded to an onboard computer system. When operated in differential mode GPS is able to provide real-time positional data and serve as a quality control check on the Loran-C system.

Vibrational Coring System

Alpine Ocean Seismic Survey, Inc. utilizes a steel hulled catamaran research vessel (R/V Atlantic Twin) with a marine model 271 B Alpine Pneumatic Vibracore™ system which is deployed onto the ocean floor from the side of the research vessel. This system is designed to recover continuous cores of sediment of up to 6.10 m (20.0 ft.) vertical penetration encased within a clear plastic core barrel liner. The Vibracore™ tower is composed of four steel legs braced widely apart on the bottom and mounted with circular foot-plates. At the top, the legs are welded to a circular steel support ring, forming a pyramidal structure. A heavy gauge steel core barrel is bolted to a pneumatically driven vibrational head which is lowered along a vertical aluminum support beam (mast) at the center of the tower. The core barrel feeds through a base-plate guide at the bottom of the tower. The barrel assembly consists of a 4 inch steel barrel with a 3.5 inch plastic inner core liner which attaches to the cutting head. A core retainer composed of overlain steel fingers angled back into the barrel is fitted inside the cutting head. The retainer allows sediment to freely enter through the center of the fingers during penetration, but expands and closes off the opening during barrel withdrawal and tower retrieval, thereby

Positioning System	Estimated Positional Accuracy (meters RMS) ²	Allowable for Survey Class		
		1	2	3
Visual Range Intersection	3-20	No	No	Yes
Sextant Angle Resection	2-10	No	Yes	Yes
Range Azimuth Intersection	0.5-3	Yes	Yes	Yes
High Frequency EPS ³	1-4	Yes	Yes	Yes
Medium Frequency EPS ³	3-10	No	Yes	Yes
Low Frequency EPS ³ (LORAN)	50-2000	No	No	Yes
Satellite Positioning:				
Doppler	100-300	No	No	No
Starfix	5	No	Yes	Yes
NAVSTAR GPS ⁴				
Absolute Point Positioning (no SA ⁵)	15	No	No	Yes
Absolute Point Positioning (with SA ⁵)	50-100	No	No	Yes
Differential Pseudo Ranging	2-5	Yes	Yes	Yes
Differential Kinematic (future)	0.1-1	Yes	Yes	Yes

Table 1. Allowable horizontal positioning system criteria¹ (after Uptegrove et al., 1995).

¹ From the U.S. Army Corps of Engineers, 1991.

² Root Mean Square

³ Electronic Positioning System

⁴ Global Positioning System

⁵ Selective Availability, a U. S. Department of Defense accuracy limitation.

minimizing sediment loss. When coarse, low cohesion sediment (sand) is expected to be recovered at a drill location, the retainer is covered by nylon mesh to help prevent the sediment from forming a watery suspension with a commensurate loss of sediment from the barrel. The cutter head assembly is then threaded into the core barrel and attached to the Vibracore™ tower.

The tower is lowered by crane to the sea-floor. Penetration into the sediment is achieved through a combination of vertically directed force due to the weight of the head assembly and strong vibration of the barrel. Vibrational power is provided to the core barrel by directing high-pressure compressed air through a pneumatic hose to the head vibrator assembly. The high pressure air stream drives the vibrator head rapidly up and down, which imparts an impulsive downward force along the core barrel. Vibration is halted when the vertical penetration of the barrel decreases to less than one foot in three minutes. The core barrel is then withdrawn from the sediment using a leveraged cable assembly which is attached to the ship winch via the coring rig support tower. The cable acts through a series of pulleys which pull the core barrel upward while maintaining downward force on the support tower. Once the core barrel is extracted from the sea-bed, a second cable retrieves the drill tower to the ship deck where it is placed in a horizontal position for barrel recovery. The core liner is removed from the barrel, sediment recovery measured, and the liner packaged into two meter lengths for transport to the laboratory. Core sections are stored vertically to prevent disturbance of the sediment.

Penetration is measured using a pressure shielded penetrometer which is attached to the vibrator casing. The system operates using a sprocket assembly which revolves during penetration as the vibrator casing descends along the mast. Penetration depth is transmitted via an insulated data cable and recorded on a strip chart recorder as a function of time (Wellner, 1990)

The R/V Atlantic Twin uses a Trimble 4000 Differential GPS Navigation System (real-time) which consists of an 8-channel satellite receiver and radio data link that obtains differential signal corrections from the United States Coast Guard GPS transmitter in

Cape Henlopen, Delaware. The navigation unit has an associated computer, printer, and display unit in the pilot house. Water depths were recorded using a Raytheon DE 719B survey echosounder. The unit's transducer operates at a frequency of 208 kHz with a beam width of 8, and is hull mounted (Alpine Ocean Seismic Survey, Inc., 1994).

Jetting

Sediment recovery may be less than the recorded penetration depth due to sediment loss, compaction of loose material, or pile driving. Sediment loss is most frequently caused by damage to the core retainer during the coring operation, allowing sediment to fall from the barrel during recovery. It may also be caused when large material is jammed into the retainer fingers, forcing them apart and preventing their proper closure during core withdrawal. Compaction usually occurs when coring through loosely packed sands which subsequently become more tightly packed during retrieval or while in storage. Pile driving occurs when sediment becomes jammed in the core cutter and lower barrel, thereby preventing other sediment from entering the barrel. When pile driving, penetration may continue into softer sediments which are underneath a more dense layer without recovering further sediments.

Cores which do not recover at least 80% of their barrel length were re-cored within 10 m of the initial site. The Vibracore™ tower is lowered to the ocean floor where water is forced through the core barrel under very high pressure (jetting) as the barrel descends into the sediments. The water forms a liquid slurry with the sediment and is forced to the side of the barrel while the barrel is lowered to within 1-foot of the previous penetration depth (point of refusal) as indicated by the penetrometer assembly. As the

barrel approaches its previous penetration depth, the water stream is shut off and coring continues. This is repeated until three attempts are made or until 80% core barrel recovery is attained.

In this study, the Vibracore™ was sometimes unable to penetrate or recover extremely coarse materials. In an attempt to maximize recovery and better understand the regional lithology and stratigraphy, such layers were bypassed by jetting through the resistant material and continuing recovery at a greater depth. This results in non-recovered sediment gaps at some locations, which are reflected in the core logs.

Vibracore™ Data Collection and Processing

Vibracore™ Data Collection

Vibracores™ were collected from August 30 to September 7, 1994 from aboard the R/V Atlantic Twin, a vessel owned and operated by Alpine Ocean Seismic Survey, Inc. Core locations (figure 7) were predetermined using data from the seismic reflection surveys and conformed to the following guidelines:

1. The majority of cores were collected on or near three large sand ridges which are considered high-priority targets due to:
 - a. proximity to remediation sites;
 - b. volume estimates which suggest abundant borrow material;
 - c. location of the potential borrow site within federal jurisdictional waters;
 - d. sediment located at economically recoverable depths (<20 m).
2. The majority of cores were placed along the crest of sand ridges, with fewer

cores collected along ridge flanks and in the intra-ridge swales.

3. The portion of each sand ridge chosen for coring was reasonably representative of the bulk sand ridge sediment, as best could be estimated from the seismic data.
4. Cores which were located on the same sand ridge were placed such that vertical stratigraphic resolution through the sand ridge could be maximized.
5. Cores which were not located on a sand ridge were located in a proximal intra-ridge swale such that when the core stratigraphy of the sand ridge and swale areas are combined there will exist a continuous composite stratigraphy.

Navigation during the coring operation used GPS real-time differential computations (Alpine Ocean Seismic Survey, Inc., 1994). The GPS antennae on the coring ship was located directly over the tower mast to provide positional accuracy without correction. The coring vessel placed each initial cast and any re-casts within a 10 m radius of the intended position. Ship sonar was used to verify the expected depth at each position and deviated by no more than 0.5 m. from the depth determined from the seismic cruise data. Expected depth was estimated from a conversion of the seismic two-way-travel-time which was previously recorded at each position.

Cores 1, 2, and 13 were collected on the innermost sand ridge of the northern region, 1 and 13 being representative of the shoal flanks and 2 being representative of the crest. Cores 11 and 14 were collected from within the swale that is landward of the inner ridge. Core 6 was collected from within the swale that is seaward of the inner ridge. Cores

3, 4, 5, and 12 were collected along an adjacent ridge and on ridge remnants seaward of the inner shoal. Cores 7, 8, and 10 were collected along the outer sand ridge (Avalon Shoal) in the northern region (figure 7).

Six cores were obtained in the southern region. Core 9 and 16 were collected from a small ridge at the inner portion of the region which is proximal to several southern area remediation sites. Cores 17 and 18 were collected within inter-ridge swales, and cores 19 and 20 were collected from non-ridge shelf sediments further offshore to provide information on spatial sediment distribution and lithologies.

Shipboard logs were maintained regarding the time and location of coring activity, depth of penetration, recovery data including a description of any sediment during core packaging which was visible on the core or at the ends of the core sections, re-casts, time on site, and penetration rate. Cores were stored vertically on ship but transported horizontally from Atlantic City, New Jersey to Rutgers University, Piscataway, New Jersey. Once at the core storage facility, they were once again stored upright until processed.

Core Processing

The cores were processed during the months of October and November, 1994. The 3.5 in. diameter PVC tubing was cut longitudinally on either side of the core using a circular saw with masonry blade. The cores were then split using a 14 gauge strand of wire which was drawn through the center of the core. The upper surface of each split core was cleaned of debris using a flat-edged masonry trowel or razor blade drawn across the

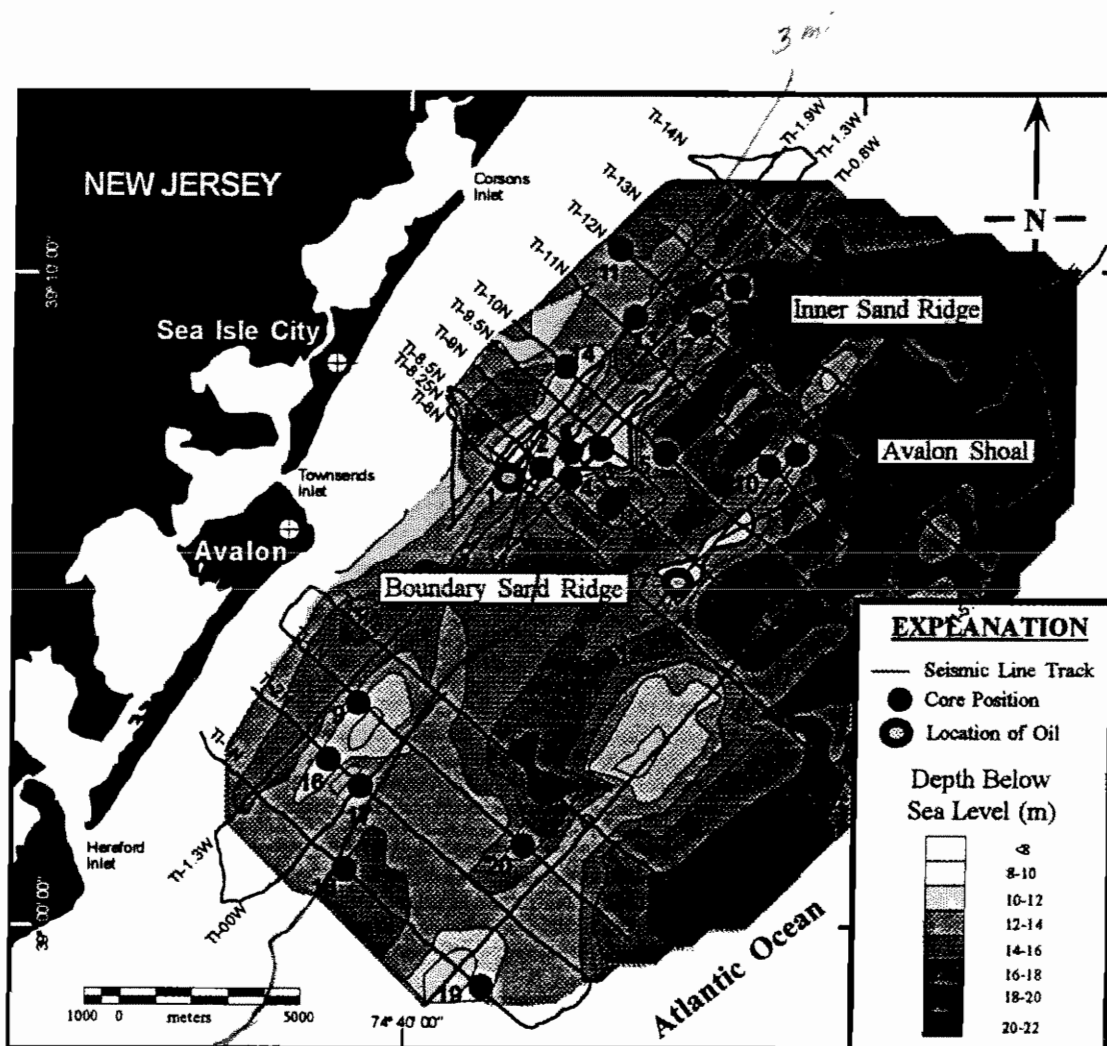


Figure 7. Twenty Vibracores™ were drilled at locations which were chosen from the seismic reflection survey results. A majority were drilled in the northern portion of the study area, particularly on or near the boundary and inner sand ridges (1, 2, 3, 4, 6), and on Avalon Shoal (7, 8, 10).

core parallel with the sediment bedding. The cores were then described, photographed, and separately sampled for grain size determination, microfossil content, organic material and mineralogy (Appendix C). Peat layers were observed and sampled, and wood fragments, including a 5 cm diameter root or branch, were recovered from the bottom of core AV-18. Remaining sediment was combined in sections and stored (composite samples).

Laboratory Procedures

Sediment samples which were taken for grain size analysis were split into two equal fractions, one to be processed and one to be archived. Sediment processing procedures follow those of Gale and Hoare (1991) and Folk (1980). Low mud-content sediment was dry sieved using a mechanical Ro-Tap at 1/4 phi intervals. Samples which contained a high percentage of mud were pre-processed using standard wet sieve techniques to separate mud from the sand and gravel. Mud content of the wet sieved samples was determined using standard pipet techniques. Sediments which contain more than 50% mud are unsuitable as beach remediation fill, so samples with a very high percentage of mud were not processed. Data were entered into a Quattro Pro™ spreadsheet and statistically analyzed using an automated program to calculate for graphic mean, inclusive graphic standard deviation, and inclusive graphic skewness (Folk, 1980). Lithic analysis was run on 6 gravel samples following procedures outlined in Gale and Hoare (1991) in order to assess the overall petrological composition of sediments on this portion of the New Jersey shelf.

Seismic Reflection Profiling

Seismic reflection profiles are produced by converting reflected acoustical (seismic) waves to electrical impulses, and then recording the resultant signal on strip chart paper or in digital format. Acoustic pulses which are produced by the towed ORE GEOPULSE™ sound source reflect from the seafloor or from sub-bottom surfaces before being received by the accompanying hydrophone array. Each hydrophone within the array converts the mechanical energy (pressure waves) to electrical impulses. These impulses travel to the GEOPULSE™ pre-amplifier/filter where they are processed and combined to generate a positive or negative polarity signal. The compilation of these signals are plotted continuously on a graphical strip chart recorder (analog format) and downloaded to a computer (digital format) during the survey cruise.

Analog records relate the polarity of the reflected acoustical signal to time/time space. The horizontal axis is a function of recording time and represents a relative position along the traverse. The strip chart recorder advances the paper in discrete intervals which are timed to coincide with the signal sampling rate. This produces a continuous record which manifests itself as a series of horizontal to sub-horizontal lines of the signal polarity being recorded. By including manually generated fix lines on the seismic record approximately every five minutes, horizontal positions on the seismic record can be determined directly from the GPS records. This allows other positions along the seismic traverse to be inferred, assuming a constant ship velocity.

The vertical axis of the reflection profile is a measure of two-way travel time between the initiation of the acoustic pulse and its detection by the hydrophone array after being reflected from the substrate. Because only part of the acoustic signal is reflected at

any given interface, a series of depth dependent reflections can be detected. Progressively deeper reflections require more time to return to the surface and consequently appear further down the seismic record than do the initial reflections. This time dependency is a function of seismic travel time, which in turn is a function of compressional wave velocity. Because the velocity of seawater is known and is reasonably uniform at shallow water depths (<30 m), the recorded two-way travel time (TWTT) to the seafloor can be used to calculate water depth at any position along the traverse. To a first approximation, depths to shallow subsurface reflections (<60 m below sea-level) can be inferred since compressional wave velocity in shallow, unlithified sediments is not sufficiently greater than seawater as to cause significant error in shallow surface calculations (less than 0.5 m error difference).

The strip chart automatically includes a series of horizontal guide lines on the seismic record which record TWTT from the initial acoustic pulse. Assuming that the acoustic pulse maintains a relatively uniform velocity through shallow sediments, the guide lines can be used in making depth estimates. Each line represents approximately 6.5 m (20 ft.) of depth based upon acoustic velocity in sea-water. Comparison of the seismically calculated water depths at each coring location with echosounder determined depths demonstrated that the two figures did not differ by more than 0.5 m at any location.

Reflectivity and Attenuation

Theory of seismic propagation states that a fraction of seismic wave energy will be reflected as the wave enters a medium of contrasting density, velocity, or both. The remaining energy will continue through the new medium until it is dissipated by additional

reflection events or through attenuation. Attenuation of the seismic pulse occurs due to conversion of the mechanical energy to heat or through mechanical dispersion of the energy into the medium.

The amplitude of a reflection event is governed by the density/velocity contrast across a boundary. The product of medium density and seismic velocity (v) is known as acoustic impedance (I). The higher the ratio of the initial acoustic impedance to the subsequent acoustic impedance (I_1/I_2) across a boundary, the greater is the amount of reflected energy at that boundary (wave amplitude) and the stronger is the return signal which arrives back at the surface. This relationship is also dependent upon the incidence (angle) of wave approach to the boundary, where a greater incidence will reduce the amplitude of the reflected wave. Since most boundaries in the shallow subsurface are close to horizontal (with the exception of high angle fault surfaces), problems due to angle of incidence are negligible.

Two types of boundaries produce particularly strong reflections due to strongly contrasting acoustic impedance: water-sediment and air-water. Upon striking the seafloor, a large fraction of the seismic wave is reflected back to the surface where it is detected by the hydrophone array. This produces an exceptionally pronounced reflector on the recording instruments which is usually characterized by a reverberatory pulse (2-4 parallel follow-cycles) due to seismic oscillation at the water-sediment interface. As the return wave strikes the air-water boundary, a large portion of the energy is reflected back towards the seafloor where it again is partially reflected upward. The return wave produces multiple reflections at twice the depth as the initial return pulse. This pattern of multiple reflections continues at regular intervals until the signal is attenuated (figure 8).

Bubble pulses and multiple reflections hamper interpretation of seismic data by obscuring primary events on the seismic trace.

Because the seismic return signal becomes increasingly weak as the wave penetrates deeper into the substrate, the sensitivity of the receiver array is increased through time. Time Variable Gain (TVG) is an automated process of linearly increasing the sensitivity of the receiver array after an initial delay. As gain is increased, the effect of background signals (noise) on the recorded signal becomes increasingly important. The gain limitation is reached when background noise overwhelms the increasingly faint return signal and no further useful information is collected from that pulse. TVG which was applied during the cruise permitted usable information to be collected from sub-bottom depths as great as 25 m (80 ft.).

Vertical Resolution

Vertical resolution is the smallest increment of vertical space in acoustic horizons which can be discerned by the seismic signal. Vertical resolution generally increases with acoustic velocity and burial depth, whereas it decreases with acoustic frequency (Christie-Blick et al., 1990). Using a simplified calculation to determine vertical resolution (Sheriff and Geldart, 1982-83), where:

velocity of primary wave/frequency of seismic equipment = wavelength

$$\frac{1700 \text{ m/s (simplified sediment velocity)}}{1 \text{ kHz (common frequency)}} = 1.70 \text{ m}$$

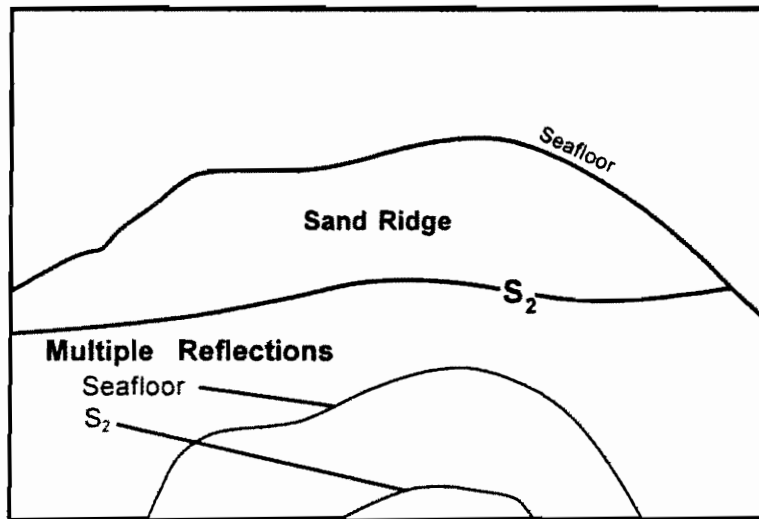
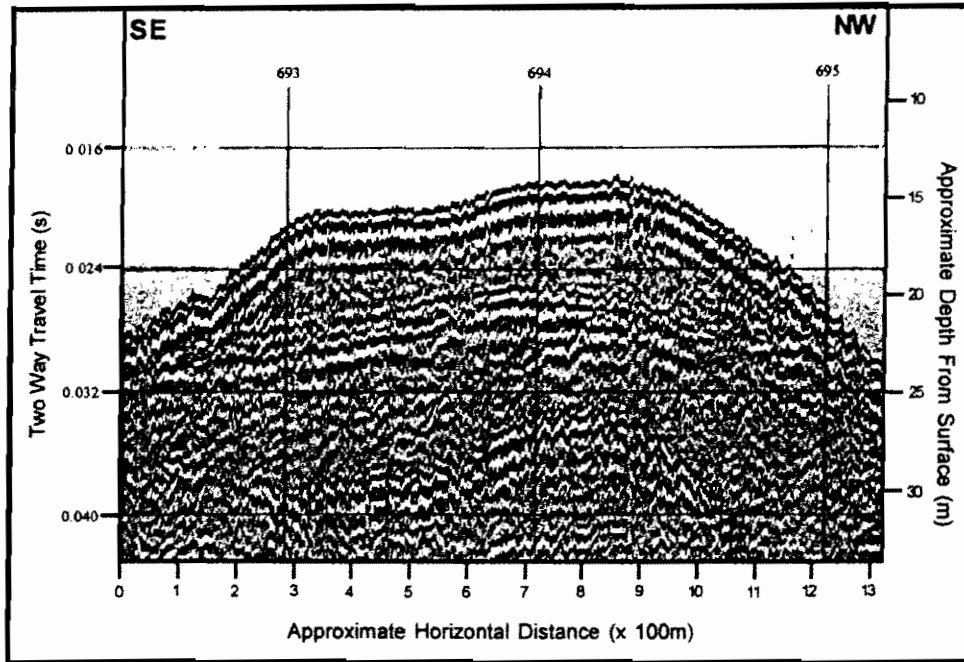


Figure 8. Multiple reflections occur when the returning acoustic wave reflects off of the air/water boundary and back to the seafloor, creating a repetitive reflection at twice the amplitude and depth as the original reflection. Multiple reflections can be produced at any strongly contrasting acoustic boundary such as the seafloor and the S_2 boundary (from seismic line T1-13N).

New wavelets are apparent in the seismic record when the distance between seismic interfaces are at least half the wavelength apart:

$$1.70 \text{ m} \times 0.50 = 0.85 \text{ m}$$

This means that the maximum theoretical vertical resolution which can be observed on the seismic records will be just under 1 m when using a 1.0 kHz profiler. Vertical precision of the reflections (time and depth position) of the ORE GEOPULSE™ system is:

$$\begin{aligned} \text{Vertical Precision} &= \text{Pulse Length} \times \text{Sediment Velocity} \\ &= 64 \text{ microseconds} \times 1700 \text{ m/s} \\ &= 0.109 \text{ m.} \end{aligned}$$

The surface wave motion affecting the catamaran and hydrophone array cause static offsets of the seismic traces of up to 0.5 ms, which at (1500 m/s)/2 is +/- 0.375 m. This causes a significant lack of precision and resolution of data.

Seismic Analysis

Seismic sequence and facies analysis is a method of inferring lithologic composition and structure in the subsurface through the use of seismically derived images. It is most effective when used in association with core control data. Acoustic reflections are generated at boundaries of density or velocity contrast which often parallel geologic boundaries such as bedding planes, faults, and erosional surfaces. Rocks which lie stratigraphically above such surfaces must be younger than rocks which lie below those

surfaces (at a given location) unless tectonic events have inverted the stratigraphy (Vail et al., 1977; Christie-Blick et al., 1990). In the case of shallow sediments on the New Jersey continental shelf, such vertical relationships will exhibit valid chronostratigraphic patterns.

Seismic sequence analysis identifies stratigraphic units which are genetically related and which are bounded by unconformities or their correlative conformities (Vail et al., 1977; Van Wagoner et al., 1987; Posamentier and Vail, 1989). Unconformities are recognized by the oblique termination of seismic reflections along the unconformity surface (figure 9). Unconformities create differing relationships with the bounding sequences depending upon the geometrical termination pattern of the seismic reflections. Reflections which terminate against an underlying boundary are defined as stratal onlap or downlap. Onlap and downlap refer to the direction of termination with respect to the underlying surface; onlap terminates updip, whereas downlap terminates downdip (assuming non-juxtaposed sediments). Reflection patterns which terminate against an overlying surface with a tapering relationship are defined as toplap; this pattern often indicates bypassing of sediments on a prograding shelf. Angular termination of parallel reflections indicates erosional truncation of sediments. Toplap can occur without truncation where sediments contribute to a prograding sedimentary wedge which builds outward without eroding the underlying sediments (Christie-Blick et al. 1990).

These stratal relationships often change with distance along the associated boundary surface, particularly if the boundary surface is non-erosional. In sections with erosional boundary surfaces, the surface of erosion must often be inferred from the termination patterns since not all unconformities generate acoustic contrasts between the bounding lithologies. Because unconformity boundaries may have changing lithologies

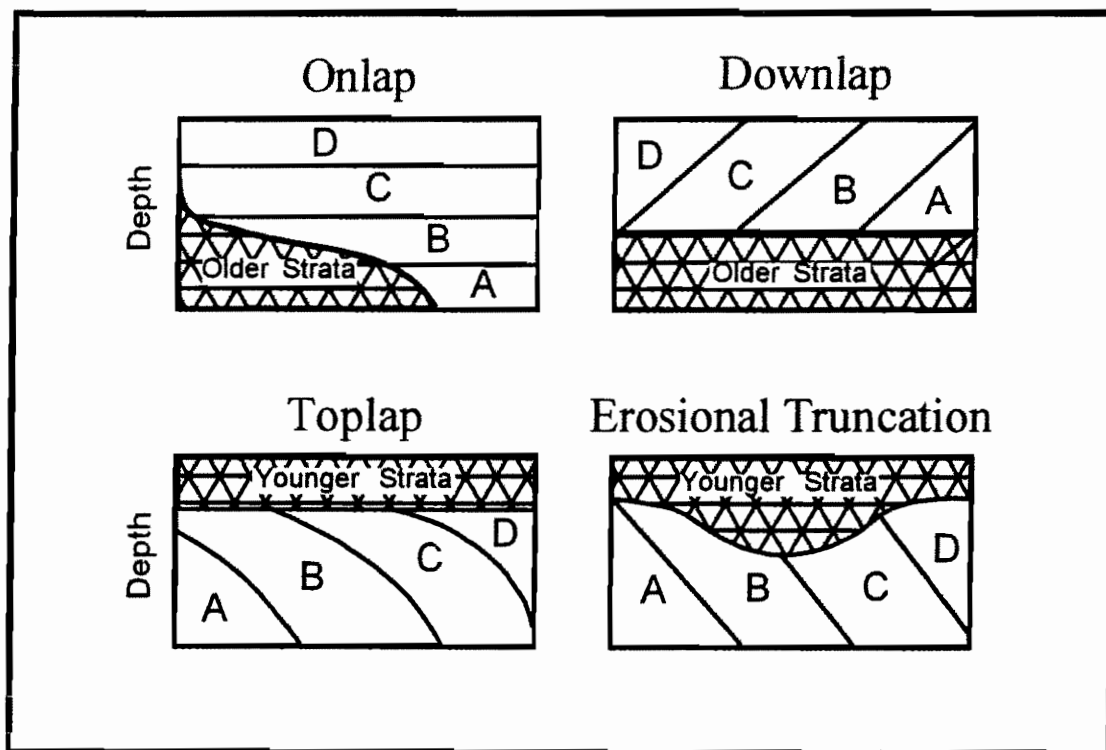


Figure 9. Sedimentary relationships of seismic reflection patterns which help to define seismic sequences (after Christie-Blick et al., 1990).

along their length (and hence changing impedance contrasts), unconformity reflection horizons may be discontinuous in profile (Vail and Todd, 1981).

Analysis of seismic profiles allow the following interpretations to be made regarding the stratigraphy and structure of the subsurface:

- 1) definition of genetically related depositional units;
- 2) relative time correlations of the depositional units;
- 3) general paleobathymetry of the depositional units;
- 4) thickness, areal extent, and relief of depositional units;
- 5) seismic cross-section;
- 6) Three dimensional or topographical map reproduction of some buried surfaces (unconformity, fault).

Continuously collected seismic data permits the creation of objectively defined tie-lines between core locations and will often allow 3-dimensional geologic structures to be inferred with a high degree of confidence. When seismic data are combined with lithological borings, the architectural elements which comprise the seismic sequence can often be matched with the core lithologies, which in turn may relate directly to the mode of deposition and the depositional environment. By tying together discrete lithological borings with continuous seismic sections, stratigraphy can be correlated across a large region. Examination of local seismic sequence patterns and core lithologies may aid in the determination of depositional settings and can allow inferences to be made concerning which lithological pattern is expected in similar, localized areas.

RESULTS

Bathymetry

Bathymetric topography was obtained by digitizing water depths at known positions along each seismic line and entering the data into Surfer™ Surface Mapping System software. Data were digitized at the 5 minute fix positions along the lines, at changes in depth, and at structural changes in between. Depths were adjusted to agree with tie points of lines. The data were contoured for mathematical best fit using fixed point triangulation with linear interpolation methodologies, applying maximum smoothing to the resultant contours. The mathematically generated surface contours were then compared with the actual seismic records along each traverse to ensure consistency with the original data set, applying corrections to the contour lines as required. This technique provides an objective basis for the contouring of a large data set while allowing interpretation and correction into the final product.

The bathymetric surface was reasonably consistent using both linear interpolation and kriging methods, but linear interpolation limited the generated surface to only that area enclosed within the seismic grid, and so was used as the starting method. The adjusted surface shows a gentle, southeasterly sloping continental shelf of small relief (figure 5). The shelf contains a series of northeasterly trending, shore-oblique linear sand ridges with deep swales surrounding some of the ridges. Sediment thickness above the regional (S_2) unconformity correlates well with the sand ridge locations (figure 10). In the northern region, Avalon Shoal sand ridge is located approximately 11 km (6 nm) offshore of Sea Isle City, New Jersey. It is approximately 6.5 km long and 2.1 km wide at its widest point, oval in shape, and oriented N30 E (figure 11). Avalon Shoal is

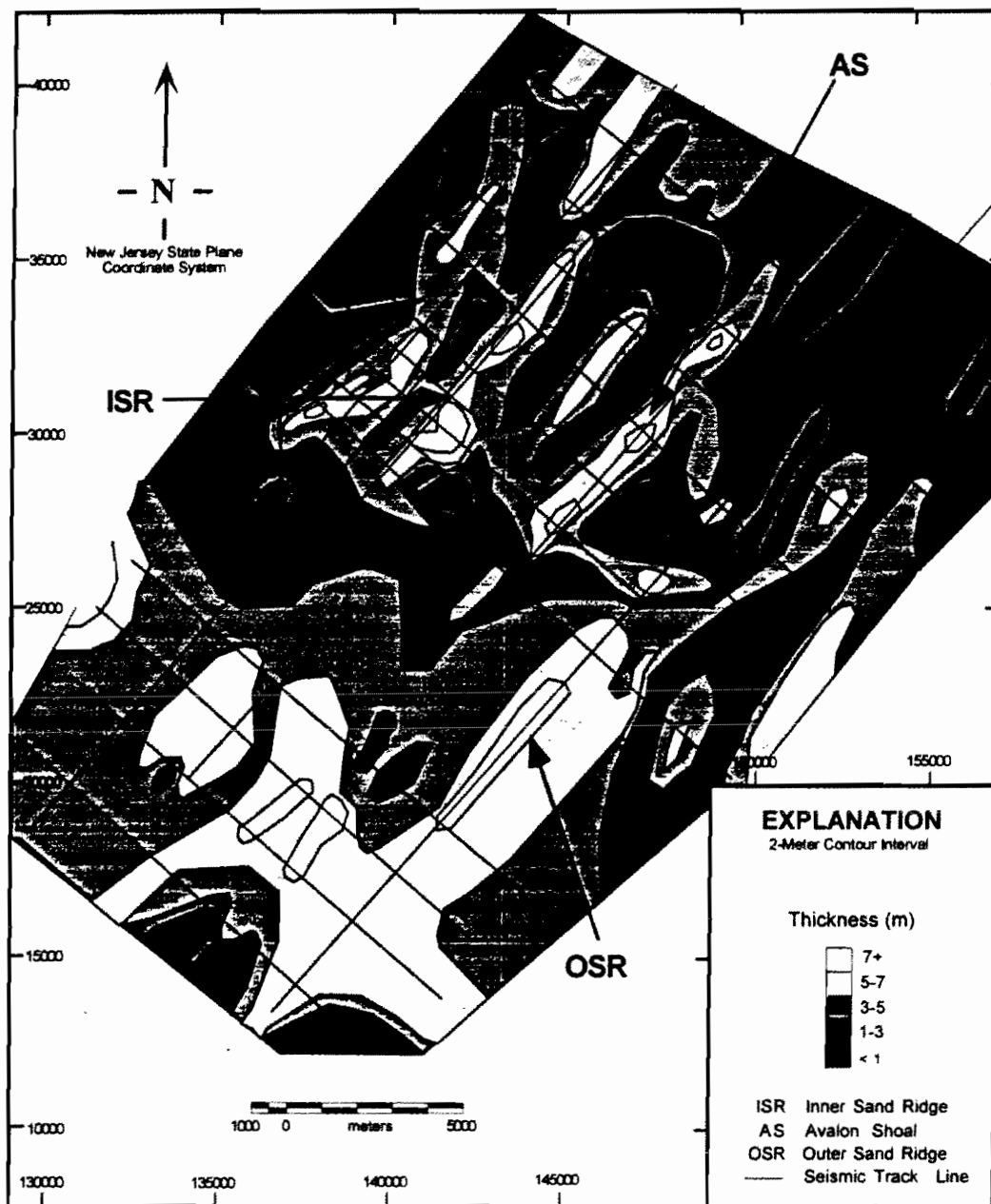


Figure 10. Sediment thickness above the S_2 unconformity closely parallels the regional sand ridge system. The thickest concentration of sediment exceeds 8 meters in thickness but lies in the seaward portion of the central/southern area (OSR), far from remediation sites and at undesirable water depths (>20m). Avalon Shoal (AS) and the inner sand ridge (ISR) contain sediment of up to 7-m thickness and are located closer to remediation sites and at more desirable water depths. The seismic track lines shown in this figure represent the portion of the lines with data usable for generation of isopach contours.

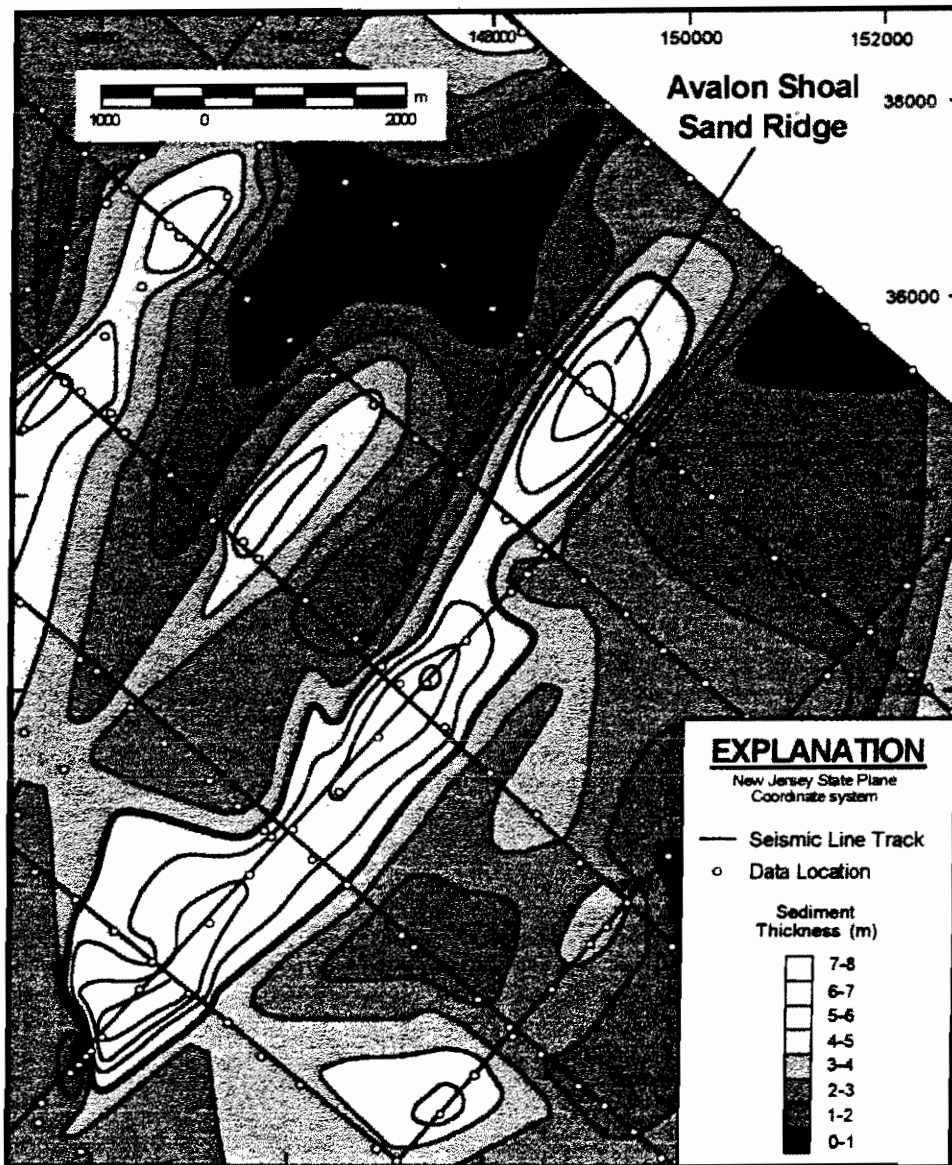


Figure 11. Sediment thickness above the S_2 unconformity in and around Avalon Shoal sand ridge, located approximately 7 miles off of Avalon, New Jersey (Figure 5). The sand ridge is an important source of sediment within the study area, containing over 35 million cubic meters of beach quality sand. Water depths over the shoal are generally less than 10 meters (30 feet). The southern end of the ridge appears to be an area of active erosion, and had very strong currents reported by divers during the seismic cruise. Bold line (5-meter thickness) approximates the surface expression of the sand ridge.

asymmetrical in axial cross-section, with a gradual slope beginning at the northeast end and abruptly terminating at the southwestern end. Divers who investigated a portion of Avalon Shoal during the seismic cruise reported strong currents moving around the southern end of the ridge. Preliminary data from the LEO-15 shelf current study on the southwest side of a nearby sand ridge (39.4615 N, 74.263 W; figure 2) also confirm the existence of very strong (>20 cm/s) cross-shore and along-shore currents in similar water depths (Glenn and Henderson, 1991, 1992, 1993, 1994).

A second sand ridge (Inner Ridge) is located approximately 5 km (3 nm) offshore of Sea Isle City, New Jersey (figure 5). It is approximately 3.8 km long and 3.3 km wide at its widest point (figure 12). A broad, low sloping sand plain extends away from the sand ridge along its southeastern side. Though exhibiting less relief than the axial portion of the sand ridge, the sand plain is prominently elevated above the surrounding topography. Another smaller sand ridge (Boundary Ridge) is located west of the Inner Ridge along the New Jersey 3-mile jurisdictional boundary. At depth, it is part of the same sediment structure as the Inner ridge due to a thin (1-3 m) connecting layer of sediment, but surficially appears to be a separate, disconnected sand ridge. Because portions of this ridge fall within state waters, it is not considered a potential candidate for offshore mining.

Investigation of the southern area was intended to fill a data gap in pre-existing seismic and coring operations along the New Jersey coastline, as well as to provide both seismic and stratigraphic continuity with the northern region. A small ridge lies approximately 5 km (3 nm) southeast of Avalon, New Jersey in the southern region (figure 5). This ridge is approximately 5 km long and 2 km wide, with similar sand accumulations and morphology as the northern area's inner ridge. A thick and extensive accumulation of

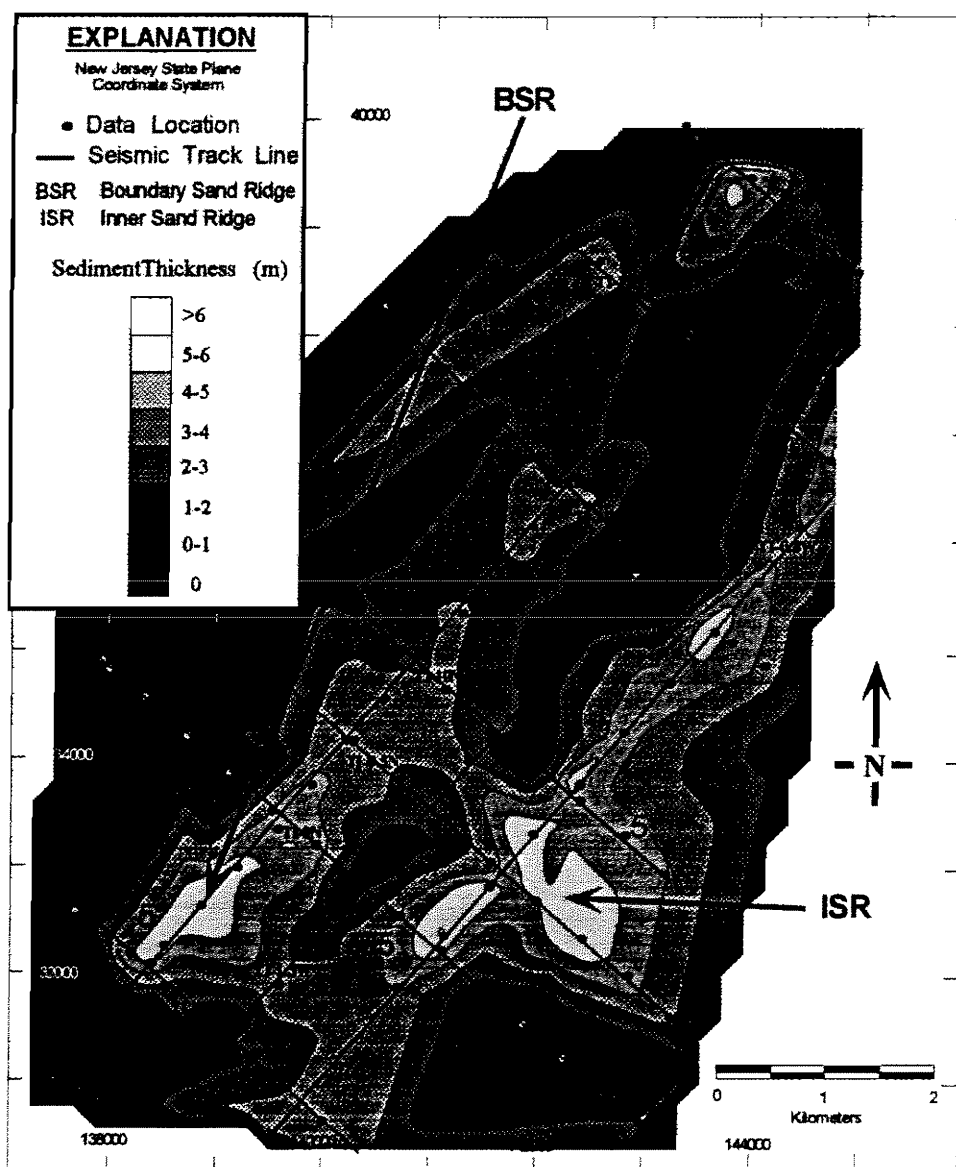


Figure 12. Sediment thickness above the S_2 unconformity in the vicinity of the inner sand ridge, located approximately 4 miles off of Avalon, New Jersey (figure 4). Water depths over the shoal are generally less than 10 meters (30 feet). Sand ridge sediment grades into similarly textured shelf sediment and is not confined to discrete locations, complicating volume calculations. Confining the calculations to the approximate surface expression of the sand ridge yields a volume estimate of approximately 48 million cubic meters of usable sediment. The surface expression of the inner ridge is approximated by the 5-meter isopach.

sediment lies further offshore in the southern region (figure 5), including a thick, linear sand shoal between the northern and southern areas. These southern area sediment accumulations lie at greater water depths than the northern ridges (often >20 m), which make them less desirable targets for mining activity.

Overall, the average slope of the continental shelf within the study area is 0.00040, with a strike N7°E (figure 13). These data were based upon depth-to-seafloor measurements at 550 data points located along the 303 km of seismic line. Average slope was calculated using a polynomial regression algorithm (Surfer™ Surface Mapping Software).

Regional Seismic Stratigraphy

The regional composite seismic stratigraphy (figure 14) can be divided from oldest to youngest into 6 depositional units (T, P₁, P₂, H₁, H₂, H₃) which are separated by 4 unconformable surfaces (S₁, S₂, R₁, R₂). Two of the unconformable surfaces (S₁, S₂) represent sequence boundaries (as defined in van Wagoner et al., 1987) which are identified where arcuate to planar reflections terminate along surfaces of erosion (figure 9). As such, they are interpreted to represent surfaces which were exposed to subaerial and fluvial processes during past sea-level regressions. These sequence bounding unconformities generally produce very strong intensity, reverberatory seismic reflections, except when the acoustic signal degrades due to attenuation at depth.

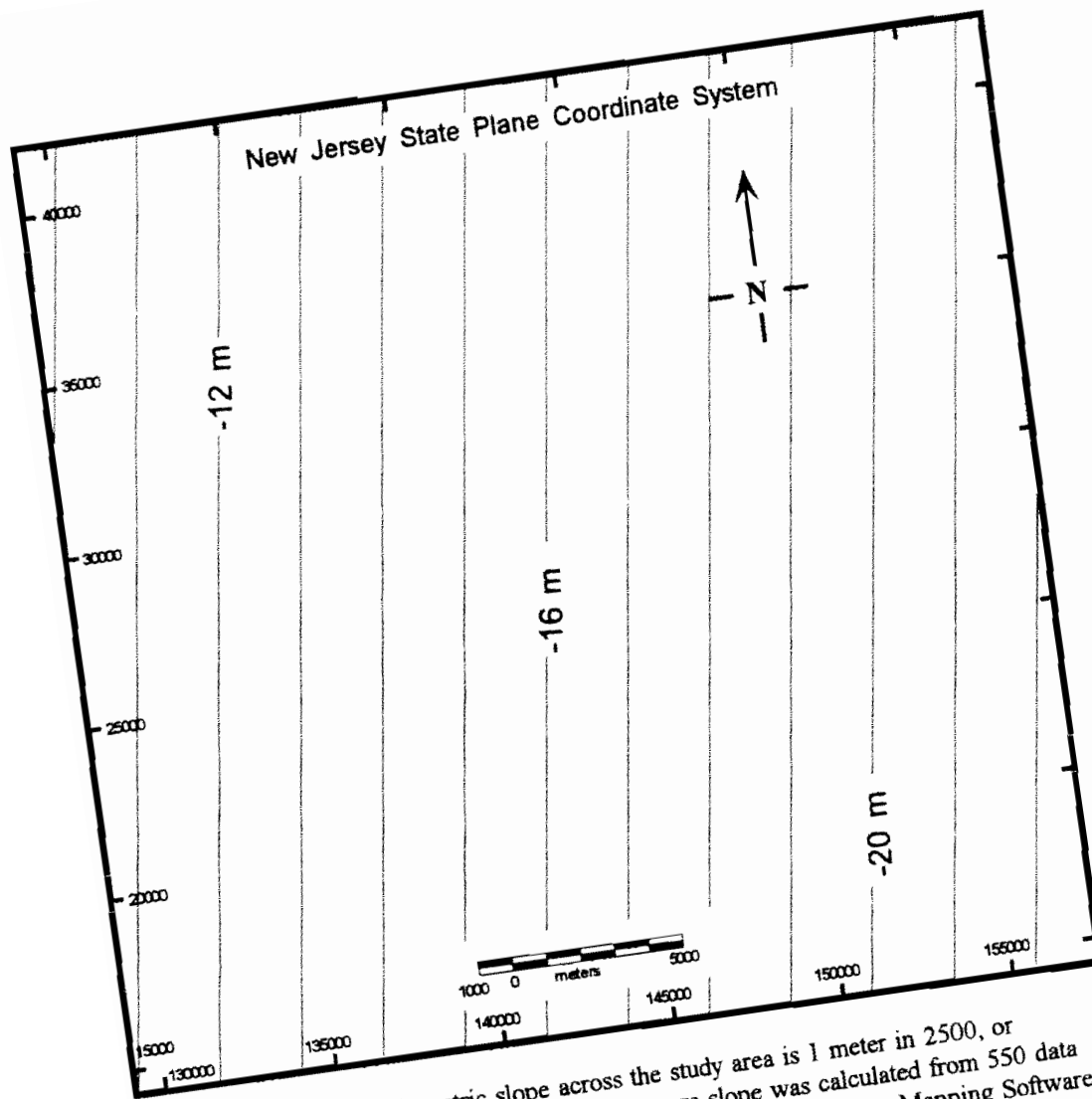


Figure 13. Average bathymetric slope across the study area is 1 meter in 2500, or 0.0004. Strike is N7°E, dip east-southeast. Average slope was calculated from 550 data points using a polynomial regression algorithm from Surfer™ Surface Mapping Software. Depth is shown relative to sea-level. Grid is in the New Jersey State Plane Coordinate System.

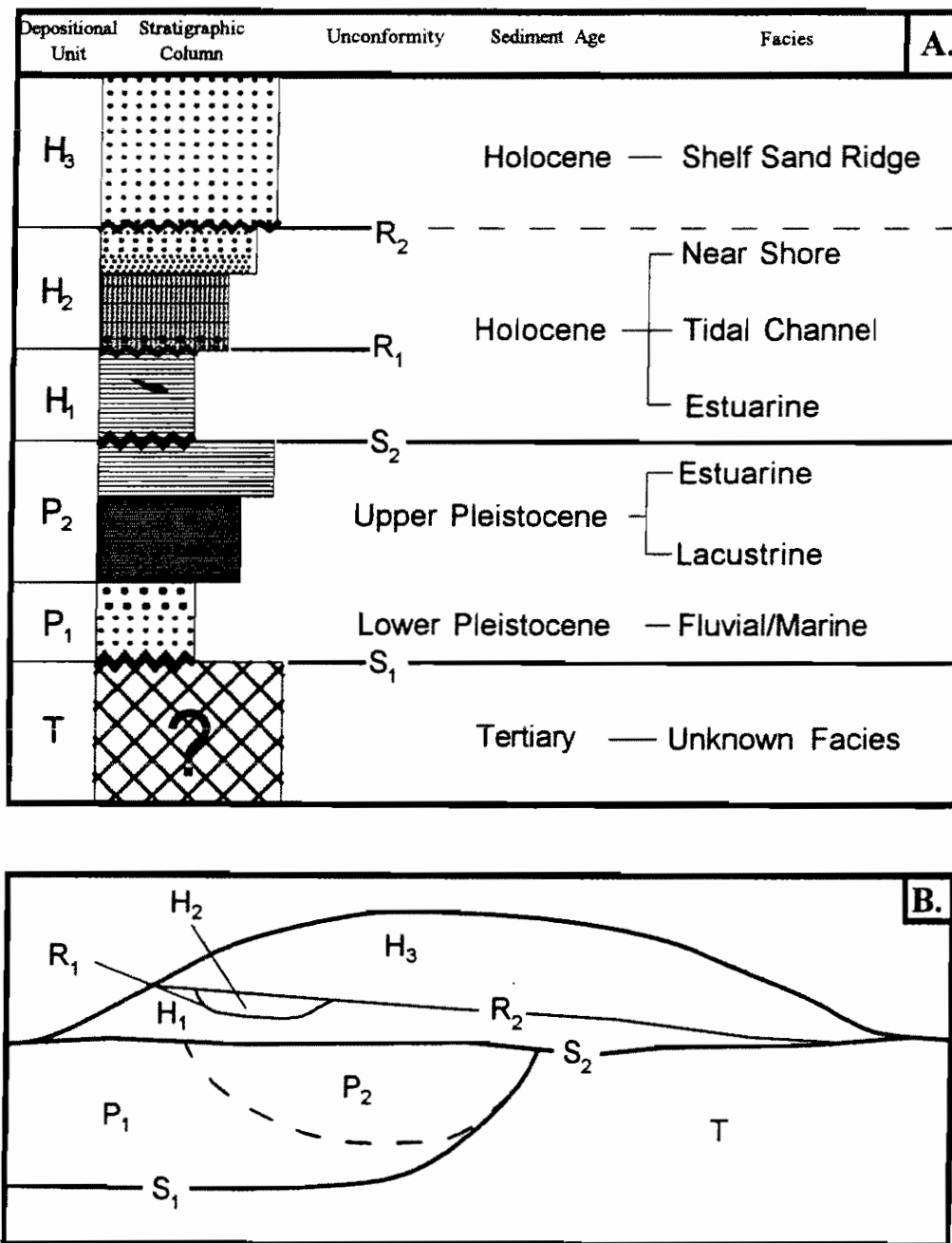


Figure 14. Composite regional stratigraphy of the study area. (A) Sediment type is indicated on the left. Tertiary (T) sediments were not recovered in core and are interpreted from seismic reflection data and data from other regional studies. Pleistocene shelf sediments (P₁ and P₂) vary from sandy gravel (P₁) to shell bearing mud (P₂ top). Holocene sediments (H₁, H₂, H₃) vary from sandy mud (H₁) to mud-depleted gravelly sand (H₃). Two regional unconformities (S₁ and S₂) formed as a result of fluctuating sea-level on the inner continental shelf. Localized unconformities (R₁ and R₂) formed as a result of channel migrational (tidal) ravinement and transgressive ravinement processes. Interpreted facies are shown on the right. (B) Generalized cross-section showing sand ridge (H₃), unconformities, and relative position of depositional units.

Unconformity Surfaces

S₁ Boundary

The lower sequence bounding unconformity (S_1) is variable in depth and relief. S_1 is regional in extent and is readily observable along some seismic profiles (i.e. TI-12N, TI-1N), although it is not reliably traced in others (i.e. TI-9N, TI-1.8E) (figure 4). S_1 locally exhibits deep (20 m), steep sided valleys, particularly in the southern region proximal to the shoreline (figure 15). It is locally truncated by the overlying regional unconformity (S_2) particularly where it exhibits a large degree of relief close to the modern seafloor (figure 16).

A contour map of the S_1 surface was not attempted due to its intermittent nature in the seismic profiles. Sporadic data will not provide meaningful topographic reproductions, particularly since it is often difficult to discriminate between S_1 and other strong reflections at depth. Locally observable channel incisions which form part of the S_1 surface along the shore-proximal portion of the seismic lines are described separately, below.

S₂ Boundary

The stratigraphically more recent unconformity (S_2) is traceable in seismic profile as a shallow, seawardly dipping reflection horizon of very low relief, which is regional in extent and continuously traceable over all of the seismic profiles (figure 16). S_2 often intersects the seafloor in erosional swales (figure 17), or where little sediment has been deposited (figure 18) and forms the underlying boundary beneath the regional sand ridges

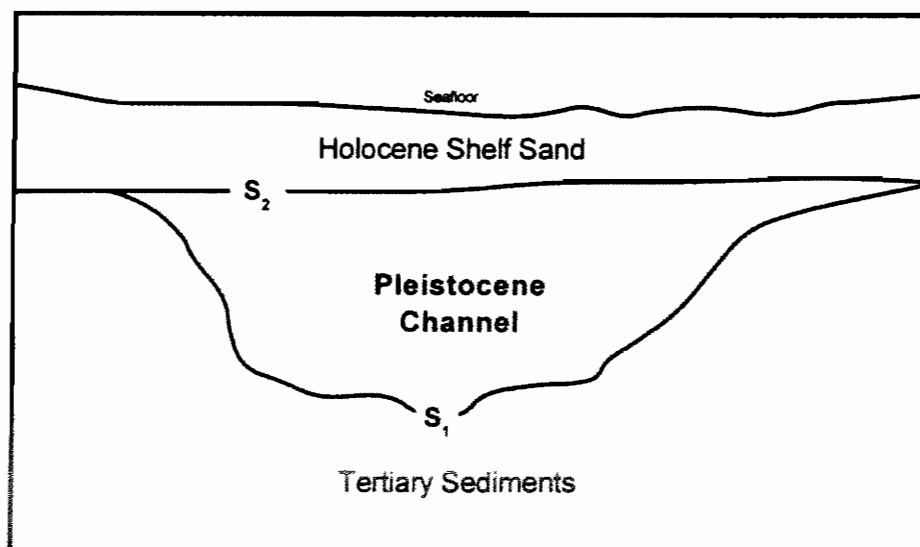
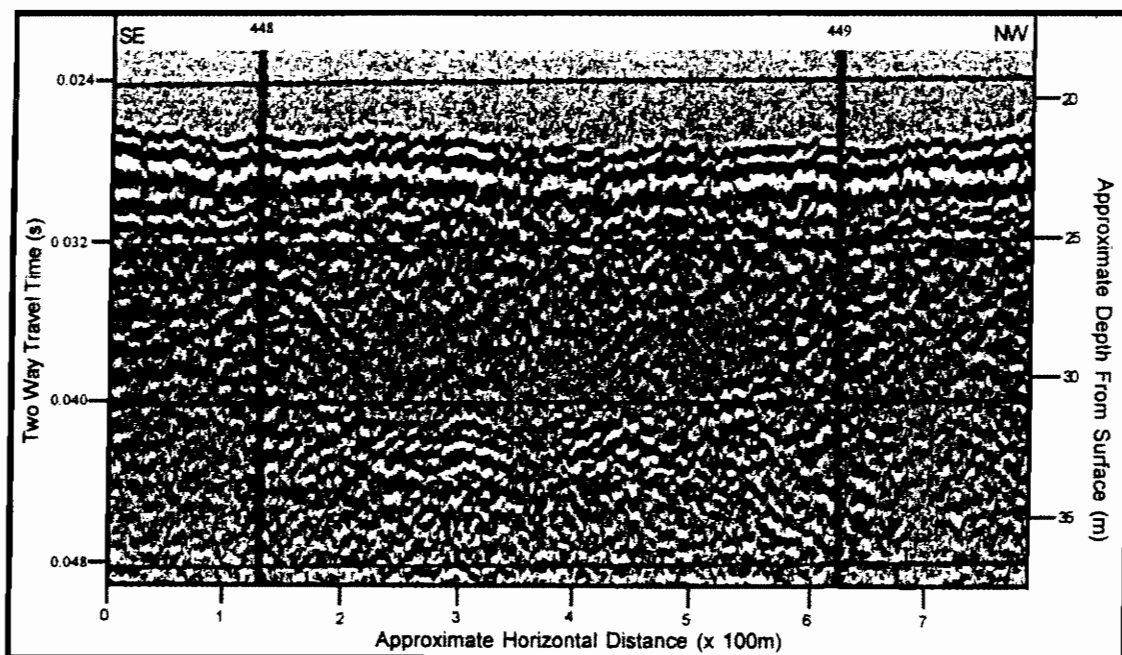


Figure 15. S_1 exhibits steep, deeply eroded valleys which lie close to the modern shoreline. The valley depicted is approximately 8 meters in depth (26 feet) and has been truncated by S_2 (from seismic line TI-4N).

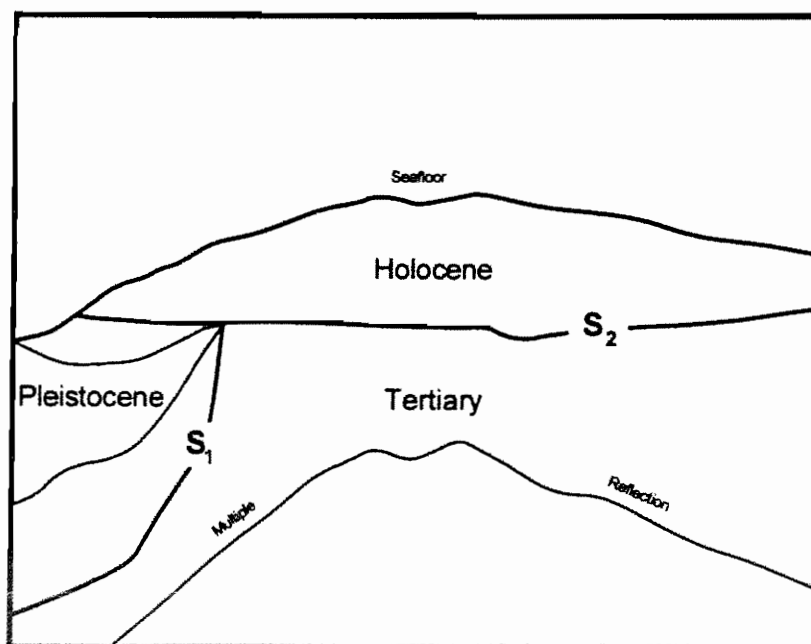
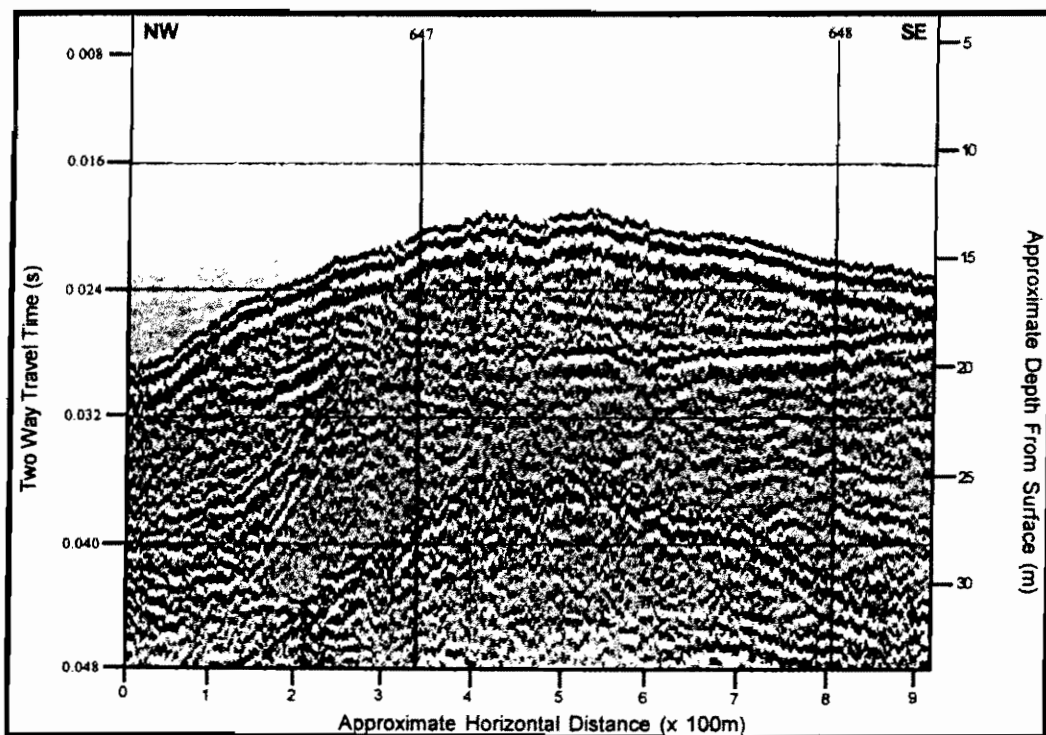


Figure 16. Termination of reflections along a surface of erosion. S_2 overlies and truncates S_1 where S_1 is close to the modern seafloor. The S_2 surface is present over the entire study area and marks the sequence boundary separating Holocene age sediments from older sediments. Interpreted age of sediments is shown relative to typical stratigraphy in the study area (from seismic line TI-12N).

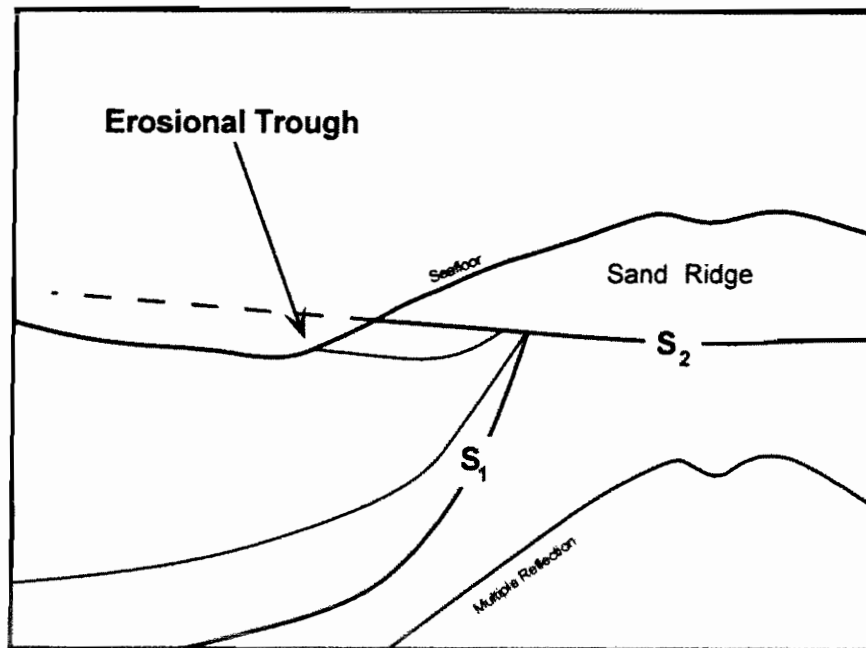
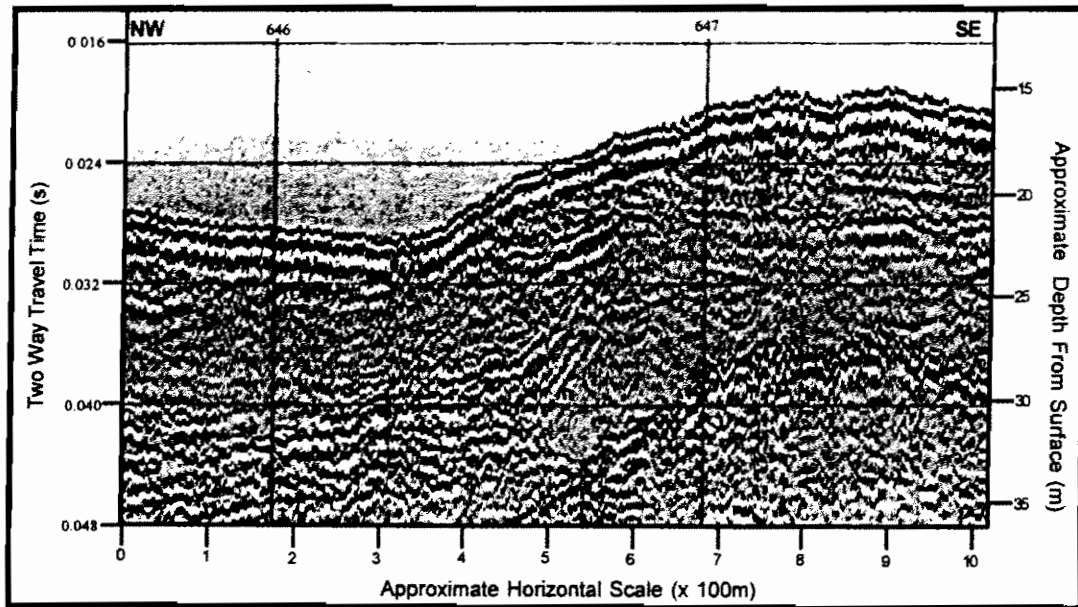


Figure 17. S_2 Erosion at the periphery of some sand ridges has exposed sediments from beneath the S_2 unconformity. This type of erosion suggests that dynamic processes continue to modify the inner continental shelf (from seismic line TI-12N).

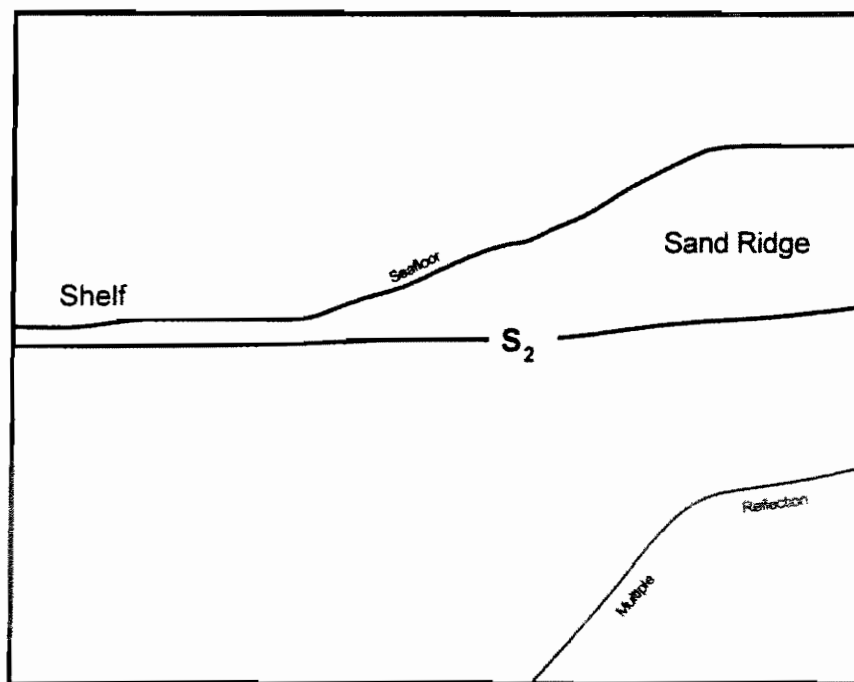
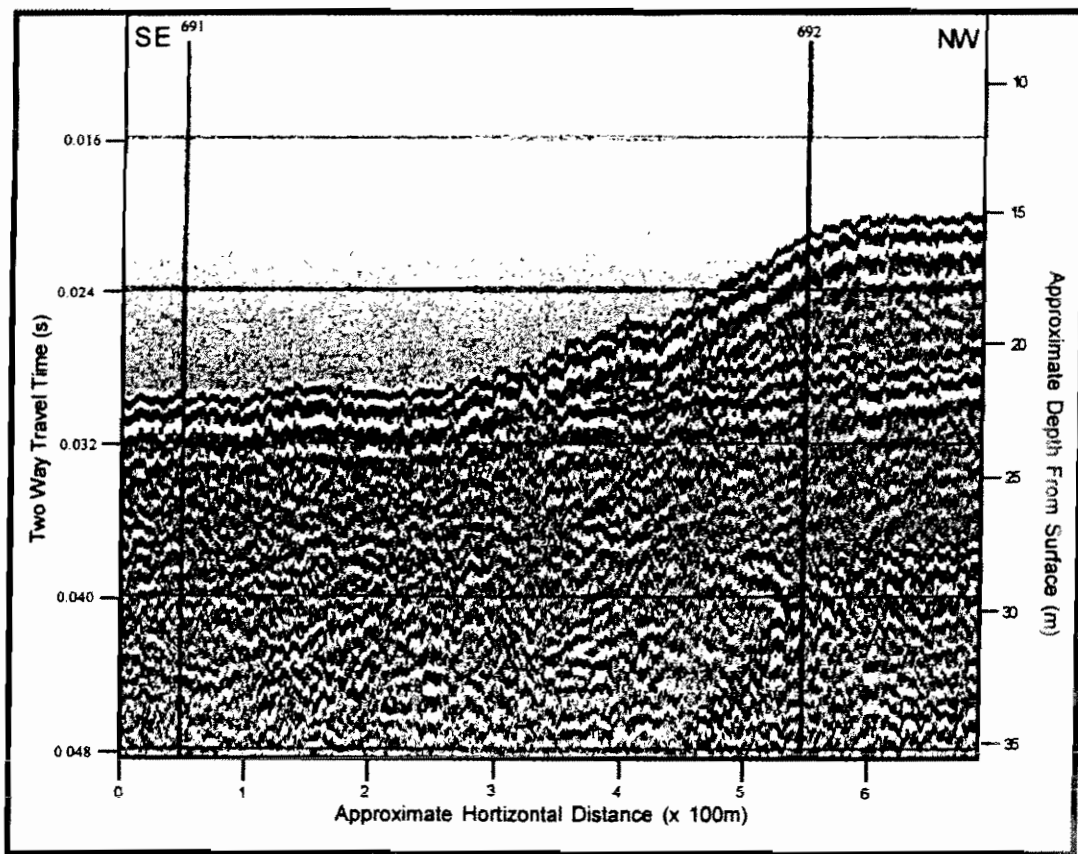
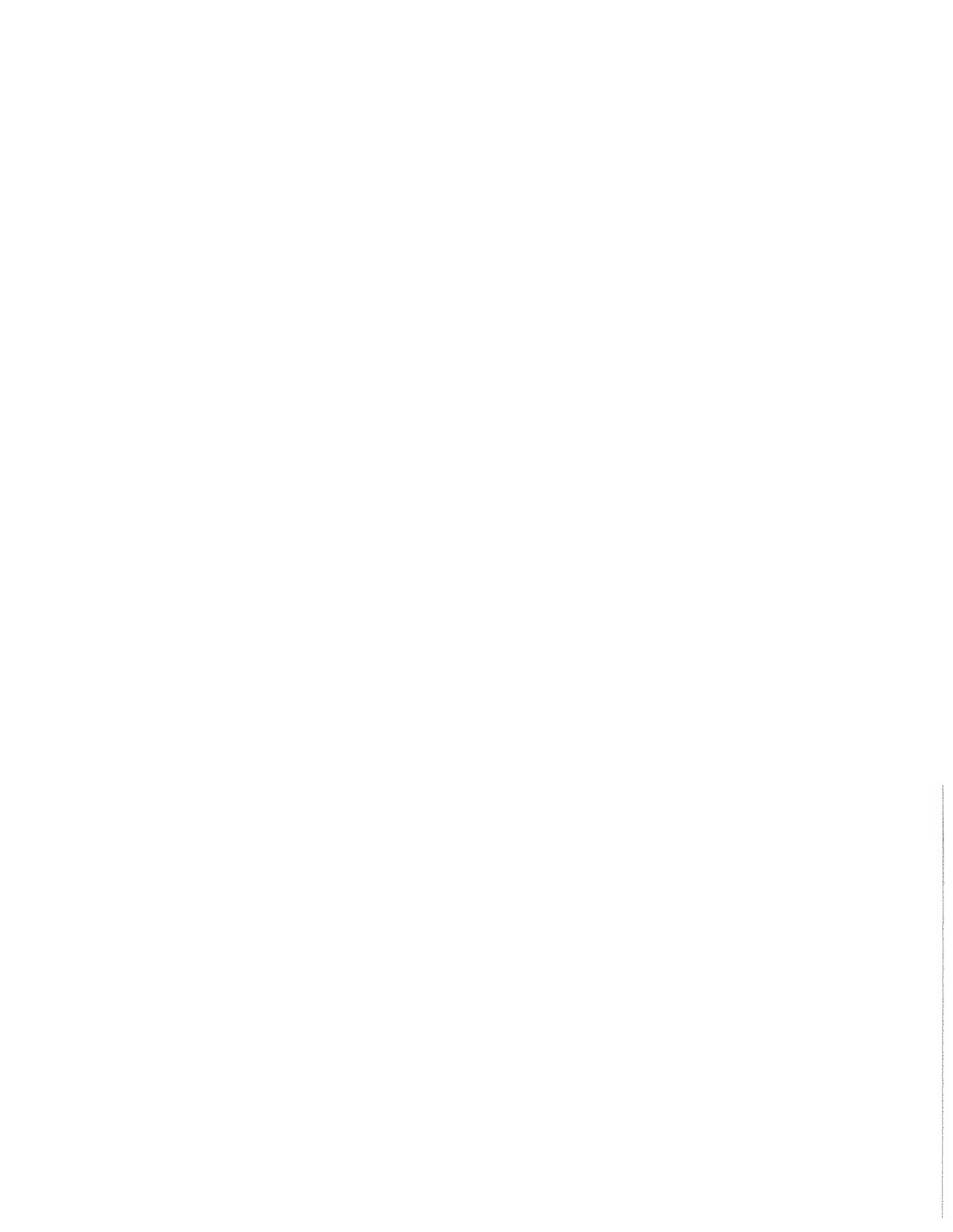


Figure 18. S_2 merges with the sea-floor at the periphery of sand ridges where there has been little deposition subsequent to its formation (from seismic line TI-13N).



(figure 19). Scouring of the seafloor has eroded through S_2 in places (determined using core analysis in conjunction with seismic sections), although it is very difficult to determine where S_2 has been penetrated from the seismic data alone. Lithologically, S_2 is usually underlain by extremely coarse, low mud sediment and overlain by fine sediment with a high percentage of mud, or (rarely) by mud-depleted sand ridge sediment. This lithological pattern is areally consistent at the S_2 unconformity, and results in an intense seismic return signal by presenting a very strong acoustical impedance contrast across the S_2 boundary surface. In addition, the existence of a regionally consistent lithology underlying the S_2 unconformity helps to determine whether shelf erosion has penetrated the S_2 unconformity surface. At core locations where the very coarse sedimentary deposit which normally underlies the S_2 surface is missing, shelf erosion subsequent to the formation of S_2 may be indicated.

Despite the relatively planar appearance of S_2 along seismic profiles, the surface exhibits several meters of relief across the seismic traverses. The average slope of the S_2 surface (figure 20) is very similar to the modern seafloor in both orientation and magnitude (table 2), although there is no indication of remnant shore-parallel sedimentary structures similar to the modern sea-floor sand ridges.

SURFACE	AVERAGE STRIKE	AVERAGE DIP
Seafloor	N7 E	0.00040
S_2	N21 E	0.00043

Table 2. Average strike and dip of the two upper surfaces in the study area.

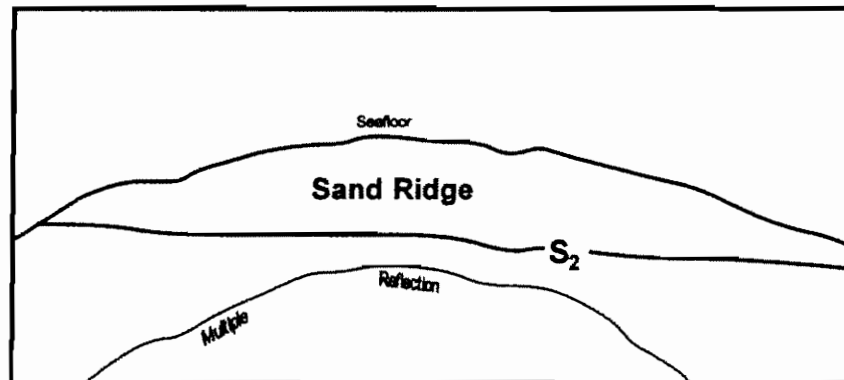
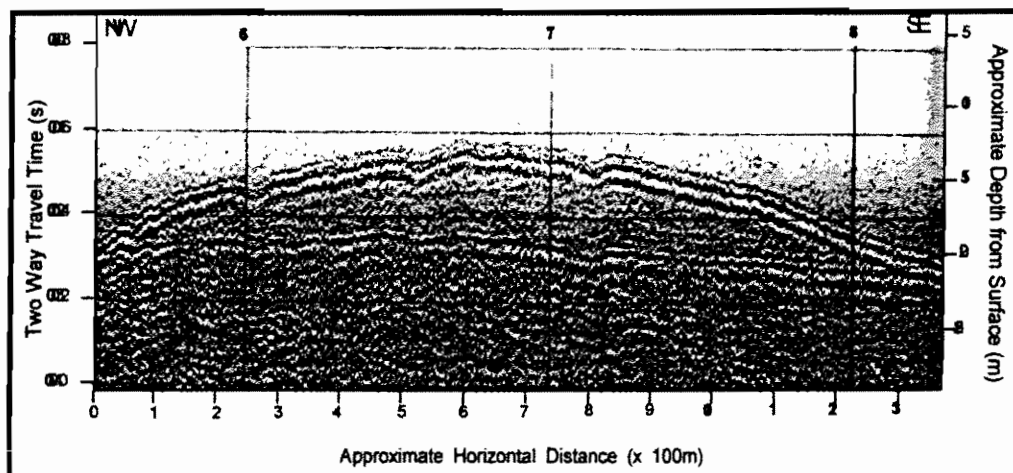


Figure 19. The S_2 unconformity underlies all sand ridges within the study area (image is from seismic line TI-9N).

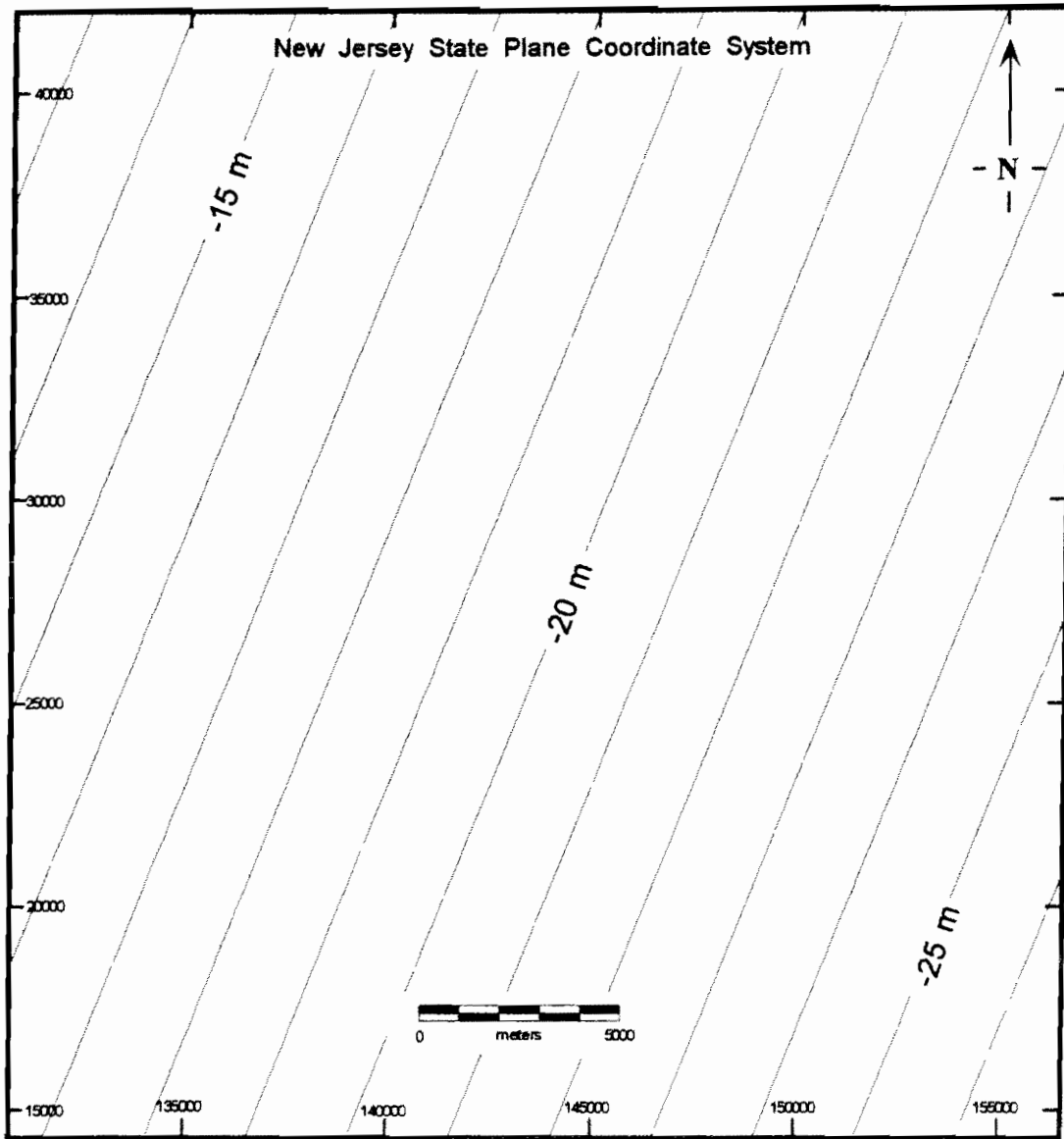


Figure 20. Average slope of the S_2 unconformity across the study area is 1-meter in 2350, or 0.00043. Strike is N21°E, dip southeast. Average slope was calculated from 550 data points using a polynomial regression algorithm from Surfer™ Surface Mapping Software. Depth is shown relative to sea-level.

Ravinement Unconformity

The third unconformable surface (R_1) is spatially discontinuous and non-resolvable in seismic profile due to its small lateral size and close vertical proximity to the R_2 surface. R_1 is identifiable in core as one or more layers of coarse, low-mud sediment which abruptly truncate muds and fine sands. In section, coarse sediment overlying the unconformity surface usually grades upward into interlaminae of fine sand and mud. R_1 is characterized by strong lithologic contrasts within estuarine-like sediments, and is usually found between the S_2 and R_2 surfaces.

The fourth unconformable surface (R_2) is discontinuous in seismic profile and variable in extent. The surface is represented by a planar, sub-horizontal to horizontal reflection which does not truncate other reflections in the seismic profiles, and is usually found within the relief of sand ridges between the S_2 boundary and the seafloor (figure 21). Examination of core sections which penetrate through R_2 (figure 22) indicate that it abruptly separates underlying very fine sediment from the much more coarse sand ridge sediment, suggesting that R_2 is truly erosional in character. Although R_2 would have originally been continuous across the study area, it is now only partially preserved within existing sand ridge structures. In addition, R_2 merges with, and is indistinguishable from, S_2 in regions where R_2 has eroded to the S_2 sequence boundary.

Depositional Units

Six depositional units are resolvable in seismic profile and correspond to specific environments of deposition as determined by sequence stratigraphic and sedimentological analysis (figure 14). The units are assigned a letter designator corresponding to their

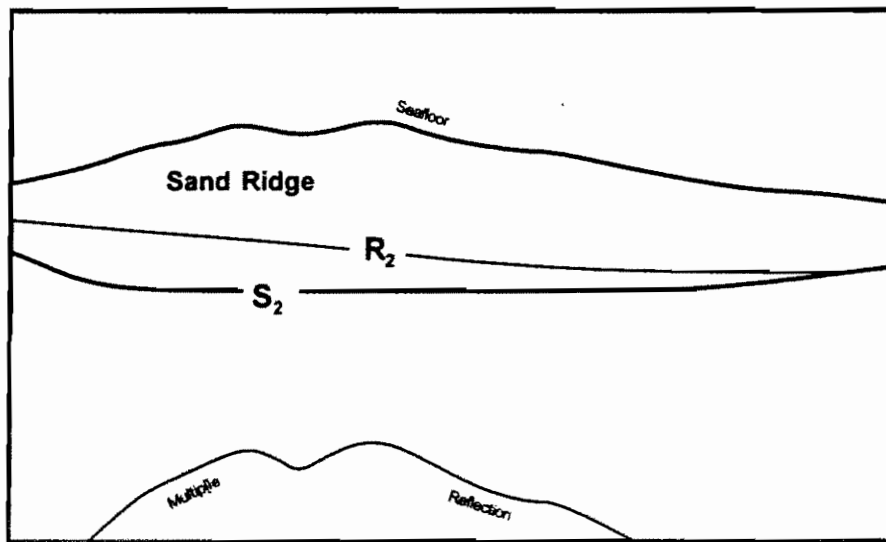
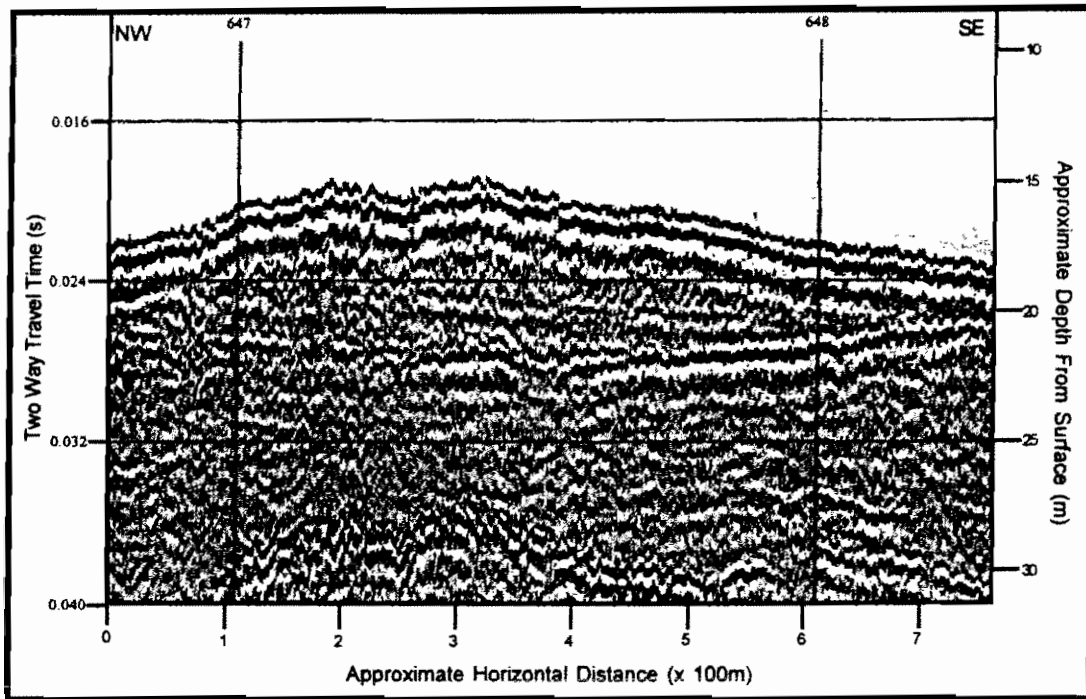


Figure 21. R_2 is a discontinuous surface of erosion formed by shoreface scour and retreat in a transgressive regime (ravinement surface). It is usually observable as a moderate to faint seismic reflection within the relief of sand ridges. Where it is found, it always overlies the S_2 unconformity (from seismic line TI-12N).

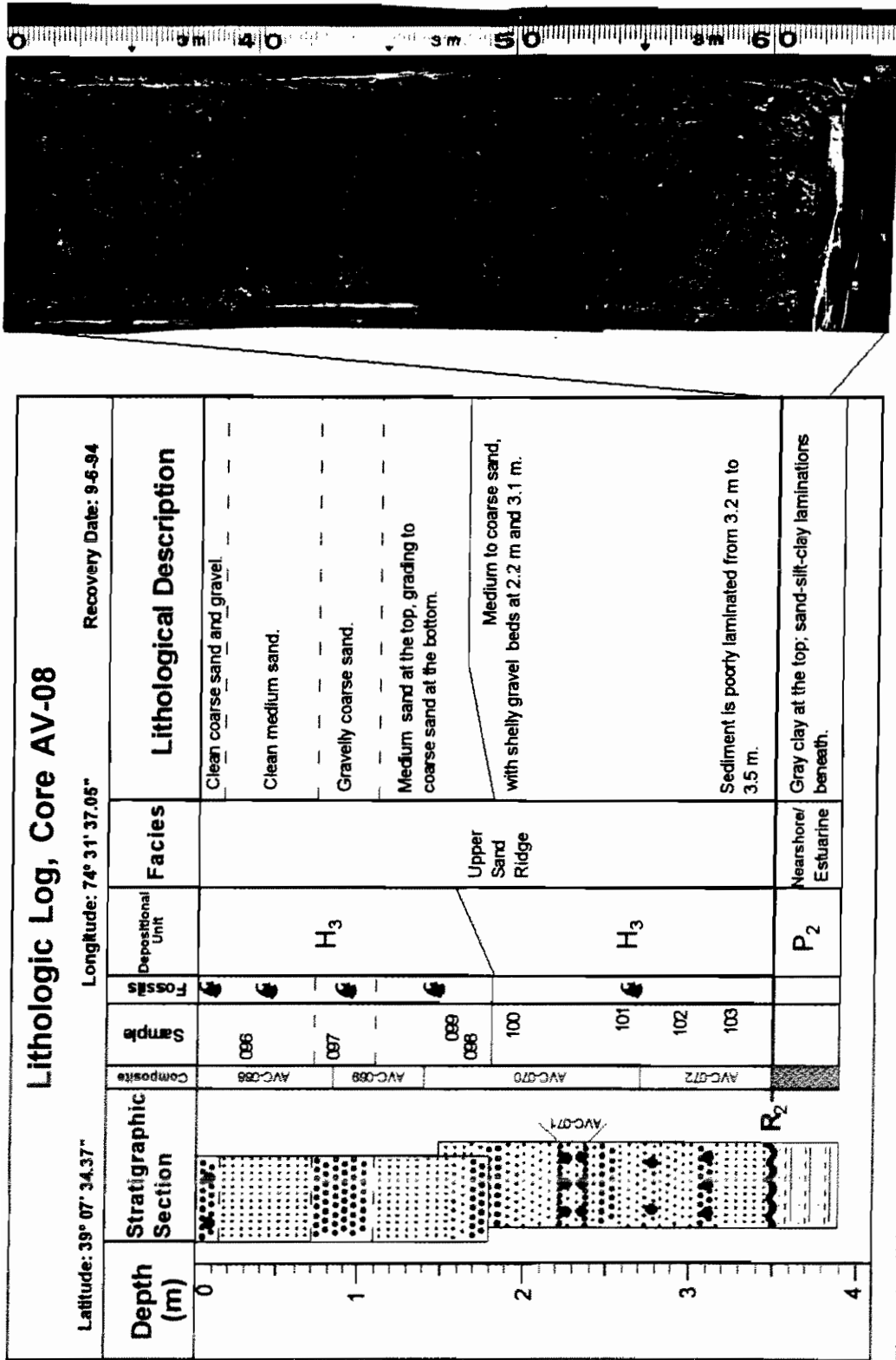


Figure 22. Within the study area, ravinement unconformities are best preserved at the base of sand ridges. Core AV-08 was drilled at the northern end of Avalon Shoal sand ridge on seismic line TI-1.8E, where it penetrated the ravinement (R₂) unconformity (figure 7). The ravinement unconformity separates the overlying coarse sand ridge sediment from fine grained estuarine and nearshore sediments, below. The photograph shows the unconformity at 3.5 meters below sea-floor.

inferred age of deposition (T=Tertiary, P=Pleistocene, H=Holocene) followed by a sequential subscript designator. T, P₁, P₂, H₁, H₂, and H₃ and are listed in relative temporal and stratigraphic order from oldest to youngest. Representative sediments were recovered in cores from each unit except T.

One or more of the units may be missing along a given seismic traverse or at a specific core location. To better explain how environments of deposition were determined for each unit and to develop a conceptual model of their development, each unit is completely described in the following sections using sequence stratigraphic concepts, sedimentological analyses, and lithostratigraphic relationships to the other units.

Depositional Unit T:

Depositional unit T underlies the discontinuous, generally deep (>40 m below sea-level) unconformity S₁. Seismic reflection patterns from beneath S₁ are variable in intensity and pattern, from very strong, parallel to slightly arcuate single reflections to ovalar regions of acoustical transparency which may represent concentrations of methane gas within fine grained sediments. Many deep reflections are obscured by the multiples, which makes interpretation of the reflections less certain. No core reached the T sediments, but based upon lithological descriptions from the U.S. Geological Survey Marine Observation Well 2 off of Atlantic City, New Jersey, T sediment is most likely a variety of silty marine muds which are interbedded with sand and gravel layers (Mullikin, 1990).

Depositional Unit P_1, P_2 :

P_1 and P_2 underlie the S_2 unconformity over most of the study area, except in restricted regions where older, high-relief Tertiary sediments crop out against the S_2 surface. Slightly arcuate, concave upward reflections of variable intensity characterize P_1 immediately beneath the S_2 surface (figure 23). Arcuate reflections extend down to approximately 15 m beneath the unconformity, and can be seismically traced for several kilometers. Some reflections terminate against stratigraphically higher arcuate reflections while others terminate at depth (25-40 m b.s.l.) against a very intense, sub-parallel reverberatory reflection horizon (S_1) (figure 24).

P_1 is composed of very coarse sand, gravel and pebble sediment which overlies a well sorted sandy sediment (figure 25). Most of the sediment which was recovered at the same depths as the seismic, arcuate reflections is very coarse, containing little to no fine grained muds other than a thin, white clay coating of the sediment grains. The white clay appears to be of kaolinitic composition. An intensely yellow, limonitic clay underlies the P_1 sediments (figure 26) at core AV-09 (figure 7). A micropaleontological search revealed no carbonaceous material, nor foraminiferal or diatomaceous organisms within the yellow clay. Other more coarse sediments with limonitic coatings are found in thin (>0.2 m) beds immediately underlying the white clay coated sandy gravels. These sediments lie close to the S_2 surface at core AV-04 (figure 7).

On seismic line TI-12N (figure 4), sub-parallel, steeply dipping, lateral clinoforms extend from the S_2 surface 15 meters in depth to the deep, planar S_1 surface (figure 27). 1.5 m of P_1 sediments were recovered from these clinoforms at core AV-11 (figure 7) and are composed of relatively clean sand and gravel with some burrow traces. This sediment

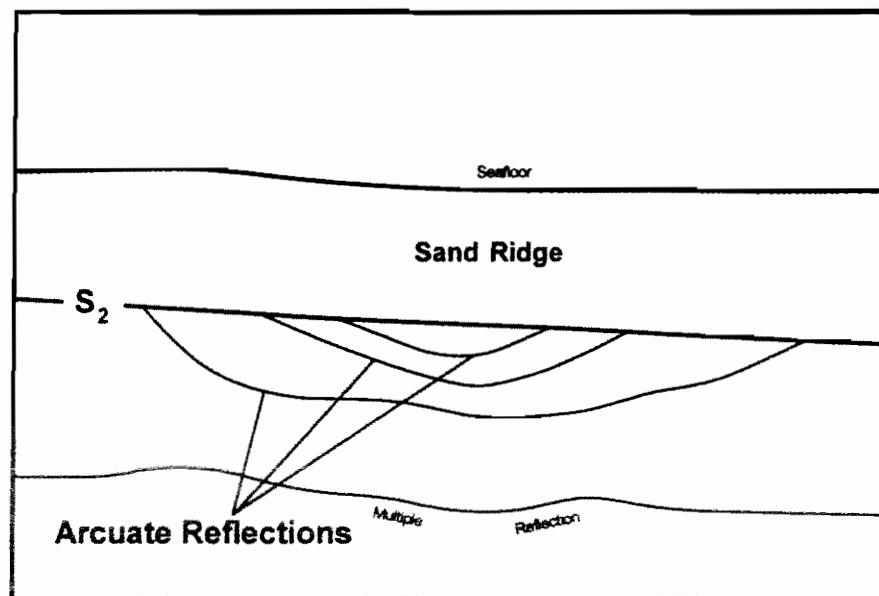
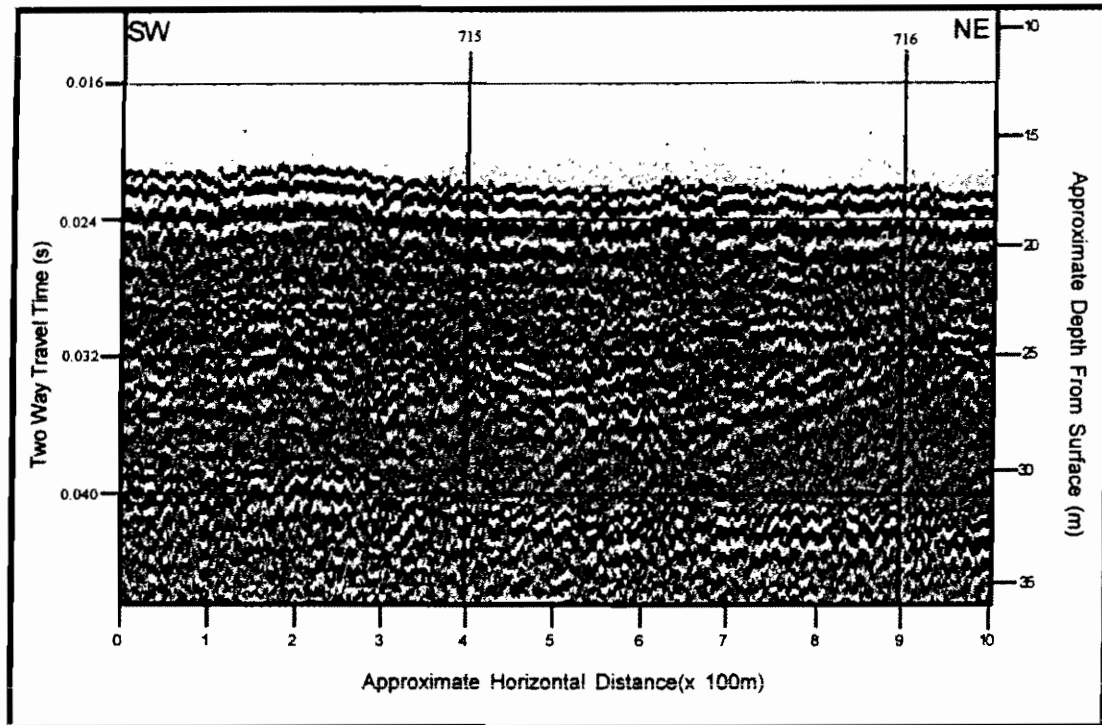


Figure 23. Slightly arcuate, concave upward reflections of medium to strong intensity underlie and are truncated by the S_2 unconformity (from seismic line TI-1.8E).

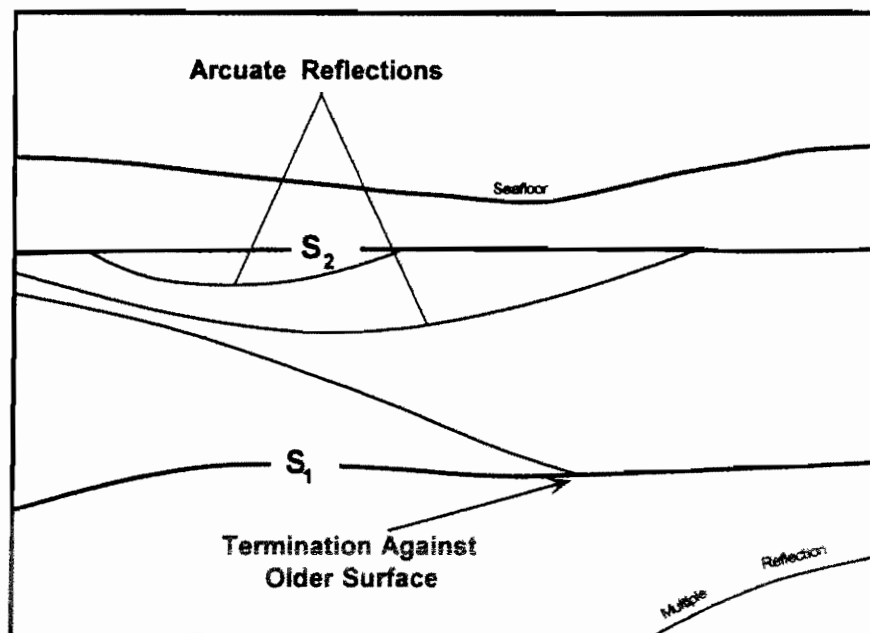
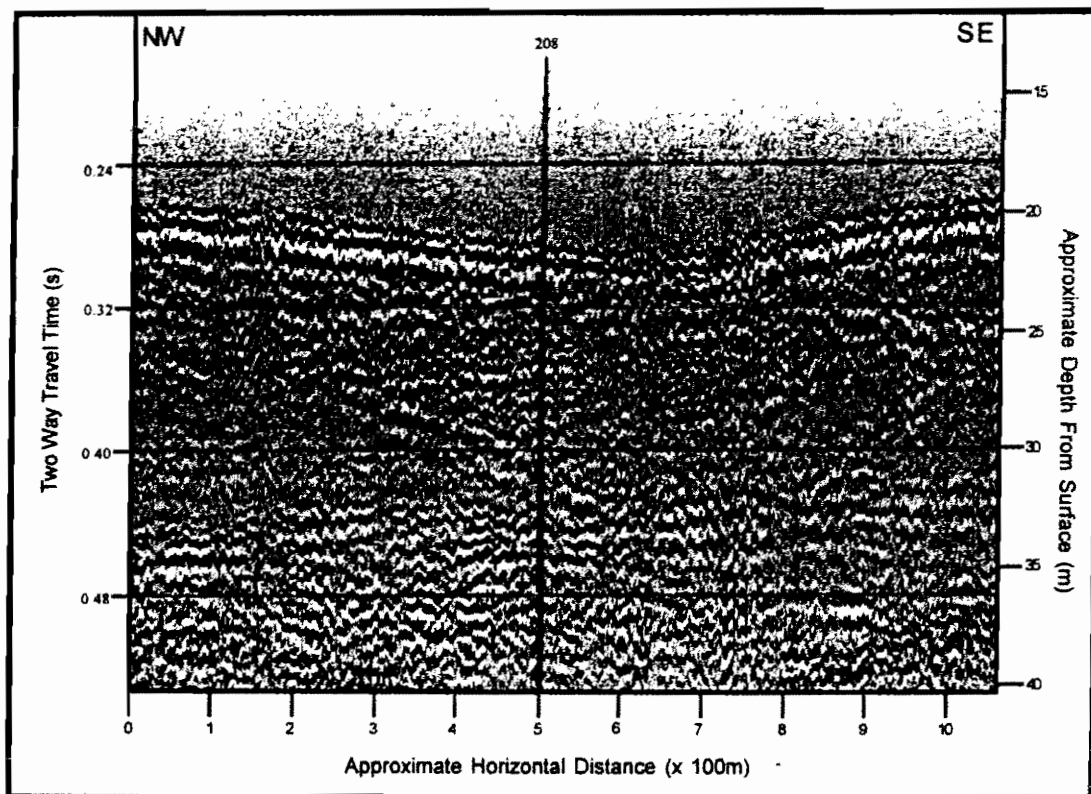
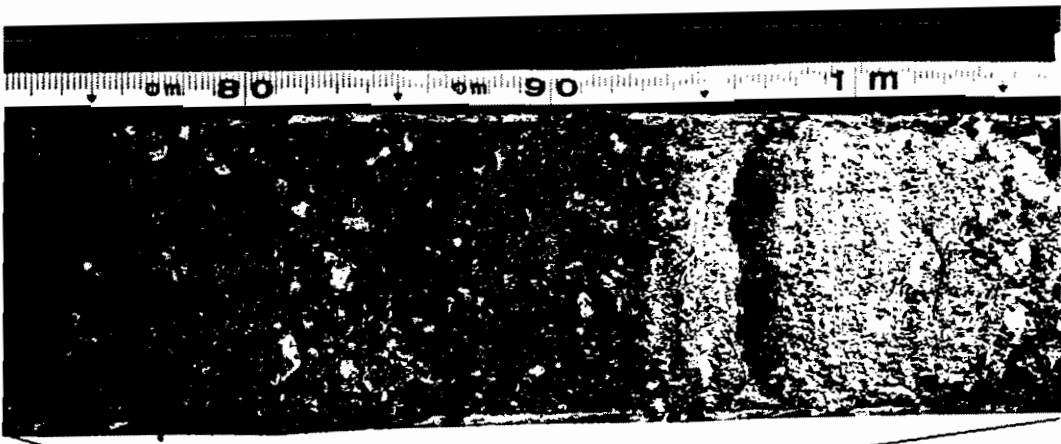


Figure 24. S_1 is often located at depth and can be resolved where reflections caused by bedding planes, lithological changes, and fault planes terminate against the surface. Often, a sharp amplitude change caused by a strong acoustic contrast is associated with the boundary. The surface morphology of S_1 could not be accurately determined, as the boundary was not consistently resolvable across the study area (from seismic line TI-14N).



Latitude: 39° 07' 39.22"		Longitude: 74° 36' 38.01"		Lithologic Log, Core AV-06		Recovery Date: 9-3-94
Depth (m)	Stratigraphic Section	Composites	Sample	Depositional Unit	Facies	Lithological Description
0			021	H ₃	Shelf Sand	Coarse sand and gravel.
			022	H ₁	Nearshore/Estuarine	Well sorted white, medium sand, heavy mineral laminae, and some pebbles toward the bottom.
			023	H ₂		Gravel and pebble (lag?) with v. coarse sand.
			024	H ₁		Interlaminated fine sand and mud; white and greenish sand at 0.57 m.
1	R ₂ ? S ₂	AVC-013	026			Muddy coarse gravel and pebbles, most coarse in center.
		AVC-014	027		(Pleistocene)	Interlaminated fine sand and mud.
		AVC-015	028		Coastal Plain	Non-bedded whitish-pink, medium sand, faint bands of heavy minerals. Sewage smell.
2	2 SY 8/1 SY 7/1 NB	AVC-016	029	P ₁		1.05-1.12: Gravely CS with white clay at top. 1.12-1.32: A normally graded bed of m to c sand. 1.32-1.72: M to c sand with clay laminae at base. 1.72-2.35: Interlaminated clean cs, ms, and white, muddy fs.
Non-Recovery						
3		AVC-017	030		(Pleistocene)	Coarse sand and fine gravel with pebbles at the base. No bedding apparent.
			031	P ₁	Coastal Plain	Gravely medium to coarse sand, poorly sorted.
		AVC-018	032			Interlaminated fine to medium sand, with mud in the coarser sediment. Fine sand has visible concentration of dark minerals.
4						Pebbly, sandy gravel, gravel layer at base interlaminated fine sand and mud.
						Fine to medium sand.

Figure 25. The S₂ regional unconformity separates overlying Holocene sediments from the underlying Pleistocene sediments. P₁ usually has a very coarse sandy gravel (lag) just below the S₂ regional unconformity, probably caused by shallow, meandering streams during the last Pleistocene lowering of sea-level. In this example, the coarse sediment abruptly truncates the underlying interlaminated sand and white mud of the Pleistocene unit.

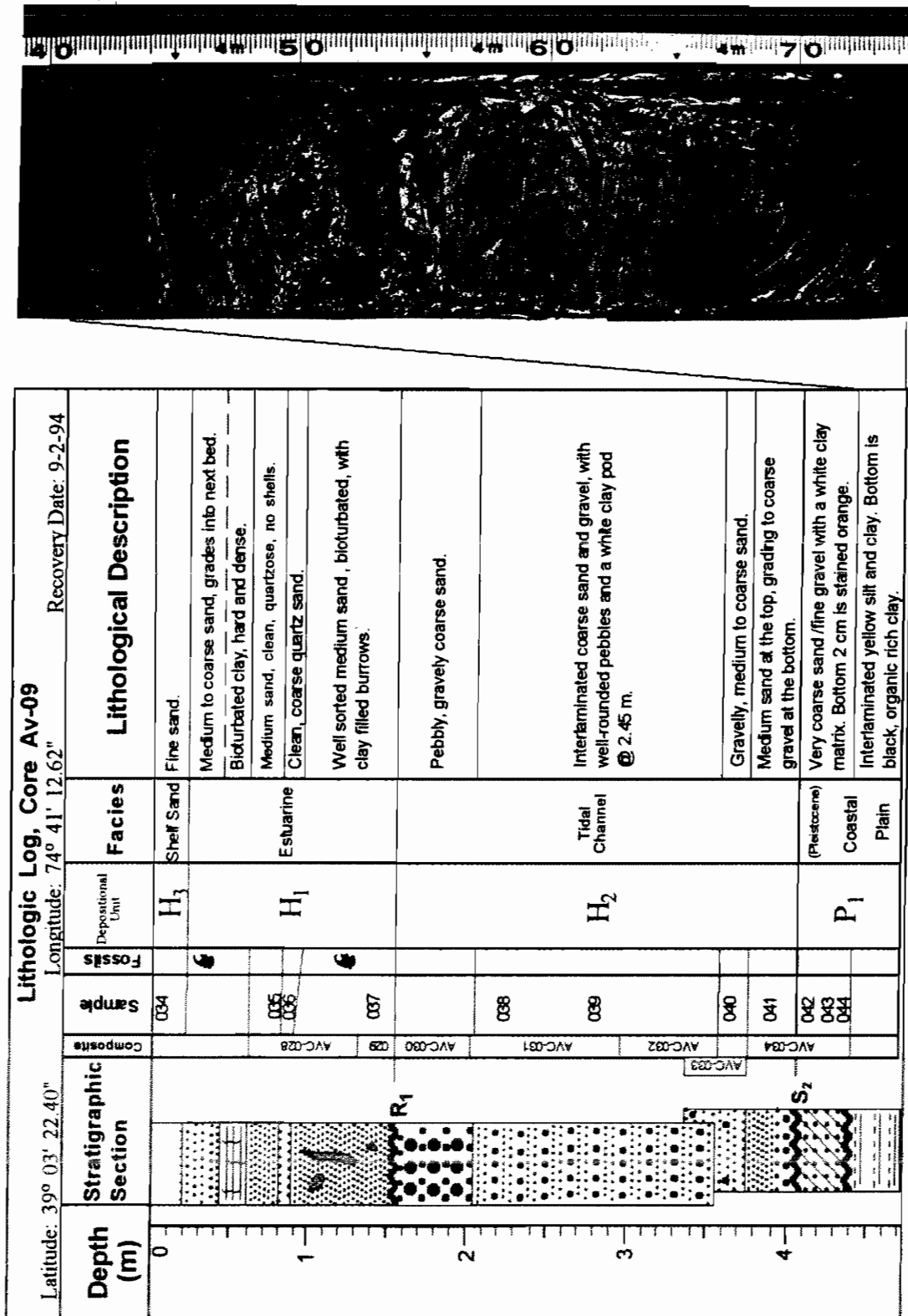


Figure 26. An intensely yellow clay underlies the S₂ unconformity at this location (seismic line TI-3.0 N). The clay appears to be limonitic, contains no microfossils, an may have been deposited in a quiet estuary or lake during the Pleistocene lowering of sea-level.

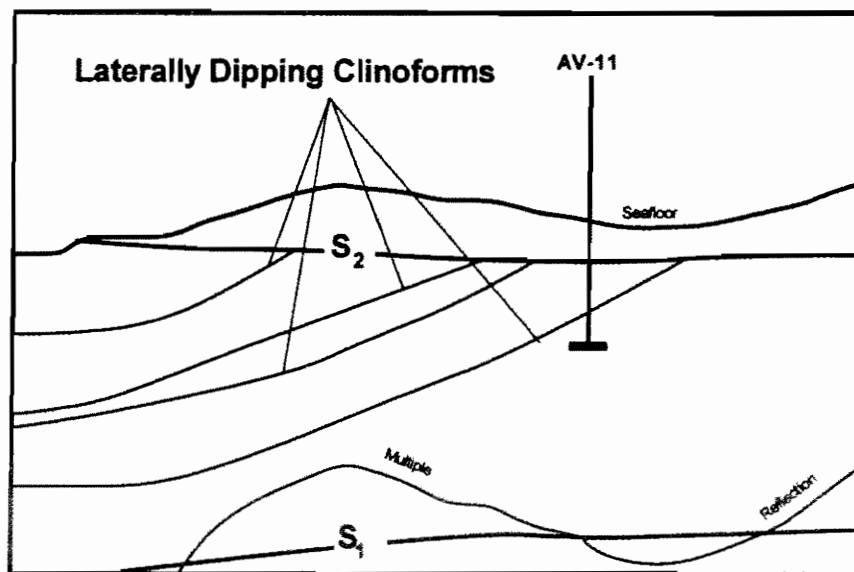
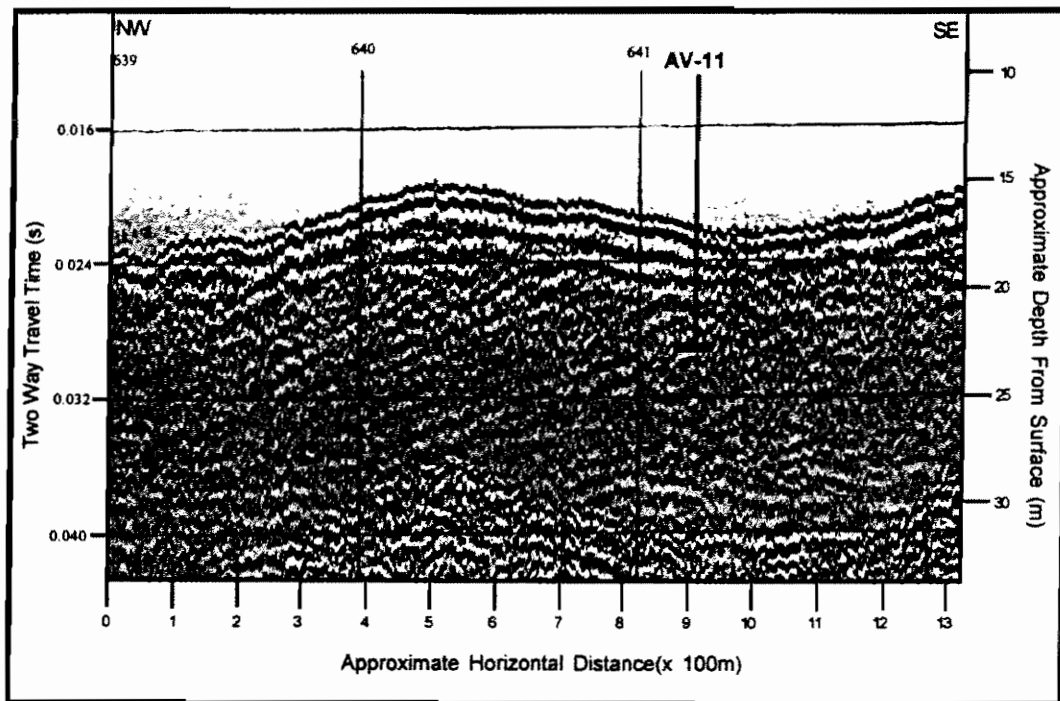


Figure 27. Sub-parallel, steeply dipping, lateral clinoforms extend from the planar S_2 surface 10 meters in depth to the S_1 surface along the shoreward portion of seismic line TI-12N. Core AV-11 recovered bedded coarse grained sediments from below the S_2 unconformity surface. The gravelly sand structure may represent a laterally accreting bay-mouth shoal complex (from seismic line TI-12N).

is similar in composition and clast size to the uppermost H_3 sediment, but underlies the S_2 unconformity.

Core AV-18 (figure 7) was collected in the swale between two sand ridges in the southern region and recovered a thin mantle of coarse sediment overlying fine mud and sandy mud. The sharp lithological contact between P_1 and H_1 is indicated in seismic profile by a very high amplitude reflection which is easily resolvable despite its proximity to the seafloor. It is immediately underlain by shallow, concave upward reflections which terminate against the S_2 surface (figure 28). In core section, these P_1 sediments are composed of coarse grained sandy gravels which are similar to the P_1 sediments found at other core locations. However, AV-18 also recovered wood fiber and a portion of tree branch or tree root which were entrained within the P_1 sediments. This well preserved terrestrial organic material in the shallow, upper portion of the P_1 sediments suggests that the sediment is likely to have been deposited in or near a sub-aerial environment. ^{14}C dating of the wood fiber returned a date in excess of 42,890 ka (Beta Analytical Laboratory No. 90134; $13C/12C = -25$).

Two deep (5-15 m) river valleys (P_2) are incised into T and P_1 sediments along the shore-proximal portion of the seismic lines and along the outer portion of the southern seismic lines (TI-1N, TI-2N, TI-3N, and TI-4N). In some cases, the valley is locally truncated by the S_2 unconformity surface. The southern area river valley is approximately 600 m across and 10 meters in depth (figure 29), exhibits an asymmetric profile, and contains an apparent width to depth ratio of 60 to 1. Channels of similar depth are observable along seismic lines TI-2N, TI-3N and TI-4N (figure 4), although the width to

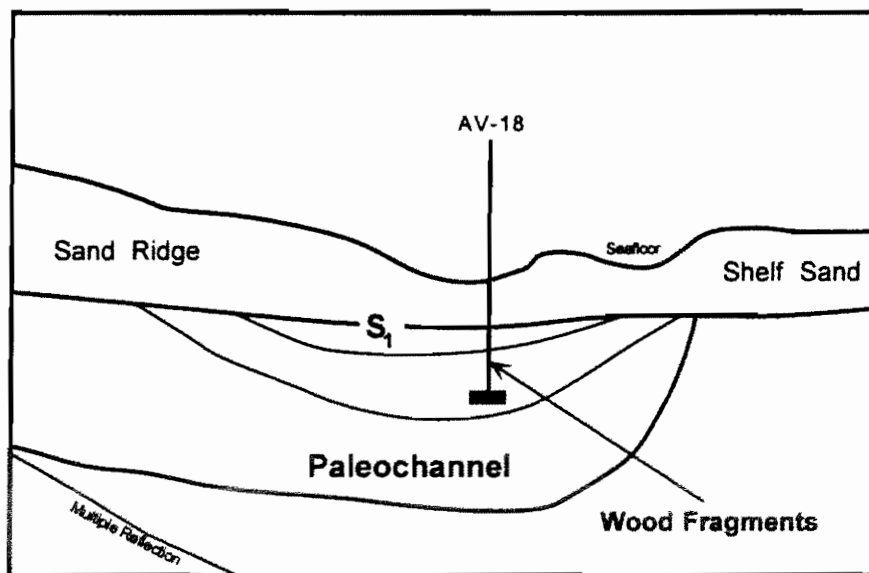
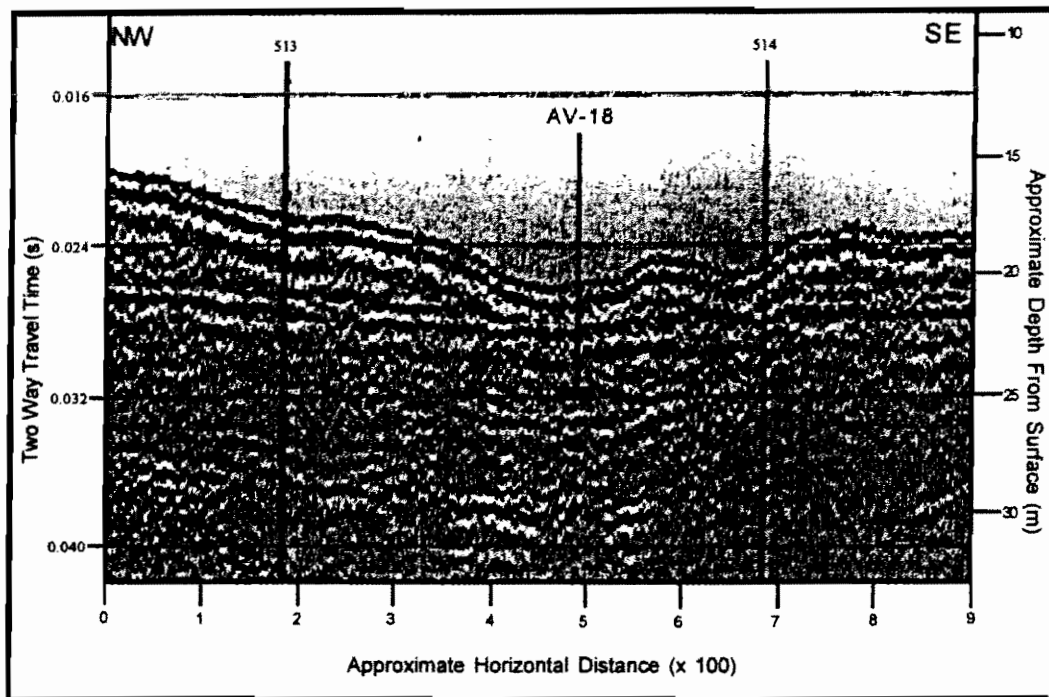


Figure 28. Core AV-18 recovered wood fragments from coarse sand and gravel. The wood was ¹⁴C dated at greater than 42,890 b.p., and apparently was fluviially transported to its present location. The arcuate reflections probably result from the filling of a paleochannel which traversed the inner continental shelf during the Pleistocene (from seismic line TI-1N).

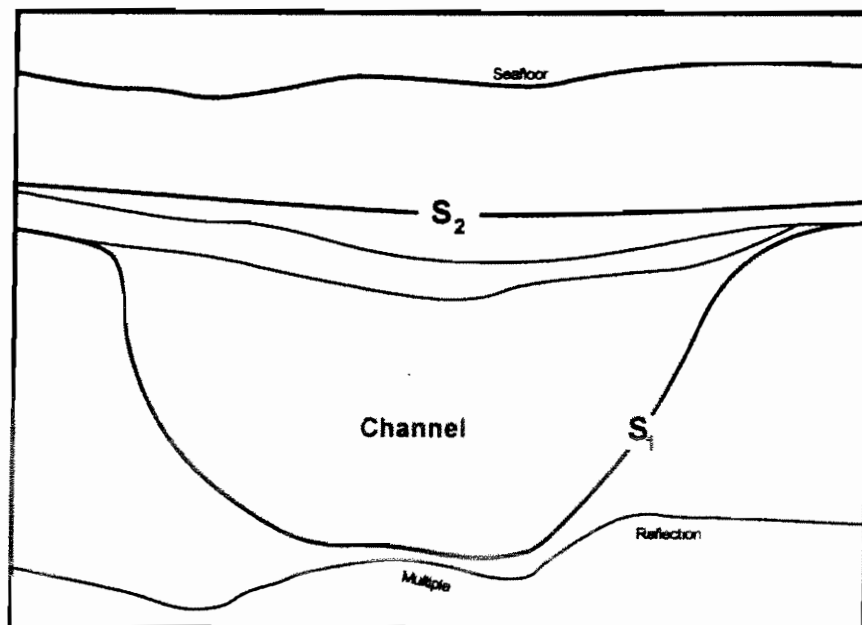
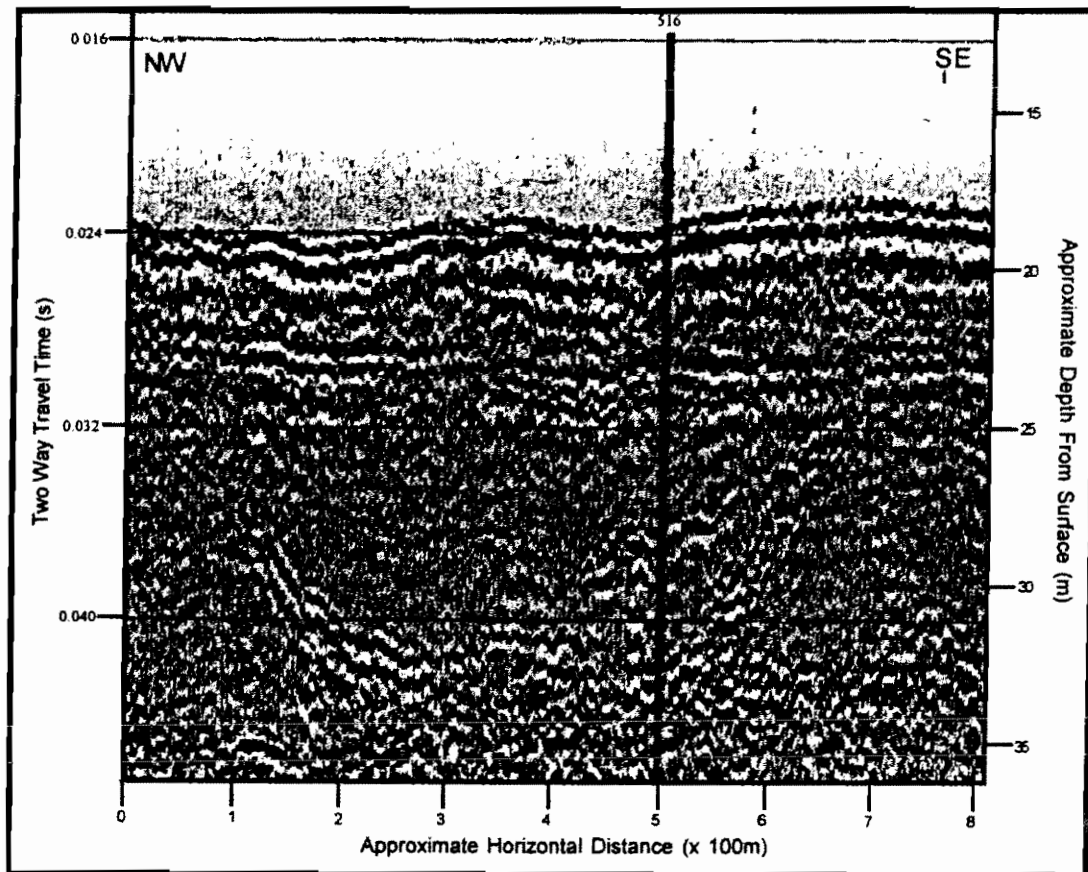


Figure 29. Sections of a deep paleochannel are resolvable on each of the shore-perpendicular seismic lines. This portion of the paleochannel is approximately 600 m across, 10 m deep, and exhibits an asymmetric profile. Lack of symmetry can be caused when the seismic line is run obliquely to the trend of the channel (from seismic line T1-N).

depth ratios are not always equivalent. Different apparent widths of meanders would affect the width to depth ratios.

The northern valley typically exhibits a series of high amplitude seismic reflections along the bottom few meters of the channel (figure 30), which may represent a lithology change from fine grained organic-rich sediment (recovered from core AV-12) to coarse grained, relatively clean sand and gravel sediments. Typically, the high amplitude reflections become indistinct, low amplitude reflections toward the top of the channel. This upper, low amplitude zone correlates with fine grained, burrowed, shell bearing silts and clays in the lower portion of core AV-12 and at AV-14 (TI-10N, figure 7). Towards the north, the valley widens and extends in width beyond the range of seismic coverage.

Based upon limited spatial data, the northern channel appears to run approximately shore parallel through the study area where it is relatively close (< 5 km) to the modern shoreline (figure 31). It exhibits a very large width to depth ratio (in excess of 300 to 1) on the inner portion of the seismic lines. In the southern area, the channel is less wide and is more shore perpendicular. Future seismic studies may better delineate the paths of these buried valleys through expanded seismic coverage.

Depositional Units H_1 , H_2 , and H_3 :

H_1 and H_2 are widely distributed in the study area, but are not present at all core locations. They usually underlie H_3 but are also found exposed at the seafloor in some areas which lack the H_3 sediments. Because these units are often less than 2 m in combined thickness, they are difficult to discriminate in seismic profile. H_1 and H_2

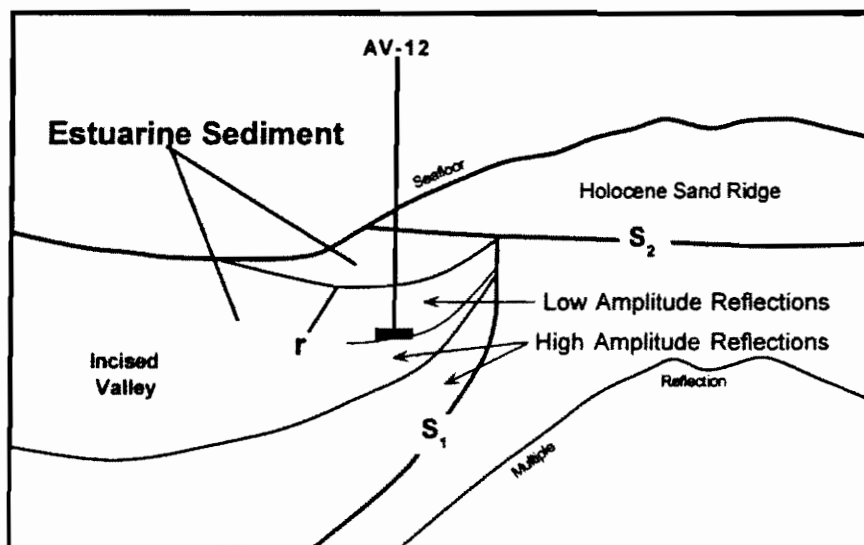
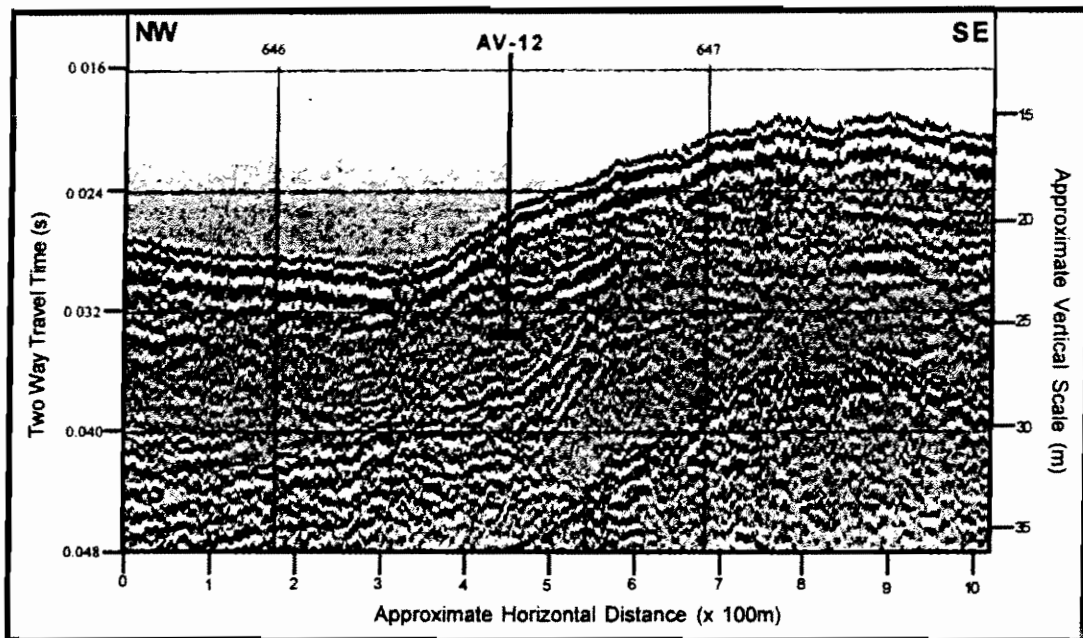


Figure 30. A deeply incised valley is filled with fine grained H_3 type estuarine sediments in the cored interval indicated (Core AV-12). The high amplitude reflections filling the lower half of the channel are probably composed of coarse grained fluvial channel sediments which formed during the last Pleistocene lowering of sea-level. The sharp reflection in the upper portion of the channel (r) is caused by a strong lithology change across a muddy sand layer. In this image, the S_1 unconformity is truncated by S_2 (from seismic line TI-12N).

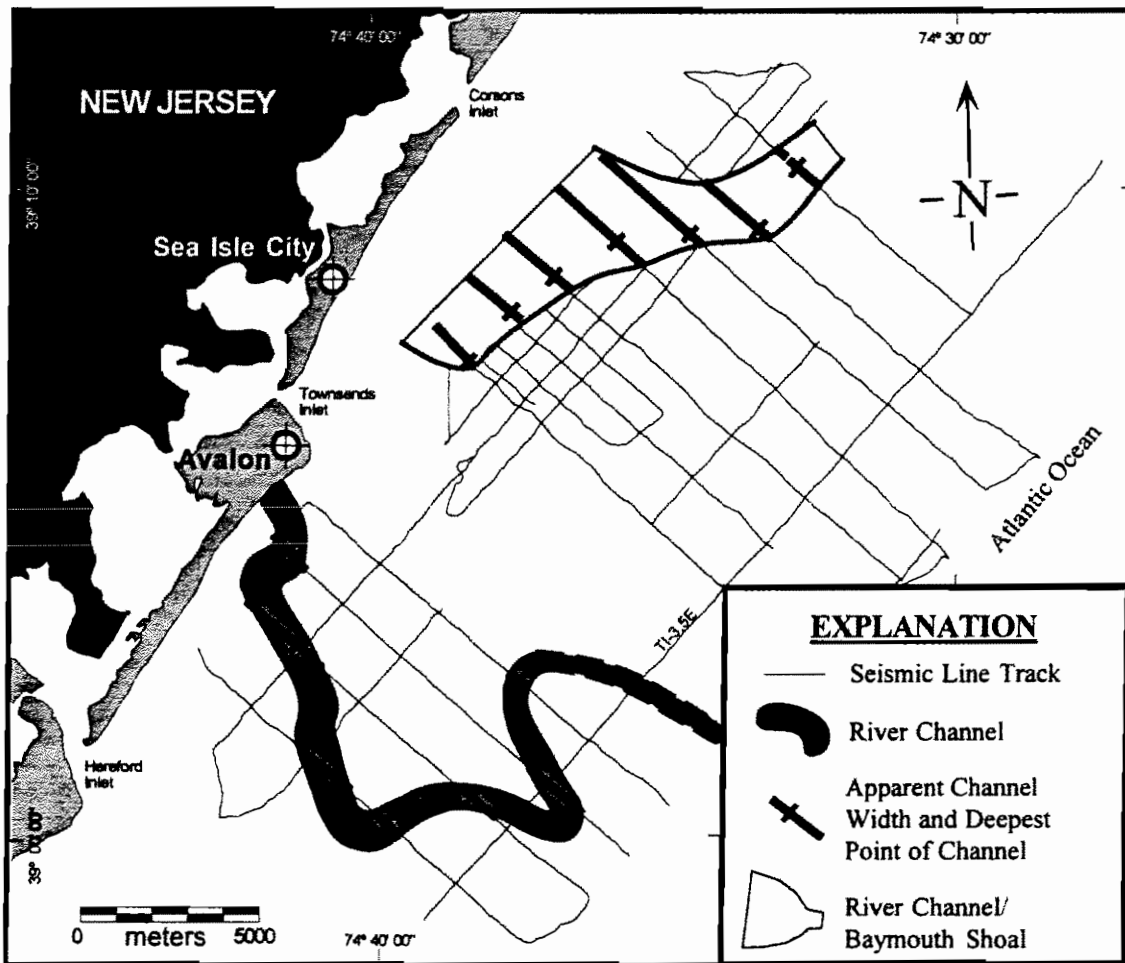


Figure 31. Deeply incised channels are apparent in seismic profile below the S_2 unconformity. Short, black lines (bold) indicate the position of the channels along the seismic lines. Small lines which are drawn perpendicular to the channel lines indicate the deepest portion of the channel and provide an impression of channel orientation along the seismic transect. Channel paths are shaded gray, with inferred paths shown dashed (seismic resolution along the long tie-line TI-3.5E was inadequate to resolve the inferred channel crossing).

sediments always underlie a low amplitude reflection (R_2) which is interpreted as a ravinement surface when it is found within the relief of sand ridges. Because the process of shoreface ravinement often completely erodes through back-barrier/estuarine sediments (Nummedal and Swift, 1987; Hine and Snyder, 1985), R_2 may, in some locations, merge with the regional unconformity S_2 and place the overlying H_3 sand ridge sediment in direct contact with the underlying Pleistocene units.

H_1 is a fine grained, high mud sediment which contains large quantities of organic plant material (peat) and shell detritus. Whole shells are common and tend to be found clustered in discrete, confined beds. Sandy beds or laminations are less common but occasionally interfinger with finer grained sediments. H_1 core recovery varied between 0.2 m and 7.1 m in thickness. In some locations, H_1 sediment thickness exceeds the 6.5 meter limit of core penetration (caused by expanding clay sediment in cores with multiple cast attempts). Seismic (figure 30) and core data (AV-12; Appendix A) demonstrate that fine grained muds fill a deep incised valley complex with over 5 m of sediments.

Depositional unit H_2 is found stratigraphically within or immediately overlying H_1 sediments. H_2 is composed of coarse grained sand and gravel sediments with variable proportions of mud. Sediments often form indistinct beds with the most coarse sediment at the contact with H_1 . H_2 rarely contains whole shells, but often contains shell detritus. Plant material was not found within H_2 sediments. The contact between H_1 and H_2 sediments is usually erosional, with a gradual transition from the coarse sand and gravel sediment back to the finer grained estuarine sediment. In some cases, the upper surface of H_2 may be in erosional contact with H_3 or exposed at the seafloor.

Like H_1 and H_2 , H_3 always lies stratigraphically above the S_2 sequence boundary surface. It overlies H_1 and H_2 when they are present, and always forms the majority of relief above the S_2 unconformity. H_1 , H_2 , and H_3 comprise the entire relief of sand ridges and other surficial sediment above the S_2 unconformity. When neither H_1 nor H_2 are present, H_3 is always in unconformable contact with P_1 , P_2 , or less frequently, T. When H_1 or H_2 are present, one of those depositional units are in unconformable contact with P_1 , P_2 , or less frequently, T. H_3 is always separated from its underlying unit by an unconformity.

The seismic reflection pattern within H_3 is indistinct to transparent (figure 32), with any observable horizontal to sub-horizontal reflections always located within the relief of sand ridges and exhibiting an apparent northeast dip along the ridge axis at from $0 - 10^\circ$. H_1 reflections appear horizontal in ridge cross-section, and seem to be correlative in core with minor, conformable lithologic transitions such as bedding planes. The combination of sand ridge bedding and longitudinally dipping weak reflections suggests that sediment may have accumulated on the sand ridges in a pattern similar to that of longitudinal landforms, by migrating up the sloping landform surface in response to at least two dominant current flow directions. The seismic pattern of H_3 is generally transparent along portions of the seismic lines without prominent sand ridge morphology (figure 33), although the small (< 3 m) relief of those areas and the close vertical proximity to the seafloor reverberation pattern often precludes resolution of any internal reflection patterns.

Lithologically, H_3 is composed of medium to coarse sand, gravel, and pebbly gravel, all of which is mixed with shelly detritus. Bedding is variable, from distinct, but

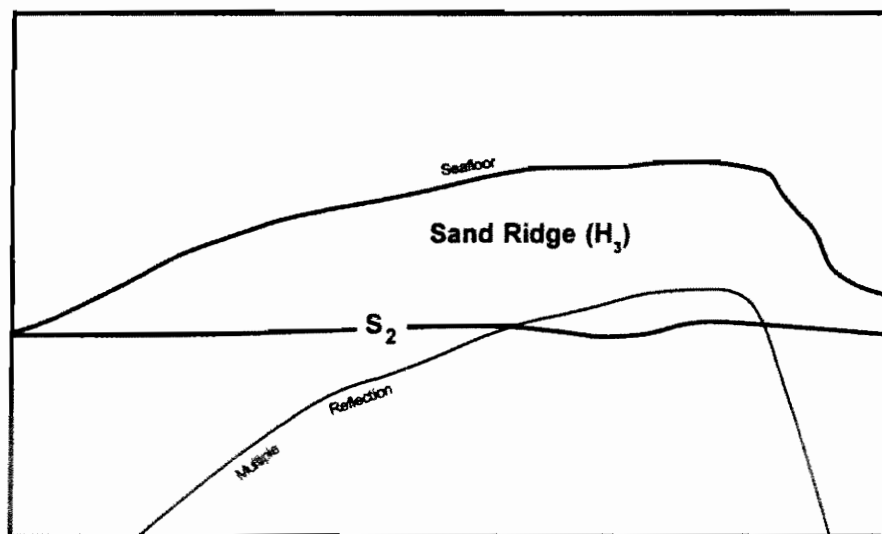
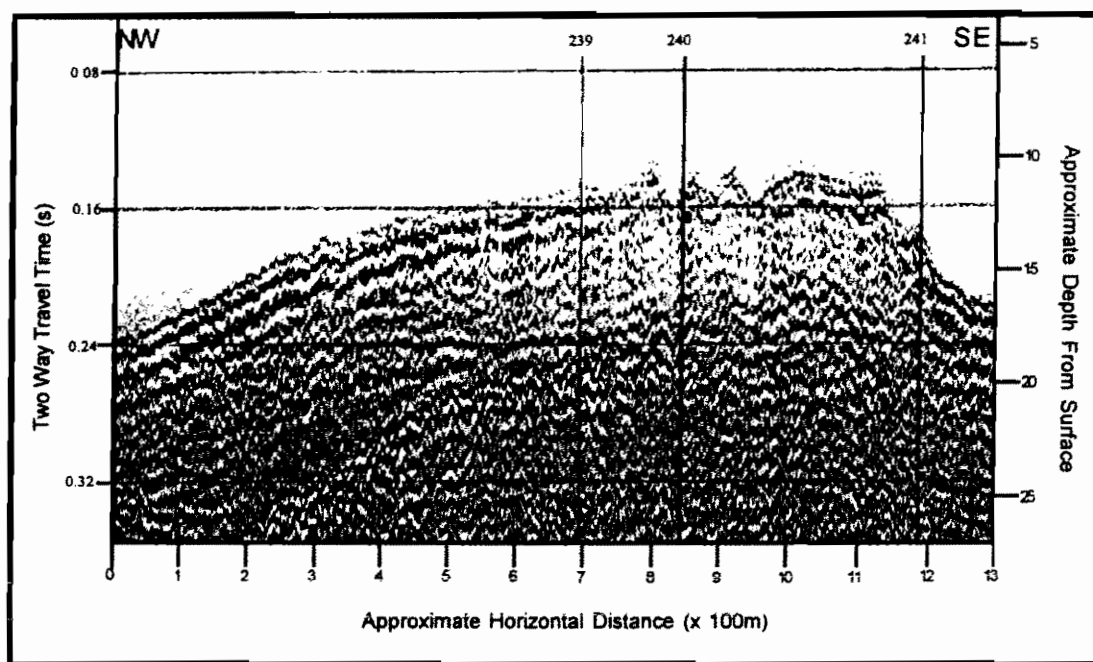


Figure 32. The seismic reflection pattern within the H₃ sand ridge sediment is indistinct, suggesting a relatively homogeneous composition. Core samples confirm an homogeneous gravelly sand composition within the H₃ sediments (from seismic line TI-8N).

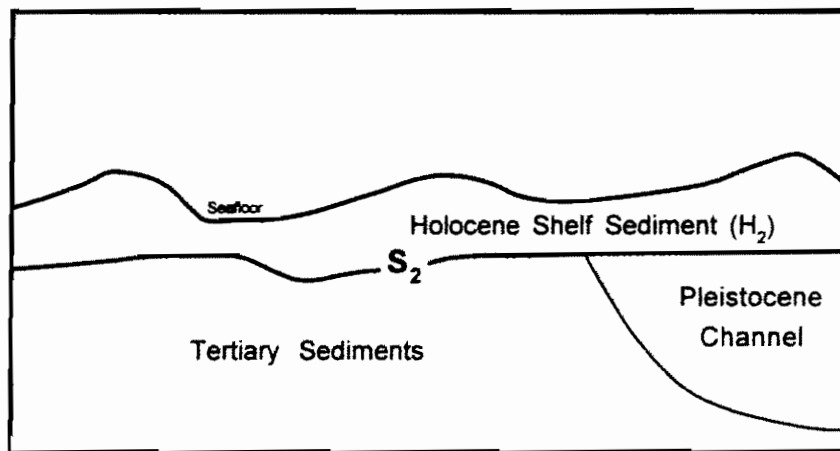
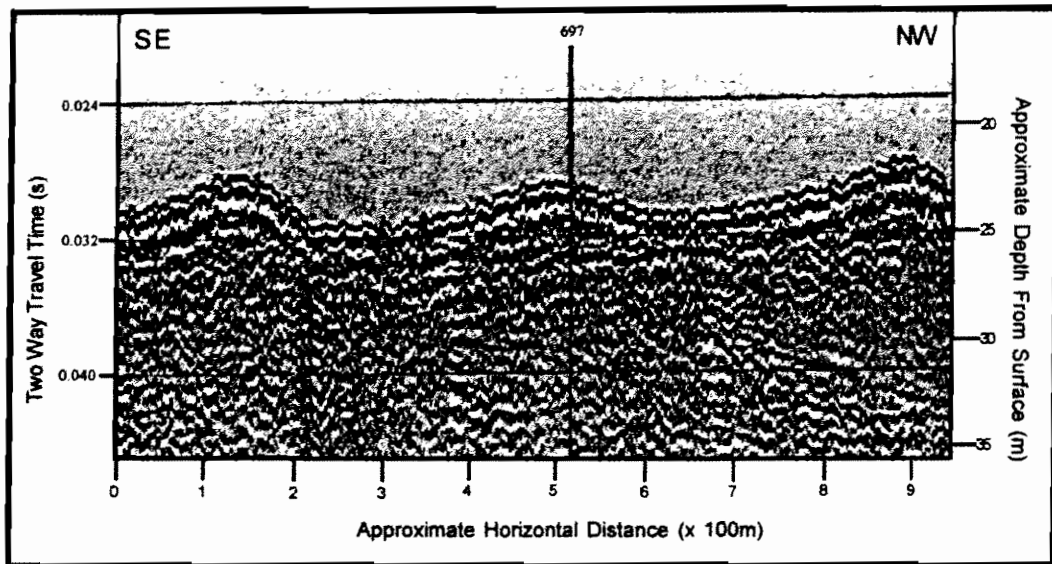


Figure 33. Where seafloor reverberation patterns do not obliterate the seismic reflections within non-sand ridge shelf sediments (H_1/H_2), the seismic pattern is relatively transparent (image is from seismic line TI-13N).

conformable, to indistinct. Bioturbation is frequently evident and in some locations has obliterated bedding surfaces. All core sections show remnant bedding variations in their horizontal clast size patterns throughout the H_3 sections. In cores which exhibit distinct bedding planes, the beds vary in thickness from 5-50 cm, the smaller beds usually being composed of well sorted, medium sand, and the larger beds being composed of coarse, gravelly sand. Gravel/pebble beds up to 20 cm thickness are commonly found between the larger layers of gravelly sand. Cores were not oriented, which precludes any determination of bedding orientation. Apparent inclination angles varied between 0° and 20° .

Mean grain size of 60 samples which were taken from the H_1 unit in 13 cores is 0.56 mm (0.82 Φ), that of medium sand. The smallest mean grain size of the samples was 0.19 mm (2.35 Φ) corresponding to fine sand, and the largest mean grain size was 2.04 mm (-1.02 Φ) corresponding to gravel. The samples were predominantly poorly to moderately sorted, with a few being moderately well to well sorted. The sediment averaged less than 1% mud (0.76 % mean), with a maximum of 5.35% and a minimum of 0%. Clay was usually non-existent. Gravel content averaged 10%, with a maximum of 44.8% and a minimum of 0.04% (table 3). Clean, coarse sediment is characteristic of this unit.

Based upon a limited number of gravel fraction samples, the vast majority of the H_1 sediment is composed of iron oxide stained quartz and quartzo-feldspathic minerals. Minor quantities (0-10%) of sandstone, siltstone, metamorphic rock fragments, and recrystallized limestone are also found in the samples. The recrystallized limestone is non-reactive with hydrochloric acid and appears to have formed through silicic replacement of

Environment	<i>Sand Ridge</i>	<i>Channel</i>	<i>Estuarine</i>	<i>Fluvial (Pleistocene)</i>
Number of Analyses	60	14	16	14
Sorting (phi)	0.98	0.87	1.77	1.59
Maximum value	1.86	1.29	4.16	2.48
Minimum value	0.41	0.52	0.79	0.52
Description	moderate	moderate	poor	poor
Mean (phi)	0.82	1.35	2.91	0.83
Maximum value	2.35	2.45	5.42	2.11
Minimum value	-1.02	-0.22	1.36	-0.64
Corresponding sediment type	c. sand	m. sand	f. sand	c. sand
Skewness	-0.19	-0.12	0.35	0.13
Max. Value	0.45	0.38	0.74	0.60
Minimum Value	-0.63	-0.44	0.00	-0.50
Descriptor (Folk, 1980)	coarse	coarse	strongly fine	fine
% Gravel, Mean	9.96	3.33	0.80	12.36
% Gravel, Median	3.85	1.60	0.17	6.66
Max. Value	44.80	16.35	4.36	41.10
Minimum Value	0.04	0.17	0.00	0.00
% Sand, Mean	89.32	94.20	81.54	81.55
% Sand, Median	95.96	95.25	89.83	86.10
Max. Value	99.72	99.73	95.09	97.42
Minimum Value	54.61	80.24	43.55	56.57
% Mud, Mean	0.76	2.47	17.64	6.08
% Mud, Median	0.04	2.08	9.72	5.54
Max. Value	5.35	6.82	55.49	14.77
Minimum Value	0.00	0.10	3.42	0.47
Suitability	Good	Poor	Poor	Variable

Table 3. Sediment summary statistics for coarse grained sediments in four different depositional environments. Sediments with a total mud content of over 50% (estimated) were not analyzed for this study. Sand ridge sediment is predominantly coarse grained and contains a very low percentage of mud, making it an ideal sediment for beach remediation. Fluvial sediment which is found underlying the regional unconformity is also often suitable for remediation. Between the Sand Ridge and Fluvial sediments is a variable layer of mud-rich estuarine sediment which is often unsuitable for remediation.

carbonate. Some fragments of recrystallized limestone grade into fossiliferous siltstone along an edge of the fragment, while other similar fossiliferous siltstone fragments have undergone partial replacement of the fossil carbonate with silica. The fossilized material includes fragments of zoantharians and is most likely of reefal origin, although no reefal structures are known to exist in the immediate region. Because these fragments are found in H_1 , H_2 , H_3 , and P_1 (no samples were taken from T) but are most strongly concentrated in H_2 , they are probably reworked from older deposits and may have been transported for a considerable distance from their place of origin by fluvial transport. Each depositional unit contains similar gross lithological compositions of their gravel fraction.

Sand Ridge Characterization

Additional topological and volumetric data were generated for the two northern region sand ridges to better delineate their structure, morphology, and usable sand volumes. The determination of sand ridge morphology is somewhat subjective since the H_1 sediments do not terminate abruptly at the periphery of the ridge, but thin gradually outward from the ridge axis until influenced by the proximity of another sand ridge axis. Therefore an arbitrary region must be chosen in which the sediment is considered 'sand ridge' sediment, and from which all other sediment is excluded. The base of the sand ridge, as defined for sediment volume calculations, is coincident with the S_1 regional unconformity surface. Sand ridge thickness must be derived from apparent seismic thickness, which is calculated based upon the apparent thickness from the seafloor to the S_1 boundary as identified in seismic profile (figure 34).

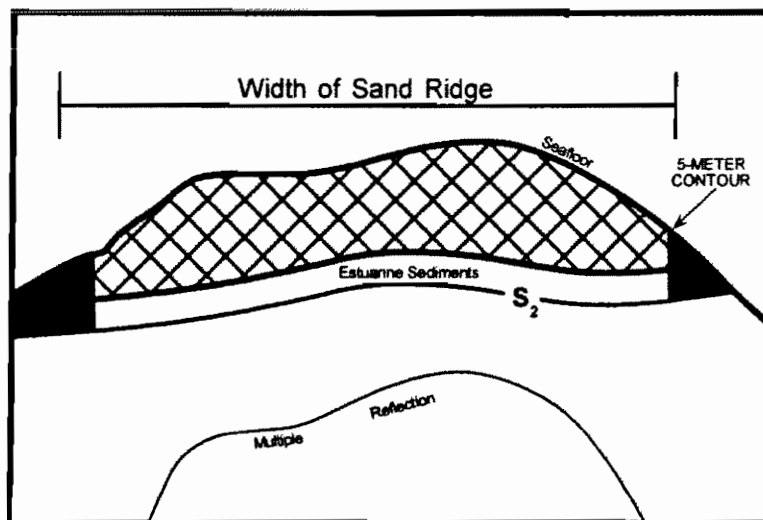
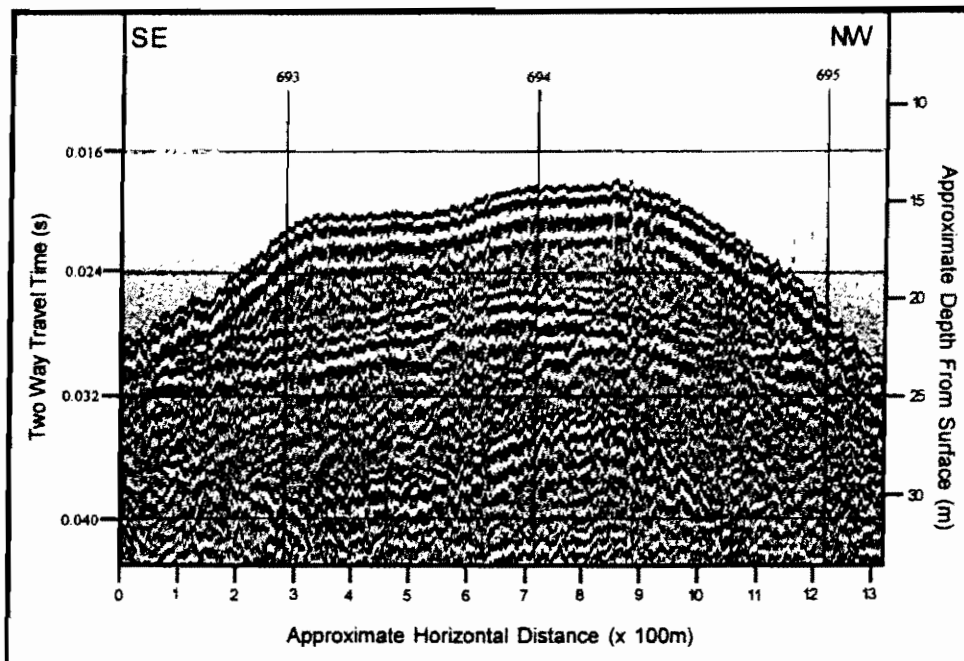


Figure 34. Sand ridge volume is calculated using seismically derived data. Because sand ridge sediments thin away from the ridge but may not terminate, a bounding area must be defined to calculate the ridge thickness. The bounding area is defined as the 5-meter contour line above the regional S_2 boundary. These contours approximate the surface expression of the sand ridges. Sediment thickness is measured from the seafloor to the contour boundary at each fix point, then integrated along the width and length of the sand ridge within the 5-meter contour limit (hatch). The lower two meters above the S_2 boundary are considered unusable estuarine sediments based upon core observations, and are not included in the calculations. Using this method, the inner sand ridge and Avalon Shoal sand ridge yield over 85 million cubic meters of usable sediment (from seismic line TI-13N).

The following method is used to estimate sand ridge sediment volume: seismic depth from the seafloor to the S_1 surface is measured at the known traverse (fix) positions along each seismic line which bisects the sand ridge. Seismic line spacing did not allow more than one axial line to intersect either ridge. Ridge periphery is defined by the starting depth contour value of 5 meters above the regional S_1 unconformity surface. These contours approximate the surface expression of the sand ridges. Two meters of unusable fine grained sediment is assumed to underlie the sandy portion of the ridge bodies (based on core observations). The sediment volume contained within the starting contour and above the S_2 unconformity, less the underlying 2-meters of unusable fine-grained sediment, comprises the sand ridge volume estimate.

A 2-dimensional representation of the sand ridge is generated using Surfer™ Surface Mapping Software. Sand ridge contours are generated using a linear interpolation algorithm with a 39 column by 50 row computer generated data grid. Volumes are calculated using three standard mathematical methods: Trapezoidal Rule, Simpson's Rule, and Simpson's 3/8 Rule. Maximum variance between the calculations was less than 0.5% for both ridges (table 4). Volume estimates from each method are compared, rounded, and an average value determined:

Inner Sand Ridge: 48.4 million m^3

Outer Sand Ridge: 37.3 million m^3
(Avalon Shoal)

Combined, these two sand ridges should provide at least 85.7 million cubic meters of usable material for remediation of local beaches. *(112,095,600 cu. yds)*

	Inner Ridge	Avalon Shoal
Volume (millions of cubic meters):		
Trapezoidal Rule	48.44	37.34
Simpson's Rule	48.42	37.31
Simpson's 3/8 Rule	48.62	37.40
Maximum Variance	0.20%	0.09%
Planar Area (millions of square meters)	4.08	2.03
Length, maximum (km)	9.0	9.5
Width, maximum (km)	3.9	2.2
Distance from shoreline (km)	7	12

Table 4. Sand ridge summary statistics. Sand ridge volume estimates are based upon total sediment thickness above the regional seismic unconformity. Volumes are constrained within the approximate surface expression of the sand ridge, and exclude fine grained estuarine sediments at the base of the ridge.

Oil

A black, oily substance coated the sediment grains in a portion of two separate ridges: in core AV-01 on the southern end of the inner ridge, and in core AV-07 on the southern end of Avalon Shoal (figure 7). At least 1.5 m of sediment in AV-01 was saturated with the volatile, black material, while globules of similarly coated sediment were recovered from AV-07. The coated sediment in core AV-01 was overlain by over 1 meter of clean, very coarse sediment, while the AV-07 coated material was mixed with clean sediment throughout the upper two meters of core. This material is most likely oil which is derived from one of many tanker spills known to have occurred along the coast of New Jersey. Because of the volume of oil needed to saturate over 1-meter of sediment, this spill probably occurred during World War II when many oil tankers were sunk off of the New Jersey shoreline.

INTERPRETATION AND DISCUSSION

Geophysical Interpretation

The late Quaternary paleoenvironmental history of the inner New Jersey continental shelf is inferred based upon interpretations of high-resolution seismic profiles, the lithostratigraphy of core sections, and sedimentological analysis of sediments which were recovered from sites within the study area. The seismic stratigraphy is divided into six depositional units which are bounded by three continuous and one intermittent unconformities (figure 14). Two of the surfaces (S_1 , S_2) are easily resolvable in seismic profile due to their high acoustic reflectivity, termination of internal reflections against the surface, and their known stratigraphic positions relative to other surfaces.

The S_1 reflection is interpreted as a sequence bounding unconformity which developed when sea-level regressed to the outer shelf in response to Pleistocene buildup of continental ice. As the deepest sequence bounding unconformity, it must have formed during or before the $\delta^{18}\text{O}$ isotope stage 4 lowstand at approximately 70 ka (figure 35), and may have eroded older (Tertiary) coastal plain sediments. Bloom et al. (1974) estimated that paleo-sea level was at least 65 m below its modern level during this eustatic minimum, which is sufficient to expose sediments to the middle shelf. Vail et al. (1977) developed the original stratigraphic concepts which associate sequence boundaries with large scale eustatic changes; sequences are defined by their bounding unconformities, which are interpreted as having formed on exposed shelves during a eustatic fall in sea-level.

Following the stage 3 sea-level rise, sea-level fell in response to the last buildup of Pleistocene continental ice. Sea-level reached a minimum by 20 ka and exposed the entire New Jersey continental shelf to erosional processes. S_2 is a sequence bounding

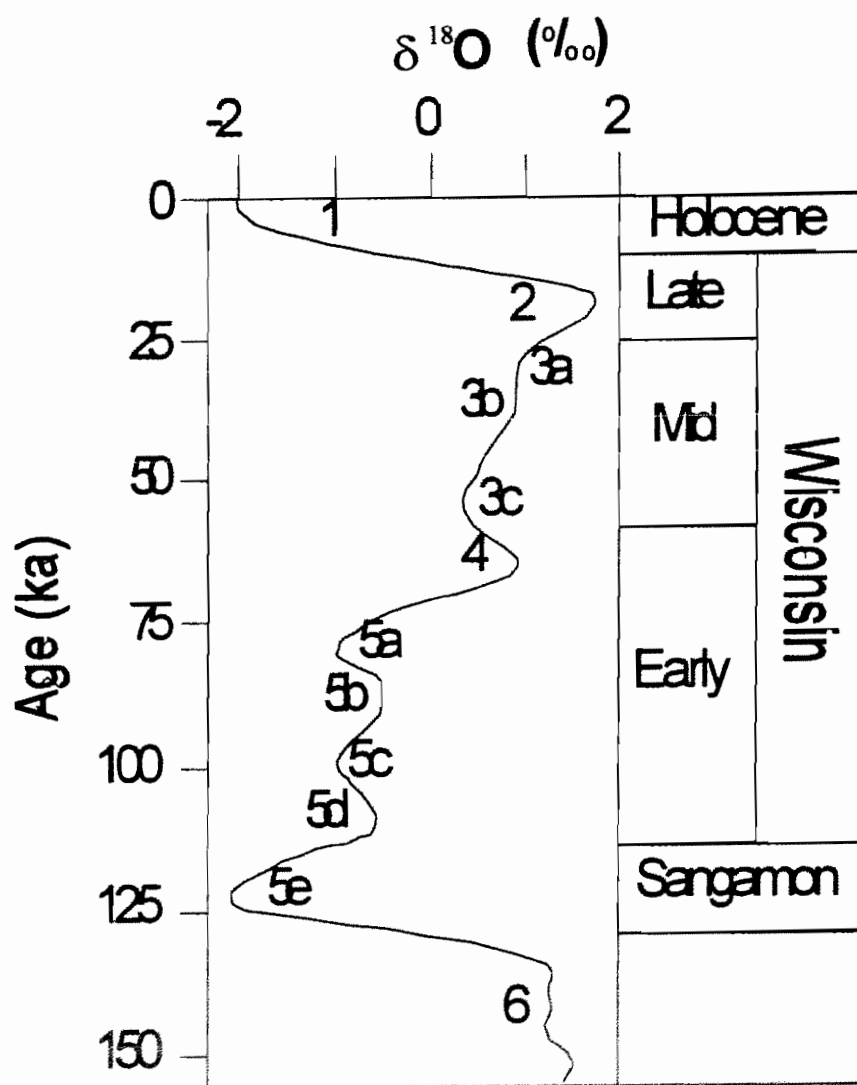


Figure 35. δO^{18} curve from 150 ka to the present (modified after Chappell and Shackleton, 1986).

unconformity which is interpreted to have formed during the $\delta^{18}\text{O}$ isotope stage 2 lowstand at approximately 20 ka because there is no stratigraphically higher surface of erosion which can be correlated with that lowering. Unlike S_1 , S_2 exhibits very little relief over short (1-2 km) distances and appears nearly planar in seismic profile; Snedden et al. (1994) refer to this surface as a sand plain which formed by the amalgamation of braided streams. This is consistent with an arid, arctic environment proximal to the ice margin.. Small arcuate, concave-upward reflections which underlie the S_2 surface (figure 28) indicate that small, low velocity, low volume streams were common on the exposed shelf, but that stream channels were typically incised only a few meters into the shelf sediments.

The S_1 and S_2 surfaces correspond to the R1 and R2 surfaces, respectively, of Ashley et al. (1991) which were identified near Barnegat Inlet, New Jersey, a coastal embayment which lies approximately 75 km north of the study area (figure 2). In that study, Ashley et al. were able to associate the R2 surface with the late Pleistocene lowering in sea-level (stage 2) and inferred an earlier isotope stage for their R1 surface. Similar seismic patterns within the line profiles coupled with similar sedimentological characteristics between this study and those of Ashley et al. (1991) and Snedden et al. (1994) enable the stratigraphy between the sites to be correlated with reasonable confidence.

The third surface (R_1) is acoustically weak in seismic profile and was typically resolvable only in core. When the sediments across the R_1 unconformity are carefully examined and understood in relation to the general sea-level history of the region, the origin of R_1 can be interpreted as a tidal-current channel cut which formed by tidal channel migration in a barrier island/estuarine environment (Ashley and Sheridan, 1994). Tidal

channels form where currents breach barrier island systems and erode through the underlying sediments (Dalrymple et al., 1992).

The fourth surface (R_2) is much less acoustically reflective but is easily located in seismic profile where it is found within the topographic relief of sand ridges. R_2 always lies stratigraphically above the S_2 boundary. As a ravinement surface, R_2 does not constitute a sequence bounding unconformity as defined by Vail et al. (1977) because the boundary does not represent a significant hiatus in deposition caused by sea-level fall. Ravinement surfaces are time transgressive erosional surfaces where the age of sediments being deposited at the front of the ravinement plane (stratigraphically beneath the surface) can be of similar age to the sediments which are deposited at the rear of the ravinement plane (stratigraphically above the surface) (Vail et al., 1977). The potentially small difference in age (a few hundred to a few thousand years, typically) of the sediments across the boundary is insignificant in comparison with the age difference considered by Vail et al. (1977) to be representative of a sequence boundary (hundreds of thousand to millions of years). Additionally, ravinement surfaces are created during rising sea-level, while sequence boundaries are formed during falling sea-level.

However, seismic stratigraphic relationships across ravinement surfaces do meet one of the criteria established by Vail et al. (1977) for a sequence boundary, ravinement unconformities represent distinct and sharp erosional surfaces along which there are discordant seismic relationships (truncation, onlap) of seismic reflections on either side of the surface. Because erosion of up to tens of meters across R_2 conforms to the definition of a sequence boundary, the surface could potentially be misidentified in seismic profiles and core sections as a sequence boundary.

In a study at Barnegat Inlet, New Jersey (figure 2) (Ashley et al., 1991) and in another study 55 km north of the study area (Snedden et al., 1994), unconformable surfaces were identified in the subsurface and interpreted as transgressive ravinement surfaces. These ravinement surfaces are similar in stratigraphic position and in seismic description to the ravinement surface (R_2) which is described in this study, and demonstrate that regional patterns of erosion have produced consistent lithologic patterns within the sediments. The sedimentological and stratigraphic characteristics of this type of unconformity are very similar to those of foreshore ravinement surfaces but are much less continuous in seismic profile. R_2 type surfaces may locally truncate R_1 type surfaces, making the discrimination and identification of these surfaces very difficult, particularly when relying principally upon core section data.

Depositional Units

The Atlantic continental shelf of New Jersey is characteristic of a passive margin with a very low sediment supply (Uptegrove et al., 1995). Most of the Pleistocene sediment is derived either from nearby glacial deposits in the northern portion of the state or from reworked and redistributed coastal plain sediments (McMaster, 1954). Ashley et al. (1991) estimate that only 30 m of sediment has accumulated above the stage 4 unconformity in nearshore areas. In contrast, Quaternary sediments in the Gulf of Mexico have attained thicknesses of several hundred meters due to loading caused by the tremendous sediment load supplied by the Mississippi River (Weimer, 1989). Even with the modest quantity of sediment which has been supplied to the New Jersey margin over

the past 120,000 years, a series of clearly delineated, regionally consistent sediment successions are preserved on the shelf (Carey et al., 1995).

Tertiary Succession:

The lowermost sedimentary succession of sediments underlie the S_1 unconformity. Although no cores from this study penetrated to this unit, correlation with deep boreholes at the Coast Guard Station in Atlantic City, New Jersey and at the U.S. Geological Survey monitoring well offshore of Atlantic City, New Jersey (Mullikin, 1990) suggest a probable depositional history of this unit. Prior to the stage 4 lowstand which produced the S_1 unconformity, an interglacial highstand occurred at approximately 125 ka (stage 5e). Sea-level was approximately 5-10 m higher than modern levels (Mayewski et al., 1981) and probably formed the prominent inland escarpment which parallels the coast from Barnegat Inlet to Cape May, New Jersey. During this period, sediment was transported and accumulated along the continental shelf in a series of barrier island systems. These old barrier islands were formed proximal to the modern coastline. The sediments which comprise the Tertiary succession are marine in nature but vary greatly in composition, from coarse sand and gravel which were transported along the inner shelf, to estuarine sand and fine mud which accumulated behind the barrier systems. Shoreface ravinement and tidal ravinement unconformities developed along the shore-proximal zones of tidal influence, creating complex depositional and erosional patterns. The Tertiary succession acoustical patterns which are observable in seismic profile lie at a stratigraphic depth which is equivalent to that of marine sands and muds which were recovered from nearby

U.S. Geological Survey monitoring wells (Mullikin, 1990). Marine sand and mud deposits would be consistent with the observed acoustical patterns of this unit.

Pleistocene Succession:

Beginning approximately 115 ka, sea-level began to drop in response to increasing glacial ice accumulations on the continent (Toscano and York, 1992) which reached peak accumulation by approximately 70 ka (stage 4). The build-up of continental ice sheets caused sufficient water to be removed from the oceans that shelves were exposed to the middle shelf (-60 m). The exposed shelf sediments were subsequently reworked by subaerial and fluvial processes, causing significant alteration to the regional geomorphology and surficial sediment layer. Miller et al. (1973) report that a thin gravel layer was deposited over extensive portions of the shelf during this period, probably in response to fluvial reworking of coastal sediments.

Seismic profiles reveal deep channels of up to 15 m in depth which were incised into the older marine sediments. These channels were partially filled with a variety of very coarse channel sediments. Excavation of deep, incised channels requires the existence of large water discharges, suggesting that the region was either exceptionally wet due to extensive precipitation, or that glacial meltwater which originated at the periphery of the northern New Jersey glaciers was able to reach the southern coastal shelf via stream transport. If the later is true, the drainage pattern in New Jersey would have been radically different from the modern pattern, as no streams which presently flow from the northern, formerly glaciated portion of the state approach the southern coastal zone.

Following the stage 4 maximum ice advance and sea-level minimum, sea-level started rising through the late Pleistocene to a maximum stage 3 highstand approximately 20 m below present sea-level (Feeley et al., 1990) at about 55 ka (Wellner et al., 1993). Barrier island systems reportedly migrated within 0.2 km of the modern shoreline (Wellner, 1990; Wellner et al., 1993) depositing a succession of unconformity bounded sediments between the S_1 and S_2 sequence boundaries of this study. On the northwest side of the study area, an accreting sequence of sediments filled a wide marine depression. This succession of deposits is transgressive in nature and resulted from a shoreward migration of sediments during a rise in sea-level. As the marine limit moved landward, a laterally accreting barrier island or baymouth shoal complex deposited a succession of sediments on the landward side of the barrier islands, forming a series of steeply dipping lateral clinoforms (figure 28). Apparent dips on the seismic profiles show a NW strike for the accreting complex, with sand flow to the southwest (a similar southwestward flow of sand occurs on the modern New Jersey shelf). Sediments accumulated to a depth of at least 10 m as the barrier island system advanced landward. The sediments which comprise this structure are composed of mud-depleted sands similar in texture to modern barrier island sands. This laterally accreting complex is resolvable on seismic profiles for 5 km landward of the buried channel, to the limit of the seismic coverage.

Sea-level fell for the last time and reached a minimum by 20 ka (stage 2). During this lowstand, no major erosional valleys were incised in the study area sediments, and the landscape was formed into a planar surface of very low relief. Shallow streams reworked the upper surface of the exposed shelf sediments in an arid, ice-proximal environment. These shallow stream deposits are seismically recorded as a series of arcuate reflections

which underlie the S_2 erosional surface. The sediments just under that surface are coarse grained and interpreted as fluvial channel sands.

Holocene Succession.

Sea-level rose rapidly from 20 ka to 3 ka, inundating the coastline and forcing the shoreline to move steadily landward. Rine et al. (1986; 1991) indirectly document the landward migration of the shoreline by dating carbonaceous shell detritus within sand ridge structures. Their analysis indicates that the mid-shelf ridge system developed in inner shelf water depths at approximately 16 ka, and that the inner shelf ridge system was in existence no later than 5 ka, by which time the shoreline had migrated to nearly its modern position. Dating of shell detritus within the inner shelf estuarine muds and sand ridges indicates that the inner shelf ridge system continuously developed as the shoreline moved landward (Rine et al., 1986, 1991). The landward transgression rate derived from the ages of shell detritus from the mid to inner shelf sand ridges is comparable with the known rate of Holocene sea-level rise (presently 1-3 mm/yr (Braatz and Aubry, 1987; Nichols, 1989)).

Sand Ridge Development

Numerous models have been proposed regarding the origin and evolution of shore attached and detached sand ridges. These models fall into one of two categories: passive and active. The passive model views the ridge system as relict, having formed at some time in the past as part of a barrier island complex. In the active model, sand ridges are mobile, ephemeral structures which are in quasi equilibrium with modern shelf processes.

Both models have supporting evidence which seemingly refutes the other. Both models cannot be entirely and simultaneously correct.

One solution proposed by Knebel and Spiker (1977) suggests that there are really two (or more) varieties of sand ridge which evolve from different processes, and therefore can exhibit different internal characteristics. This model implies that significant differences exist in the structure of actual sand ridges and that ridges can be classified into different categories based upon their differential development. Swift and Field (1981) demonstrated a relationship between current induced shear stress and the development of large scale bedforms. By tying mechanical processes with the development of large scale bedforms in a dynamic shelf setting, sand ridge morphology and development do not require an association with abandoned barrier island systems, except for a means of concentrating sediment.

A major step in understanding the developmental history of the Atlantic margin sand ridges was made with a publication which associates the structure and sedimentological composition, faunal assemblages, and lithologies of sand ridges on the New Jersey shelf with specific depositional environments. Rine et al. (1986, 1991) recognized that sand ridges are composed of distinct lithological layers, even though the lithological layers are not always resolvable in seismic profile. They deduced that the layers are indicative of different environments of deposition within the same ridge morphology, and that the lithologies are correlative between sand ridges of different orientation and morphology. Rine et al. (1986, 1991) and Ashley et al. (1991) suspected that the morphology of sand ridges are governed, at least in part, by modern current activity. These findings are particularly important when attempting to construct a model of

ridge formation based upon ridge morphology and orientation. If currents are modifying the topography of the shelf, morphology of sand ridges may be more related to modern current vectors than to the environment of deposition. Little detailed information is available about regional current patterns and velocity structures on the shelf to generate useful associations. However, preliminary information from an ongoing study by Glenn and Henderson (1991, 1992, 1993, 1994) at LEO 15 (figure 2, inset) show that modern average current vectors trend strongly alongshore (southwest) but maintain an onshore component, the net flow orientation being consistent with many inner shelf ridge orientations (average azimuth 217° from summer 1991 to summer 1993). Storm generated currents trend strongly onshore and may contribute significantly to the net sediment flow patterns along the sand ridges.

To determine properly the evolution of continental shelf sand ridges, the layered physical construction and sedimentological characteristics of sand ridges should be associated with appropriate environments of deposition which occur within a sequence stratigraphic framework. By making two reasonable assumptions governing the New Jersey pattern of sedimentary deposition during the last marine transgression, the development of sand ridges on the New Jersey shelf can be explained by a single formative process, even accounting for differing internal characteristics among sand ridges. These assumptions are made from a temporally restricted viewpoint: 1) that the general pattern of inner continental shelf deposition at any time during the last transgression was the same and that it conforms to a modern analog; that is, that the New Jersey coastline possessed a barrier island/lagoonal/estuarine system which maintained the same geophysical relationship to the coastline throughout the last transgression; and 2) that sedimentation

rates have remained fairly constant throughout the transgression. These assumptions are reasonable given the present understanding of coastal processes, the gradual nature of coastal transgressions, and the low sediment supply along the New Jersey coast. As additional evidence, the +5m Cape May escarpment representing the stage 5e barrier systems nearly parallels today's barrier system.

The upper 5 depositional units which were identified in this study form a composite lithostratigraphic column which encompasses a stratigraphic sequences between the major unconformities S_1 and S_2 (figure 14). Each depositional unit retains unique structural, sedimentological and acoustical characteristics which can be jointly associated with specific environments of deposition. If no erosion had occurred on the shelf during, or following, the last transgression, a complete Holocene lithostratigraphic column would be observed at most locations. Lack of some units, or portions of units, implies net erosion subsequent to deposition. Pleistocene (P) units were deposited prior to the last transgression and are always found beneath the S_2 regional unconformity. H_1 and H_2 units were deposited contemporaneously with the coastal barrier island/estuarine lagoonal system as it migrated landward during the Holocene transgression, and represent relict sediments from the landward portion of a barrier island complex. H_3 sediment (sand ridge sediment) is derived from many sources and owes its textural, mineralogical, and morphological composition to modern shelf processes. All H_3 sand ridge sediment but the upper, active layer is 'relict' (inactive at present) to one degree or another, but the entire ridge system can be moved by the gradual erosion and redeposition of sand ridge sediment due to current activity, given sufficient time. Whether any, or all, of the Holocene

depositional units are found at a particular location is a function of past and present erosional processes related to shoreface ravinement, tidal ravinement, and current scour.

Stating that the sand ridge is active requires careful definition of terms:

structurally, the sand ridge can encompass several distinct layers within its relief (Rine et al., 1986, 1991; Snedden et al., 1994), each of which may have formed at different times. Morphologically, the shape and orientation of sand ridges are governed by the sum of erosional processes past and present. Movement of the ridge is accomplished by erosion of existing sediments, differential transportation of the sediments, and redeposition of some sediments within the existing fluid dynamic regime. This does not mean that all layers are active, nor that the sand ridge layers will move as one unit. Rather, in regions where shelf currents have eroded to beneath the H_3 layer (figure 17) and have mobilized H_2 , H_1 , or P sediments (see also Rine et al., 1986), only the coarse fraction will be redeposited on or near the sand ridge.

Various evidence exists for active transportation of sediments on the continental shelf. McClennen (1973) investigated current activity around inner shelf sand ridges and determined that currents were sufficiently strong, particularly during storm activity, to induce movement in the upper meter of sediment at inner- to mid-shelf water depths. Stubblefield et al., (1975) used petrographic data from grab samples and Vibracores on the central New Jersey shelf to conclude that up-flank suspensive transport occurred during intense storm activity. Shell ages within the New Jersey inner shelf sand ridges (Rine et al., 1986, 1991) are inconsistent and highly variable within short vertical distances, again supporting the hypothesis of sediment reworking and redeposition within the upper sand ridge structure (H_3 sediment). H_3 sediments which were recovered during

the coring operation are composed of a variety of large clast sizes, but universally contain no clay and virtually no silt. The lack of silt and clay sediments within the sand ridge structure, in a region with abundant quantities of such sediment close to the sea-floor in inter-ridge swales, suggests that energy levels on and around the sand ridges are too great to permit the deposition of muds but low enough to permit deposition of the more coarse sediments on the ridge crests.

The existence of strong, fair weather currents along ridge crests is supported by modern current studies (Glenn and Henderson, 1991, 1992, 1993, 1994) and observations during the seismic cruise by divers who investigated Avalon Shoal sand ridge during calm weather conditions. I suggest that sand ridge structures are in quasi-equilibrium with modern shelf currents. Many have been in existence for a few thousand years, but all are being constantly reworked by currents. Much of this activity probably takes place during storm events when current velocities on the inner shelf are sufficient to transport sand and gravel, and the along-shore/cross-shore current components are consistent with the orientation of the inner shelf sand ridges (Glenn and Henderson, 1991, 1992, 1993, 1994). Preserved bedding structures within the core sections also show sharp variations in average grain size which may be directly related to sharp changes in current velocities before, during, and after storm events.

McBride and Moslow (1991) suggested that ridges were associated with barriers because of the necessity of concentrating sand by tidal inlets. Other geomorphological evidence suggests that sand ridge development is independent of, and unrelated to, that of barrier islands, tidal channels, or tidal deltas. Although sand ridges and barrier islands tend to be of approximately the same size, differences exist. Barrier island systems trend

parallel with the shoreline, whereas sand ridges trend oblique to the shoreline, typically up to 30° obliquity. Most sand ridge systems are not parallel to any existing or inferred paleoshoreline, but parallel the orientation of modern shore attached ridges. Modern shore attached ridges near the study area exhibit similar internal structures and stratigraphy to many shore detached ridges (Snedden et al., 1994) and evolve concurrently with, but as separate entities to, the barrier island system. The physical similarity between shore attached and shore detached ridges has been noted by other authors (Stubblefield et al., 1984; Swift et al., 1981) and led to the suggestion that shore detached ridges evolved from shore attached ridges. Whether or not the different ridge types are genetically related to each other, their great morphological and structural similarity certainly confirms that shelf processes are able to form ridge structures seaward of barrier island systems.

The sand ridges examined on the New Jersey inner shelf exhibit asymmetrical axial profiles which produce long, gradual slopes (0.006) from northern to southern ends, followed by a precipitous reversal of slope (minimum of 0.116) at the southern terminus. This abrupt escarpment does not appear to have developed as a relict tidal channel between sand ridges since there are no symmetrical sand ridge systems opposite the ridges' ends. Sand ridge orientation and morphology also differs from barrier island tidal deltas in that tidal deltas tend to develop perpendicular to the barrier island, and exhibit a much more broad morphology than do sand ridges. Furthermore, tidal deltas are smaller features than the barrier islands with which they are associated, and no barrier type structures exist which could be associated with the offshore sand ridges.

Finally, the morphological shape of sand ridges is governed by their apparent relief relative to the bathymetric lows surrounding them. Because there is ample evidence of

current erosion at the periphery of ridges where scouring has eroded to beneath the S_2 plane (figure 17; see also Rine et al., 1991; Snedden et al., 1994), the relief (and orientation) of the ridge must be due, at least in part, to modern current activity. These characteristics of ridge morphology, composition and orientation directly contradict the models of ridge development which interpret ridges as drowned or overstepped barrier island systems. Instead, ridge development appears to be multi-staged within a modern, continuing process of current controlled erosion and redeposition. Clear evidence that modern sedimentation processes are altering ridge morphology is found within two recovered sediment cores (AV-01 and AV-07; figure 7) in which oil was recovered. The depth of the oil beneath a clean, coarse sand layer clearly demonstrates that sediment is prograding over the end of the ridge escarpment in a manner similar, perhaps, to that of giant dunes. The minimum vertical accumulation rates of 1-2 m /100 yr which are occurring at 10 km distance from the shoreline are conclusive of active shelf transport of coarse grained sediment, and cannot reasonably be attributed to new sediment transported from river systems at the shoreface. Strong currents, particularly during storm events, have eroded through the H_1 and H_2 sediments and into the Pleistocene sediments at the base of inner shelf sand ridges (i.e. figure 17), thus providing ample sediments for redeposition.

CONCLUSIONS AND SUMMARY

Stratigraphy

Near-surface stratigraphy is comprised of five distinct lithofacies separated by two regional unconformities (S_1 , S_2). Older Tertiary (T) sediments are found at depth beneath the S_1 unconformity and are not characterized due to lack of recovery during the field coring operations. Pleistocene sediments (P_1 , P_2) are found between the S_1 and S_2 unconformities, as well as at the seafloor in areas of locally active erosion. These sediments vary from fine grained muds to very coarse grained sand and gravel.

Holocene sediments (H_1 , H_2 , H_3) comprise three lithofacies separated by one to two regional surfaces (R_1 , R_2). H_1 estuarine sediments are found ubiquitously and underlie the R_2 ravinement surface. These sediments are composed of fine grained muds and fine sand, are often interbedded, and frequently contain abundant shell material. H_2 facies are found intermittently and formed concurrently with the R_1 tidal ravinement unconformity. H_2 sediment is composed of medium to coarse sand and fine gravel. The H_3 sand ridge facies is ubiquitous in the study area and formed as a result of complex tidal interactions with shelf sediments. Sediment comprising the H_3 facies is predominantly coarse grained sand and gravel with variable proportions of shell material. Silt and clay are generally found in very low quantities or are absent altogether from the unit.

Sand Ridge Evolution

Sand ridges are complex structures which must be understood within an appropriate depositional and stratigraphic framework. Sand ridge morphology is a

function of past and present erosional processes within an active shelf setting. Orientation of the sand ridge is governed by modern current flow directions which act to continually erode and redeposit shelf sand and sand ridge sediments in an active depositional regime. Sand ridge morphology is determined by the relative proportion of the three Holocene lithofacies found in a given location, the accumulation patterns of the H_3 sediment in response to tidal and storm induced current activity, and the erosional patterns in inter-ridge swales. Sand ridge relief can exceed the height of the combined Holocene sediments in regions where current activity at the base of the sand ridge has eroded into the underlying Pleistocene sediments. Inner shelf ridge systems trend obliquely to the shoreline (30°) and exhibit axial and cross-axial asymmetry. Ridge systems are ephemeral at any location and are able to (slowly) migrate in response to changing dynamic conditions on the inner shelf. The oil layer of possible WWII origin indicates a vertical sedimentation rate of 1 m/50 years. This corresponds to a lateral migration rate of 1.73 m/50 years, assuming a 30° angle of repose for sands.

Remediation Potential

Regardless of their formative mechanism, shore detached sand ridges contain abundant sediment which is suitable for beach remediation projects. Mean grain size of the H_1 sediments indicate that the sediment size falls within the parameters required (0.25-4.00 mm; medium sand to gravel) for beach remediation sediment fill (see appendix for complete statistical characterization of samples). H_3 sediment contains very high concentrations of medium to coarse sand (>70%) with most of the remainder comprising the gravel fraction. Little to no (<5%) mud is found within H_1 sediments. Conservative

estimates of sand ridge volumes yields over 85 million cubic meters (113 million cubic yards) of usable sediment within the inner sand ridge (northern region) and Avalon Shoal. These sand ridges are within economic range of high priority remediation sites between Townsends and Hereford Inlets, and may be within economic distances of remediation sites south of Townsends Inlet (figure 1). Most of the sediment within the sand ridges lies at depths of less than 20 meters, well within standard dredging limitations. Another +100 million cubic meters of usable sediment probably is contained in the other southern area ridges.

H₁-type sediments, though ubiquitous in the region, do not generally comprise a significant portion of the sand ridge volume (<15% based upon seismic cross-section estimates). This material underlies the sand ridge and, as such, poses no impediment to mining activities. In regions where the stratigraphic thickness of fine grained sediments exceeds a few meters, the sediments generally fill well defined acoustic depressions and are easily mappable in seismic profile.

Usable quantities (> 3 m) of older, coarse coastal plain sediments underlie much of the survey region. These sediments were most likely deposited in a fluvial environment during the stage 2 lowstand and are comprised of relatively mud free coarse quartz sand and gravel. Though the exact stratigraphic thickness of these deposits were not determined in core section, seismic analysis indicates that they may locally exceed 7 meters. Because the sediments may represent shallow channel fill, these deposits may be sinuous in nature and require careful mapping using closely spaced seismic data.

Another potentially valuable source of sediment is found underlying the S₂ unconformity in the northern region, where relatively steeply dipping (0.013m/m)

clinoforms suggest the existence of a baymouth shoal complex. This sediment is areally abundant, relatively shallow in depth, and found in close proximity to the modern shoreline. Because it does not form part of a sand ridge or other positive relief feature, this sediment may be more favorable for mining should sand ridge mining be deemed impractical or ecologically threatening. Other smaller relief features are abundant in the study area and may represent smaller sand shoals. They are not well resolved using a seismic line spacing of 2 km, but may be mappable with a more closely spaced seismic grid. If they contain sand ridge type sediment, they may represent an abundant alternative resource to the larger sand shoals.

Summary

Two sand ridge structures in federal waters off of Avalon Township, New Jersey contain at least 85 million cubic meters (113 million cubic yards) of well sorted quartz sand with median diameter of 0.57 mm (coarse sand) which may be of potential use as beach remediation material. These inner shelf sand ridges are located within 10 km of high priority remediation areas and in water depths of under 20 m, and can offer a viable resource to help maintain the southern New Jersey beach system.

References Cited

- Alpine Ocean Seismic Survey, Inc., 1988, Identification and delineation of potential borrow areas for the Atlantic coast of New Jersey, Asbury Park to Manasquan: final supplementary report, detailed investigation of Sea Bright sand borrow areas: Vol. 1, contract #DACW51-87-C-0011, modification # P00002, for U.S. Army Corps of Engineers, New York District.
- Alpine Ocean Seismic Survey, Inc., 1994, Offshore Vibracore sampling for NJDEPE: Final Report, New Jersey Solicitation X-21177, AOSS Contract #1185, Norwood, New Jersey, 42 pp.
- Ashley, G. M., 1987, Barnegat Inlet, Tidal Prism Study, Final Report, U. S. Army Corps of Engineers, Philadelphia District, 60 pp.
- Ashley, G. M., Halsey, S. D., and Farrell, S. C., 1987, A study of beach fill longevity: Long Beach Island, N.J., Coastal Sediments '87, A.S.C.E., New York, p. 1188-1202.
- Ashley, G. M., Sheridan, R. E., and Wellner, R. W., 1988, Seismic stratigraphy and depositional history of the ebb-tidal delta and linear shoal complex, Barnegat Inlet, New Jersey: N.J.D.E.P.E. Division of Coastal Resources Technical Report, 28 pp.
- Ashley, G. M., Wellner, R. W., Esker, D., and Sheridan, R. E., 1991, Clastic sequences developed during late Quaternary glacio-eustatic sea-level fluctuations on a passive margin: Example from the inner continental shelf near Barnegat Inlet, New Jersey: GSA Bulletin, 103:1607-1621.
- Ashley, G. M., and Sheridan, R. E., 1994, Depositional model for valley fills on a passive continental margins, *in* Incised-valley Systems: Origin and Sedimentary Sequences, SEPM Special Publication 51, p. 285-301.
- Bloom, A. L., Broecker, W. S., Chappell, J. M. A., Mathews, R. K., and Mesoella, K. J., 1974, Quaternary sea-level fluctuations on a tectonic coast: New $^{230}\text{Th}/^{234}\text{U}$ dates from the Huon Peninsula, New Guinea: Quaternary Research, 4: 185-205.
- Boczar-Karakiewicz, B., Amos, C. L., and Drapeau, G., 1990, The origin and stability of sand ridges on Sable Island Bank, Scotian Shelf: Continental Shelf Research, 10: 683-704.
- Boczar-Karakiewicz, B., and Bona, J. L., 1986, Wave dominated shelves: A model of sand-ridge formation by progressive infragravity waves, *in* Knight, R. J., and McLean, J. R., eds., Shelf Sands and Sandstones, Canadian Society of Petroleum Geologists, Memoir II, p. 163-179.
- Braatz, B. V., and Aubrey, D. G., 1987, Recent relative sea-level change in Eastern North America, *in* Nummedal, D., and others, eds., Sea-level Fluctuation and Coastal Evolution: SEPM Special Publications, 41: 29-46.
- Brinkhuis, B. H., 1980, Biological effects of sand and gravel mining in the lower bay of New York Harbor: an assessment from the literature: Special Report 34, Reference No. 80-1. Prepared for the Marine Sciences Research Center, Stony Brook, NY, 11 pp.
- Carey, J. S., Sheridan, R. E., and Ashley, G. M., 1995, Late Pleistocene sequence stratigraphy of the New Jersey continental shelf, AAPG Abstracts, Annual Convention, P. 15A.

- Caston, V. N. D., 1972, Linear sand banks in the southern North Sea: *Sedimentology*, 18: 63-78.
- Chappell, J. and Shackleton, N. J., 1986, Oxygen isotopes and sea-level: *Nature*, 324: 137-140.
- Conkwright, R. D. and Gast, R. A., 1994, Potential offshore sand resources in central Maryland shoal fields; Coastal and Estuarine Geology, File report No. 94-9, Maryland Geological Survey, Department of Natural Resources, 40 pp.
- Cousins, P., Dillon, W. P., and Oldale, R. N., 1977, Shallow structure of sediments of the U.S. Atlantic shelf, Long Island, NY to Norfolk, VA: U.S. Geological Survey Cruise Report, 23 p.
- Christie-Blick, N., Mountain, G. S., and Miller, K. G., 1990, Seismic stratigraphic record of sea-level change, *in* Revelle, R., ed., Sea Level Change; National Research Council, Studies in Geophysics, Washington, D.C., National Academy Press, p. 116-140.
- Dalrymple, R. W., 1992, Tidal Depositional Systems, *in* Walker, R. G., and James, N. P., eds., Facies Models: Response to Sea level change, edition 3, Geological Association of Canada, p. 195-218.
- Dalrymple, R. W., Zaitlin, B. A., and Boyd, R., 1992, Estuarine facies models: conceptual basis and stratigraphic implications: *Journal of Sedimentary Petrology*, 62: 1130-1146.
- Dill, C. E., and Miller, H. J., 1982, Bathymetric and geologic study of a proposed outfall at Avalon, New Jersey (Appendix C), *in* Wastewater Handling Facilities, Cape May County, Converse Consultants, Inc., 17: 1-18.
- Duane, D. B., Field, M. E., Meisburger, E. P., Swift, D. J. P., and Williams, S. J., 1972, Linear shoals on the Atlantic inner shelf, Florida to Long Island, *in* Swift, D. J. P., Duane, D. B., and Pilkey, O. H., eds., Shelf Sediment Transport: Process and Pattern, Dowden Hutchinson and Ross, Inc., Stroudsburg, PA, p. 447-498.
- Emery, K. O., 1966, Atlantic continental shelf and slope of the United States geologic background: U.S. Geological Survey Professional Paper, 529-A, 23 pp.
- Emery, K. O., 1968, Relict sediments on continental shelves of the world: *Bulletin of the American Association of Petroleum Geologists*, 52: 445-64.
- Emery, K. O., and Uchupi, E., 1972, Western North Atlantic Ocean, American Association of Petroleum Geologists, Tulsa, OK, 532 pp.
- Emery, K. O., and Uchupi, E., 1984, The Geology of the Atlantic Ocean, Springer, New York, NY, 1050 pp.
- Farrell, S. C., Meggison, A., Lyons, T., and Hafner, S., 1993, The New Jersey beach profile network analysis of the shoreline changes for reaches 1-15, Raritan Bay to Stow Creek, New Jersey, New Jersey Department of Environmental Protection Contract # 1219, Trenton, New Jersey.
- Fletcher, C. H., III, Knebel, H. J., and Kraft, J. C., 1992, Holocene depocenter migration and sediment accumulation in Delaware Bay: a submerging marginal marine sedimentary basin: *Marine Geology* 103: 165-183.
- Folk, R. L., 1980, Petrology of Sedimentary Rocks, Hemphill Publishing Company, Austin, Texas, 185 pp.
- Fray, C. T., and Ewing, J., 1961, Project 555, Monmouth County offshore borings, CU

- report no. 1, New Jersey Department of Conservation and Economic Development.
- Feeley, M. H., Moore, T. C., Jr., Loutit, T. S., and Bryant, W. R., 1990, Sequence stratigraphy of the Mississippi fan related to oxygen isotope sea level index; *American Association of Petroleum Geologists Bulletin*, 74: 407-424.
- Gale, S. J., and Hoare, P. G., 1991, Quaternary Sediments, Halsted Press, New York, New York, 323 pp.
- Glenn, S. M., and Henderson, L. J., 1991, LEO-15 preliminary data summary: Report #1, Institute of Marine and Coastal Sciences, Rutgers University, New Brunswick, NJ, 5 pp.
- Glenn, S. M., and Henderson, L. J., 1992, LEO-15 preliminary data summary: Report #2-5, Institute of Marine and Coastal Sciences, Rutgers University, New Brunswick, NJ, 24 pp.
- Glenn, S. M., and Henderson, L. J., 1993, LEO-15 preliminary data summary: Report #6, Institute of Marine and Coastal Sciences, Rutgers University, New Brunswick, NJ, 6 pp.
- Glenn, S. M., and Henderson, L. J., 1994, LEO-15 preliminary data summary: Report #8, Institute of Marine and Coastal Sciences, Rutgers University, New Brunswick, NJ, 6 pp.
- Hine, A. C., and Snyder, S. W., 1985, Coastal lithosome preservation: Evidence from the shoreface and continental shelf of Bogue Banks, North Carolina: *Marine Geology*, 63: 307-330.
- Huthnance, J. M., 1973, Tidal current asymmetries over the Norfolk sandbanks: *Estuarine and Coastal Marine Science*, 1: 89-99.
- Huthnance, J. M., 1982, On the mechanism forming linear sand banks: *Estuarine, Coastal and Shelf Science*, 14: 79-99.
- James, W. R., 1975, Techniques in evaluating suitable borrow material for beach nourishment: Technical Memorandum 60, U. S. Army Corps of Engineers, CERC, Ft. Belvoir, VA.
- Knebel, H. J., and Spiker, E., 1977, Thickness and age of surficial sand sheet, Baltimore Canyon trough area: *American Association of Petroleum Geologists Bulletin*, 61: 861-871.
- Kraft, J. C., 1969, Sedimentary facies patterns and geologic history of a Holocene marine transgression: *Geological Society of America Bulletin*, 82: 2131-2158.
- Lavelle, J. W., Gadd, P. E., Han, G. C., Mayer, D. A., Stubblefield, W. L., Swift, D. J. P., Charnell, R. L., Brashear, H. R., Case, F. N., Haff, K. W., and Kunselman, C. W., 1976, Preliminary results of coincident current meter and sediment transport observations for wintertime conditions on the Long Island inner shelf: *Geophysical Research Letters*, 3: 97-100.
- Mayewski, P. A., Daton, G. H., and Hughes, T. J., 1981, Late Wisconsinan ice sheets of North America in Denton, G. H. and Hughes, T. J., eds., *The Last Great Ice Sheets*: New York, John Wiley & Sons, p. 67-178.
- McBride, R. A., and Moslow, T. F., 1991, Origin, evolution, and distribution of shoreface sand ridges, Atlantic inner shelf, U.S.A.: *Marine Geology*, 97: 57-85.
- McClennan, C. E., 1973, New Jersey continental shelf near bottom current meter records

- and recent sediment activity: *Journal of Sedimentary Petrology*, 43: 371-380.
- McClennan, C. E., 1983, Middle Atlantic nearshore geologic hazards off the New Jersey coastline, *in* McGregor, B. A., ed., Environmental geologic studies in the United States Mid- and North Atlantic Outer Continental Shelf Area, v. II, Mid-Atlantic Region: U.S. Geological Survey Report, p. 9-1 to 9-16.
- McClennan, C. E., and McMaster, R. L., 1971, Probable Holocene transgression effects in the geomorphic features of the continental shelf off of New Jersey, United States: *Marine Sedimentology*, 7: 69-72.
- McKinney, T. F., and Friedman, G. M., 1970, Continental shelf sediments of Long Island, New York: *Journal of Sedimentary Petrology*, 40: 213-248.
- McMaster, R. L., 1954, Petrography and genesis of the New Jersey beach sands: *New Jersey Geological Survey Bulletin* 63, Trenton, New Jersey, 238 pp.
- Meisburger, E. P., and Williams, S. J., 1980, Sand resources on the continental shelf of the Cape May region, New Jersey, *Miscellaneous Report #80-4*, U. S. Army Corps of Engineers, Coastal Engineering Research Center, Ft. Belvoir, VA, 40 pp.
- Meisburger, E. P., and Williams, S. J., 1982, Sand resources on the inner continental shelf off of the Central New Jersey Coast, *Miscellaneous Report #82-10*, U.S. Army Corps of Engineers, Coastal Engineering Research Center, Ft. Belvoir, VA, 49 pp.
- Miller, H. J., Dill, C., and Tirey, G. B., 1973, Geophysical investigation of the Atlantic Generating Station site and region: *Alpine Geophysical Association Technical Report*, Norwood, NJ, 56. pp.
- Miller, K. G., Kent, D. V., Brower, A. N., Bybell, L. M., Feigenson, M. D., Ollson, R. K., and Poore, R. Z., 1990, Eocene-Oligocene Sea-level changes on the New Jersey Coastal Plain linked to the deep-sea record: *Geological Society of America Bulletin*, 102: 331-339.
- Mullikin, L. G., 1990, Records of selected wells in Atlantic County, New Jersey: *New Jersey Geological Survey Report GSR 22*, 82 pp.
- New Jersey Shore Protection Update Bulletin, June 1994, Number 5, U.S. Army Corps of Engineers, Philadelphia, 6 pp.
- Nichols, M. M., 1989, Sediment accumulation rates and relative sea-level rise in lagoons *in* Ward, L. and Ashley, G., eds., *Physical Processes and Sedimentology of Siliclastic-Dominated Lagoonal Systems*: *Marine Geology*, 88: 201-209.
- Nummedal, D. and Swift, D., J., P., 1987, Transgressive stratigraphy at sequence-bounding unconformities: some principles derived from Holocene and Cretaceous examples *in* Nummedal, P., Pilkey, O. H., and Howard, D. J., eds., *Sea-Level Fluctuation and Coastal Evolution*: Tulsa, SEPM Special Publication 41, p. 241-260.
- Off, T., 1963, Rhythmic linear sand bodies caused by tidal currents: *Bulletin of the American Association of Petroleum Geologists*, 47: 324-341.
- Penland, S., Suter, J. R., and Moslow, T. F., 1986, Inner-shelf shoal sedimentary facies and sequences: Ship Shoal, northern Gulf of Mexico, *in* Moslow, T. F., and Rhodes, E. G., eds., Modern and Ancient Shelf Clastics: a Core Workshop, SEPM Core Workshop #9, p. 73-123.
- Posamentier, H. W. and Vail, P. R., 1989, Eustatic controls on clastic deposition II: sequence and system tract models *in* Wilgus, C. K. et al., eds., *Sea-level Changes:*

- An Integrated Approach: SEPM Special Publications 42, p. 125-154.
- Reison, G. E., 1991, Transgressive barrier island and estuarine systems, *in* Walker R. G., and James, N. P., eds., Facies Models: Response to Sea Level Change: St. Johns, Geological Association of Canada, p. 179-194.
- Riggs, S. R., and Belknap, D. F., 1988, Upper Cenozoic processes and environments of continental margin sedimentation; eastern United States, *in* Sheridan, R. E., and Grow, J. A., Eds., The Geology of North America, V 1-2: The Atlantic Continental Margin, U. S., Geological Society of America.
- Rine, J. M., Tillman, R. W., Stubblefield, W. L., and Swift, D. J. P., 1986, Lithostratigraphy of Holocene sand ridges from the nearshore and middle continental shelf of New Jersey, U.S.A., *in* Moslow, T. F., and Rhodes, E. G., eds., Modern and Ancient Shelf Clastics: A Core Workshop, SEPM Core Workshop #9, p. 1-72.
- Rine, J. M., Tillman, R. W., Culver, S. J., and Swift, D. J. P., 1991, Generation of late Holocene sand ridges on the middle continental shelf of New Jersey, USA: Evidence for formation in a mid-shelf setting based on comparisons with a nearshore ridge, *in* Swift, D. J. P., Oertel, G. F., Tillman, R. W., and Thorne, J. A., eds., Shelf Sand and Sandstone Bodies, Special Publication of the International Association of Sedimentologists, Blackwell Scientific Publications, 14: 395-423.
- Sanders, J. E., and Kumar, N., 1975, Holocene shoestring sand on inner continental shelf off Long Island, New York: American Association of Petroleum Geologists Bulletin, 59: 997-1009.
- Schlee, J., and Pratt, R., 1972, Atlantic continental shelf and slope of the United States: U.S. Geological Survey Professional Paper 529-H.
- Scott, J. T., and Csanady, G. T., 1976, Nearshore currents off of Long Island: Journal of Geophysical Research, 81: 5401-5409.
- Shepard, F. P., 1963, Submarine Geology, Harper and Row, New York, NY, 557 pp.
- Sheridan, R. E., Dill, C. E., Jr., and Kraft, J. C., 1974, Holocene sedimentary environments of the inner continental shelf off Delaware: Geological Society of America Bulletin, 85: 1319-1328.
- Sheriff, R. E. and Geldart, L. P., 1982-83, Exploration Seismology (2 v.): Cambridge University Press, New York.
- Snedden, J. W., Tillman, R. W., Kreisa, R. D., Schweller, W. J., Culver, S. J., and Winn, R. D. Jr., 1994, Stratigraphy and genesis of a modern shoreface-attached sand ridge, Peahala Ridge, New Jersey: Journal of Sedimentary Research, B64: 560-581.
- Stearns, F., 1969, Bathymetric maps and geomorphology of the middle Atlantic continental shelf: *Fish. Bull.*, 68: 37-66.
- Stubblefield, W. L., Lavelle, J. W., Swift, D. J. P., and McKinney, T. F., 1975, Sediment response to the present hydraulic regime on the central New Jersey shelf: Journal of Sedimentary Petrology, 45: 337-358.
- Stubblefield, W. L., McGrail, D. W., and Kersey, D. G., 1984, Recognition of transgressive and post-transgressive sand ridges on the New Jersey Continental Shelf, *in* Tillman, R. W., and Siemers, C. T., eds., Siliciclastic Shelf Sediments, SEPM Special Publication # 34, Tulsa, OK, p.1-23.

- Swift, D. J. P., Duane, D. B., and McKinney, T. F., 1973, Ridge and swale topography of the Middle Atlantic Bight, North America: Secular response to the Holocene hydraulic regime: *Marine Geology*, 15: 227-247.
- Swift, D. J. P., and Field, M. E., 1981, Evolution of a classic sand ridge field: Mayland sector, North American inner shelf: *Sedimentology*, 28: 461-482.
- Swift, D. J. P., Young, R. A., Clarke, T. L., Vincent, C. E., Niedoroda, A., and Lesht, B., 1981, Sediment transport in the middle bight of North America; synopsis of recent observations: *International Association of Sedimentologists Special Publication*, 5: 361-383.
- Toscano, M. A. and York, L. L., 1992, Quaternary Stratigraphy and sea-level history of the U. S. Middle Atlantic Coastal Plain: *Quaternary Science Reviews*, 11: 301-328.
- Uchupi, E., 1968, Atlantic continental shelf and slope of the United States: *Physiography: U.S. Geological Survey Professional Paper 529C*, 30 pp.
- Uchupi, E., 1970, Atlantic continental shelf and slope of the United States: *Shallow structure: U.S. Geological Survey Professional Paper 600D*, 231-234.
- Uptegrove, J., Mulliken, L. G., Waldner, J. S., Ashley, G., Sheridan, R., Hall, D., Gilroy, J., Farrell, S., 1995, Characterization of offshore sediments in federal waters as potential sources of beach replenishment sand--Phase I: *New Jersey Geological Survey Open File Report OFR 95-1*, 148 pp.
- U.S. Army Corps Of Engineers, 1991, *Hydrographic surveying manual*, EM 1110-2-1003: 123 pp.
- U.S. Army Corps of Engineers General Design Memorandum, 1989, V. II, Technical Appendix, Sandy Hook to Barnegat Inlet, Army Corps of Engineers, New York, v.11.
- Vail, P. R., Mitchum, R. M., Jr., Todd, R. G., Widmier, J. M., Thompson, S., III, Sangree, J. B., Bubb, J. N., and Hatlelid, W. G., 1977, Seismic stratigraphy and global changes in sea level, *in* Payton, C. E., Ed., Seismic Stratigraphy: Applications to Hydrocarbon Exploration, American Association of Petroleum Geologists Memoir 26, Tulsa, OK, p. 49-212.
- Vail, P. R. and Todd, R. G., 1981, Northern North Sea Jurassic unconformities, chronostratigraphy, and sea-level changes from seismic stratigraphy *in* *Petroleum Geology of the Continental Shelf of North-West Europe*, Illing, L. v. and Hobson, G. D., eds., Heydon and Son, London, p. 216-235.
- Van Veen, J., 1935, Sand waves in the North Sea: *Hydrography Review*, 12: 21-28.
- Van Wagoner, J. C., Mitchum, Jr., R. M., Posamentier, H. W., and Vail, P. R., 1987, Seismic stratigraphy interpretation using sequence stratigraphy, Part 2: Key definitions of sequence stratigraphy, *in* *Atlas of Seismic Stratigraphy*, A. W. Bally, Ed., *Studies in Geology No. 27*, American Association of Petroleum Geologists, Tulsa, Oklahoma, p. 11-14.
- Veatch, A. C., and Smith, P. A., 1939, Atlantic submarine valleys of the United States, and the Congo submarine valley: *Geological Society of America Special Paper*, 7: 101 pp.
- Waldner, J. S., and Hall, D. W., 1991, A marine seismic survey to delineate Tertiary and Quaternary stratigraphy of coastal plain sediments offshore of Atlantic City, New

- Jersey: New Jersey Geological Survey Report GSR 26, 15 pp.
- Walker, R. G., 1992, Facies, facies models, and modern stratigraphic concepts, *in* Facies Models: Response to Sea Level Change, Walker, R. G., and James, N. P., eds., Geological Association of Canada, St. John's, Newfoundland, Canada, p. 1-14.
- Weimer, P., 1989, Sequence stratigraphy of the Mississippi fan (Plio-Pleistocene), Gulf of Mexico: *Geo-Marine Letters*, 9: 185-172.
- Wellner, R. E., Ashley, G. M., and Sheridan, R. E., 1993, Seismic stratigraphic evidence for a submerged Mid-Wisconsin barrier: Implications for sea-level history: *Geology*, 21: 109-112..
- Wellner, R. E., 1990, High-resolution seismic stratigraphy and depositional history of Barnegat Inlet, New Jersey and vicinity: Masters Thesis, Rutgers University, New Jersey, 109 pp.
- Williams, S. J., and Duane, D. B., 1974, Geomorphology and sediments of the inner New York Bight continental shelf: U.S. Army Corps of Engineers, Coastal Engineering Research Center, Technical Memoir 45, 81 pp.

APPENDIX A

Preliminary
Core Logs

Avalon Shoal Area
Avalon, New Jersey

Appendix A: Guide to Core Interpretations

Core sections that are shown offset indicate a re-cored section which was recovered from a subsequent cast position. Recasts were positioned within 10-meters of the initial position. Depths shown are based upon penetrometer data for each cast, and begin at the seafloor. Interpreted tie-points (as indicated by unconformities) may show an offset from the other casts due to the measurement method.

Cores were split into two half-sections. 10-cm samples were collected from section 'A' for grain size analysis at the intervals indicated on the core logs (sample). Not all of the collected samples were analyzed (see Appendix C). Remaining sediment from section 'A' was composited into 1-gallon bags over the intervals indicated (composite). Core section 'B' was archived.

CORE: AV-01

Depth (m)	Stratigraphic Section	Composite Sample	Fossils	Color	Facies	Lithological Description <i>(Preliminary Description)</i>
0		AVC-021		2.5Y 7/3		Interbedded coarse to very coarse sand and gravel beds which vary from 5-40 cm in thickness.
1		AVC-022				
2		AVC-023	☛	Black	Upper Sand Ridge	Sediment in the lower portion of the core sections is saturated with a black, oily substance.
		AVC-024		5Y 4/1		
3		AVC-025		Black		
		AVC-027		2.5Y 7/3		
4		AVC-026	☛	Black		
5						
6						

Recovery Date: 9-3-94

Latitude: 39° 07' 15.56"

Longitude: 74° 38' 10.72"

Water Depth: 32 feet (9.75 m)

Describers: Peter C. Smith & Matthew Goss

CORE: AV-02

Depth (m)		Composite	Sample	Fossils	Color	Facies	Lithological Description <i>(Preliminary Description)</i>	
0		AVC-001	001		2.5Y 5/4 Light Olive Brown	Upper Sand Ridge	Coarse to very coarse sand and gravel, with pebbles.	
1		AVC-002	002					
		AVC-003	003					
2		AVC-004	004		N7/ Lt. Gray			Silty, fine sand.
		AVC-004	005		5Y 6/1 Gray			Coarse sandy gravel and pebbles, bioturbated.
			006		5B 5/1 Bluish Gray			Gravelly coarse sand, sulfur smell.
	3	AVC-005	007		5Y 6/3	Upper Sand Ridge	Gravelly, coarse sand.	
4	AVC-006	008						
		009		5GY 7/1	Nearshore/ Estuarine	Silty medium sand with gravel.		
	010		5GY 4/1	Coarse gravel.				
	011		5Y 5/1	Fine to medium sand.				
	AVC-007	012		5GY 6/1		Sandy gravel with rounded quartz fragments.		
		013		5Y 6/1		Fine to medium sand.		
	5				N4/		Fossil rich, muddy, quartzose sand.	
6								

Recovery Date: 9-7-94

Latitude: 39° 07' 49.26"

Longitude: 74° 37' 32.33"

Water Depth: 28 feet (8.53 m)

Describers: Peter C. Smith & Matthew Goss

CORE: AV-03

Depth (m)		Composite	Sample	Fossils	Color	Facies	Lithological Description (Preliminary Description)
0		AVC-008	014	☛	2.5Y 7/3 Pale	Upper Sand Ridge	Medium to coarse bedded sand and gravel, with only a few pebbles. Some heavy mineral laminations are visible. Some dark staining of sediments at the bottom of the core section, probably from bleeding of the sock which was put on the core-catcher.
			015		Yellow		
1		AVC-009	016	☛			
		017					
		018					
2		AVC-010	019	☛			
		020		☛			
3							
4							
5							
6							

Recovery Date: 9-3-94


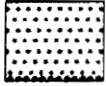
Latitude: 39° 07' 43.39"

Longitude: 74° 35' 53.35"

Water Depth: 23 feet (7.01 m)

Describers: Peter C. Smith & Matthew Goss

CORE: AV-04

Depth (m)		Composite	Sample	Fossils	Color	Facies	Lithological Description (Preliminary Description)	
0		AVC-045	057		2.5Y 7/3	Sand Ridge	Shell-rich medium sand.	
1		AVC-046	058		5GY 4/1		Dark Green Gray	Shell-rich coarse sand and gravel with black pebble clasts. Dark brown globs of sediment, possibly oil saturated.
		AVC-047	059					Shell bed.
		AVC-043	060					Medium to fine sand.
2		AVC-044						Coarse sand and gravel.
		AVC-047	061					Medium to fine sand.
		AVC-048	062		5Y 8/1 to 5Y 7/2		Pleistocene Sediments	Medium to fine white sand with clay pods (possibly burrow traces); gradational into gravel beds at 2.05m and 2.35 m.
		AVC-048	063		White			
		AVC-049			5Y 7/4 Pale Yellow			
AVC-050		064		N8/ White				Very coarse sand and gravel with pebbles; coated with white clay.
AVC-050	065		5Y 7/8 Yel		Same as above, but yellow.			
3								
4		AVC-051			2.5Y 7/8 Yellow	Pleistocene Sediments	Coarse sand with fine laminae of heavy mineral; coarse sand and gravel at base.	
5								
6								

Recovery Date: 9-3-94

Latitude: 39° 07' 08.89"

Longitude: 74° 36' 32.88"

Water Depth: 48 feet (14.6 m)

Describers: Peter C. Smith & Matthew Goss

CORE: AV-05

Depth (m)	Composite	Sample	Fossils	Color	Facies	Lithological Description (Preliminary Description)
0		066		5Y 7/1 Light Gray	Shelf Sand	Medium sand.
		067		5Y 3/1 V. Dark Gray	Estuarine	Green Clay.
		068		5Y 7/1 Light Gray	Lag	Sand with gravel.
1	AVC-062	069		5Y 7/1 Light Gray		Sand with some gravel.
		070		N 5/ Gray	Tidal Channel	Color contact only.
	AVC-064	071		2.5Y 7/3 Pale Yellow		Medium sand.
2		072			Lag	1.83-1.87 m. : clay laminae underlain by coarse gravel.
		073				
	AVC-065	074		N5/ Gray		
3		075				
	AVC-066	077				
		078		N5/	Estuarine	Sand-silt-clay laminae.
						Muddy sand.
4	AVC-067	079		5BG 4/1 Dark Greenish Gray	Tidal Channel	Sand and gravel.

R₁

Recovery Date: 8-31-94

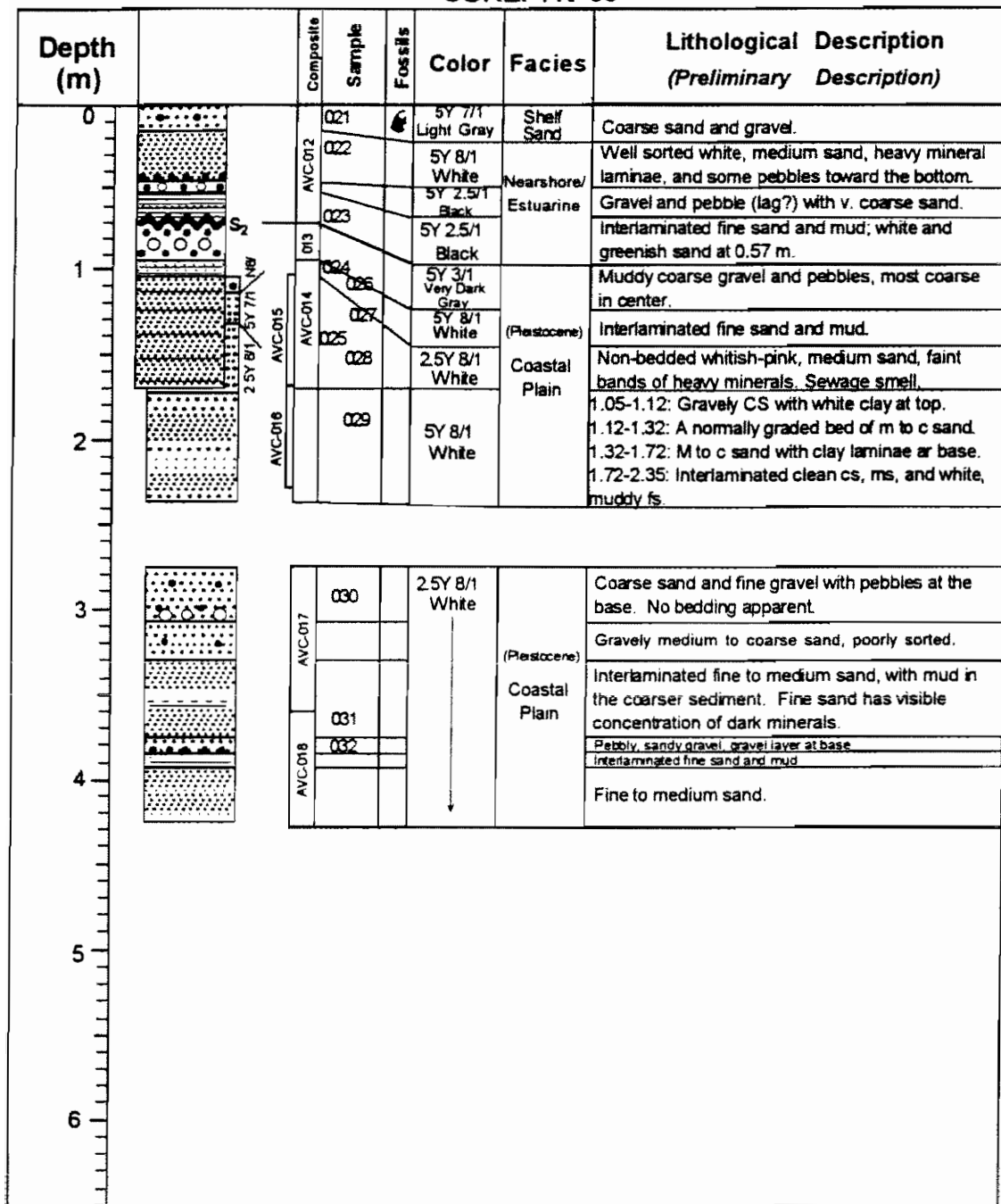
Latitude: 39° 10' 05.28"

Longitude: 74° 33' 53.35"

Water Depth: 56 feet (17.1 m)

Describers: Peter C. Smith & Matthew Goss

CORE: AV-06



Recovery Date: 9-3-94

Latitude: 39° 07' 39.22"

Longitude: 74° 36' 38.01"

Water Depth: 50 feet (15.2 m)

Describers: Peter C. Smith & Matthew Goss

CORE: AV-07

Depth (m)	Composite	Sample	Fossils	Color	Facies	Lithological Description (Preliminary Description)
0 1 2	AVC-058	080		2.5Y 7/3 Pale Yellow	Upper Sand Ridge	Medium to coarse sand, sorted and clean, with shell. Slightly orange at top, with a color change at the bottom. Bedding not apparent.
		081				
	AVC-059	082				
		086				
	AVC-061	083				
		087				
	AVC-060	084				
		088				
	AVC-062	085		N3/		
089			V Dark Gray			
3 4 5 6	AVC-064	090		2.5Y 8/2 Pale Yellow	Upper Sand Ridge	Medium to coarse sand and gravel Whitish medium sand, little gravel. Coarsens downward to coarse sand and gravel. Some blackened sediment. Medium to coarse sand, little gravel. Oil globs.
		091		N8/ Gray		
	AVC-065	092				
		093		N3/		
	AVC-066	094				
		095		N4/		

Recovery Date: 9-6-94

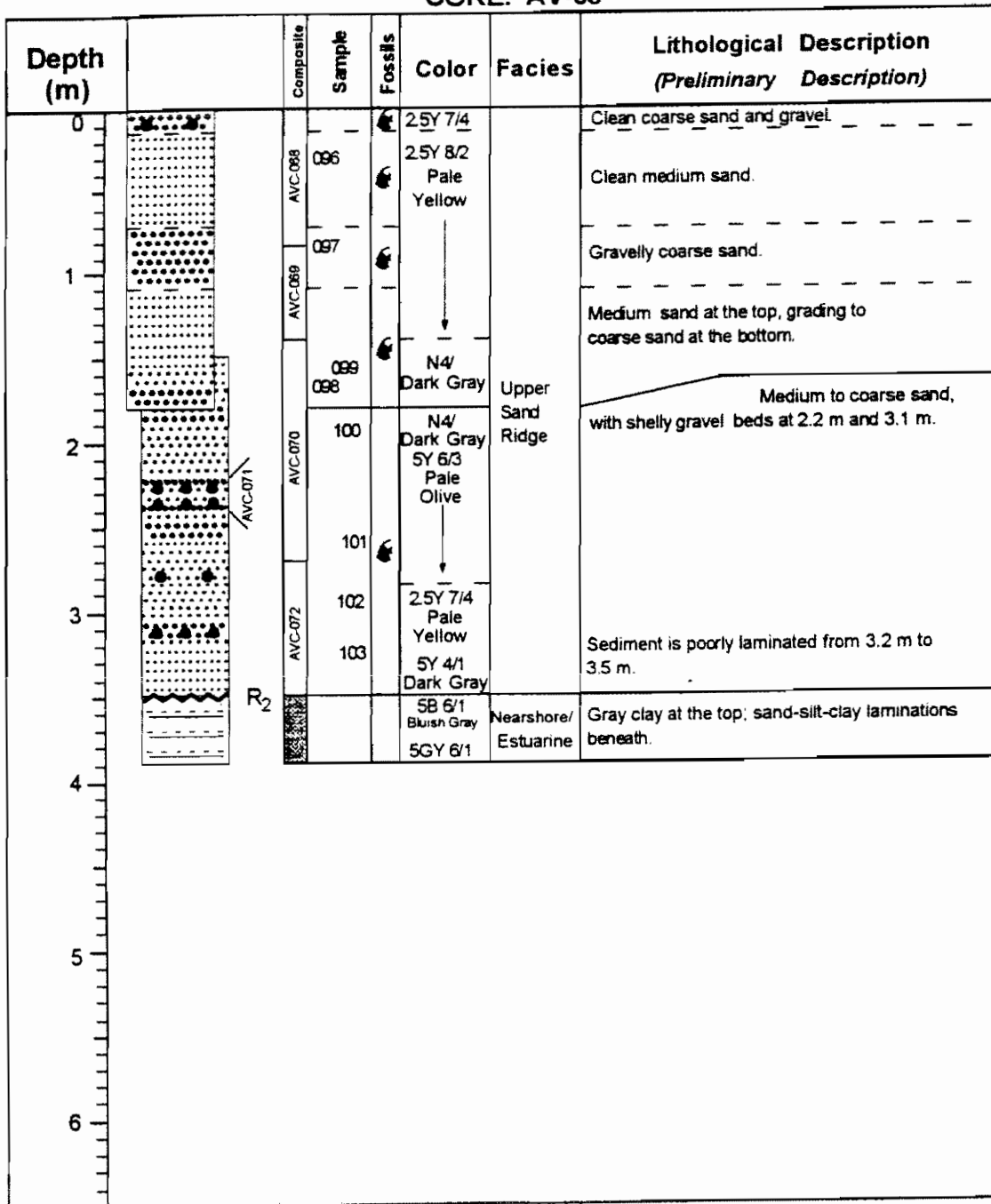
Latitude: 39° 05' 21.69"

Longitude: 74° 34' 04.38"

Water Depth: 36 feet (10.9 m)

Describers Peter C. Smith & Matthew Goss

CORE: AV-08



Recovery Date: 9-6-94

Latitude: 39° 07' 34.37"

Longitude: 74° 31' 37.05"

Water Depth: 42 feet (12.8 m)

Describers: Peter C. Smith & Matthew Goss

CORE: AV-09

Depth (m)		Composite	Sample	Fossils	Color	Facies	Lithological Description (Preliminary Description)
0			034		5Y 7/1 Light Gray	Shelf Sand	Fine sand.
					5Y 7/1 Light Gray		Medium to coarse sand, grades into lower bed.
					N4/7 Dark Gray		Bioturbated clay, hard and dense.
			035		5Y 5/1 Gray		Medium sand, clean, quartzose, no shells.
1		AVC-028	036		5Y 7/1 Gray	Estuarine	Clean, coarse quartz sand.
					5Y 5/1 Gray		Well sorted medium sand, bioturbated, with clay filled burrows.
		028	037		5Y 5/1 Gray		
2		AVC-030			5Y 5/1 Gray		Pebbly, graveley coarse sand.
		AVC-031	038		5Y 8/1 White		
3			039			Tidal Channel	Interlaminated coarse sand and gravel, with well-rounded pebbles and a white clay pod @ 2.45 m.
		AVC-032					
		AVC-033	040		N8/		Gravelly, medium to coarse sand.
4		AVC-034	041		N7/ Light Gray		Medium sand at the top, grading to coarse gravel at the bottom.
			042		N8/ White	(Pleistocene)	Very coarse sand /fine gravel with a white clay matrix. Bottom 2 cm is stained orange.
			043		2.5Y 5/6 Orange		
			044		2.5Y 7/6 Yellow	Coastal Plain	Interlaminated yellow silt and clay. Bottom is black, organic rich clay.
					2.5Y 5/1 Gray		
5							
6							

Recovery Date 9-2-94

Latitude 39° 03' 22.40"

Longitude 74° 41' 12.62"

Water Depth: 44 feet (13.4 m)

Describers: Peter C. Smith & Matthew Goss

CORE: AV-10

Depth		Composite	Sample	Fossils	Color	Facies	Lithological Description (Preliminary Description)	
0		AVC-073	104		2.5Y 7/3 Pale Yellow	Sand	Very coarse sand, gravel, and pebbles.	
1			105					
2		AVC-074	106		2.5Y 8/2 Pale Yellow	Ridge	Medium to coarse sand and some fine gravel.	
			107				Very coarse sand, gravel and pebbles.	
							Medium to coarse sand and some fine gravel.	
			AVC-075					Very coarse sand, gravel and pebbles.
3								
4		AVC-076	110		4GY 4/1 Dark Green-Gray	Estuarine	Green sandy mud, bioturbated.	
		AVC-077			5GY 5/1 Green-Gray	Nearshore	Very coarse sand, gravel and pebbles, normally graded.	
		AVC-078	108		N8/ White	Beach?	Well sorted, clean, medium sand.	
5	AVC-078				N7/ Light Gray	Fluvial Channel	Very hard and dense coarse muddy gravel and pebbles.	
		109		N8/ White	Coarse sand and gravel with white clay matrix.			
		111		N8/ White	Interlaminated medium and coarse sand. Some heavy mineral bands present. Some white clay laminae.			
		AVC-079	112		N8/ White		Very coarse sand and gravel with white clay matrix.	
6								

Recovery Date: 9-6-94

Latitude: 39° 07' 26.42"

Longitude: 74° 32' 11.82"

Water Depth: 47 feet (14.3 m)

Describers: Peter C. Smith & Matthew Goss

CORE: AV-11

Depth		Composite	Sample	Fossils	Color	Facies	Lithological Description (Preliminary Description)
0		AVC-080	113		5G 4/1 Dark Greenish Gray	Shelf Sand	Medium to fine, mottled, silty, bioturbated sand.
		AVC-081	114		5Y 8/1 White	Tidal Channel	Sandy mud, with 3 cm bed of coarse sand and gravel at top.
1		AVC-082	115		5G 4/1 D. Gr. Gray		Baymouth Shoal (Pleistocene)
		AVC-083	116		5Y 7/1 N6/	Indistinctly bedded muddy sand. Relatively clean 4 cm bed of sand at 0.93 m.	
2		AVC-084	117		5G 4/1 D. Gr. Gray	Tidal Channel	Very coarse sand, gravel and pebbles which fines downward to medium sand.
		AVC-085	118		5Y 8/1 5Y 7/1 N6/		Clean medium to fine sand; burrow trace at 1.6 m.
3		AVC-086	119		5G 4/1 D. Gr. Gray	Baymouth Shoal (Pleistocene)	Interlaminated fine sand, silt, and clay. Bioturbated.
		AVC-087	120		5G 4/1 5Y 8/1 White		Reverse graded coarse sand and gravel. 1 cm clay laminae at base.
4		AVC-088	121		2.5Y 7/2 Light Gray	Baymouth Shoal (Pleistocene)	Coarse sand, gravel and pebbles with dark clay staining sediment grains.
		AVC-089	122		N6/ Gray		Clean medium to coarse sand, massive, with thin burrow or root traces, and some gravelly laminae.
5		AVC-090	123		N6/ Gray		Clean medium to coarse sand with some gravelly laminae.
6							

Recovery Date: 8-30-94

Latitude: 39° 11' 01.82"

Longitude: 74° 35' 32.03"

Water Depth: 49.5 feet (15.0 m)

Describers: Peter C. Smith & Matthew Goss

CORE: AV-12

Depth		Composite	Sample	Fossils	Color	Facies	Lithological Description (Preliminary Description)		
0		R ₂			5Y 6/3 Pale Olive	Shelf Sand	Coarse sand and gravel. Pebble lag on top.		
			124		5Y 6/3 Pale Olive (sand)	Nearshore	Bioturbated sand and gravel, fining downward. Burrow traces are filled with clay from below.		
1			125		5B 5/1 Greenish Gray (mud)	Estuarine	Interlaminated sand, silt, and clay. Fine material is deposited over a coarse sand bed.		
			126						
2		AVC-087	128		N8/ White (sand)	Fluvial (Pleistocene)	Coarse sand and gravel with white clay matrix. Dark clay laminae at 1.6 m separates this unit from the one above.		
			129		N8/ White	Fluvial (Pleistocene)	Slightly muddy coarse sand ad gravel.		
3		AVC-088			5G 5/1 Greenish Gray	Estuarine Channel Fill (Pleistocene)	Burrowed and bioturbated green massive, dense mud with black organic material (possible peat). No evidence of shells. Silt bed at 4.7 m.		
4									
5				AVC-089					
6				AVC-090					
7				AVC-091					

Latitude: 39° 09' 57.87"
Longitude: 74° 33' 52.07"

Water Depth: 59 feet (17.9 m)

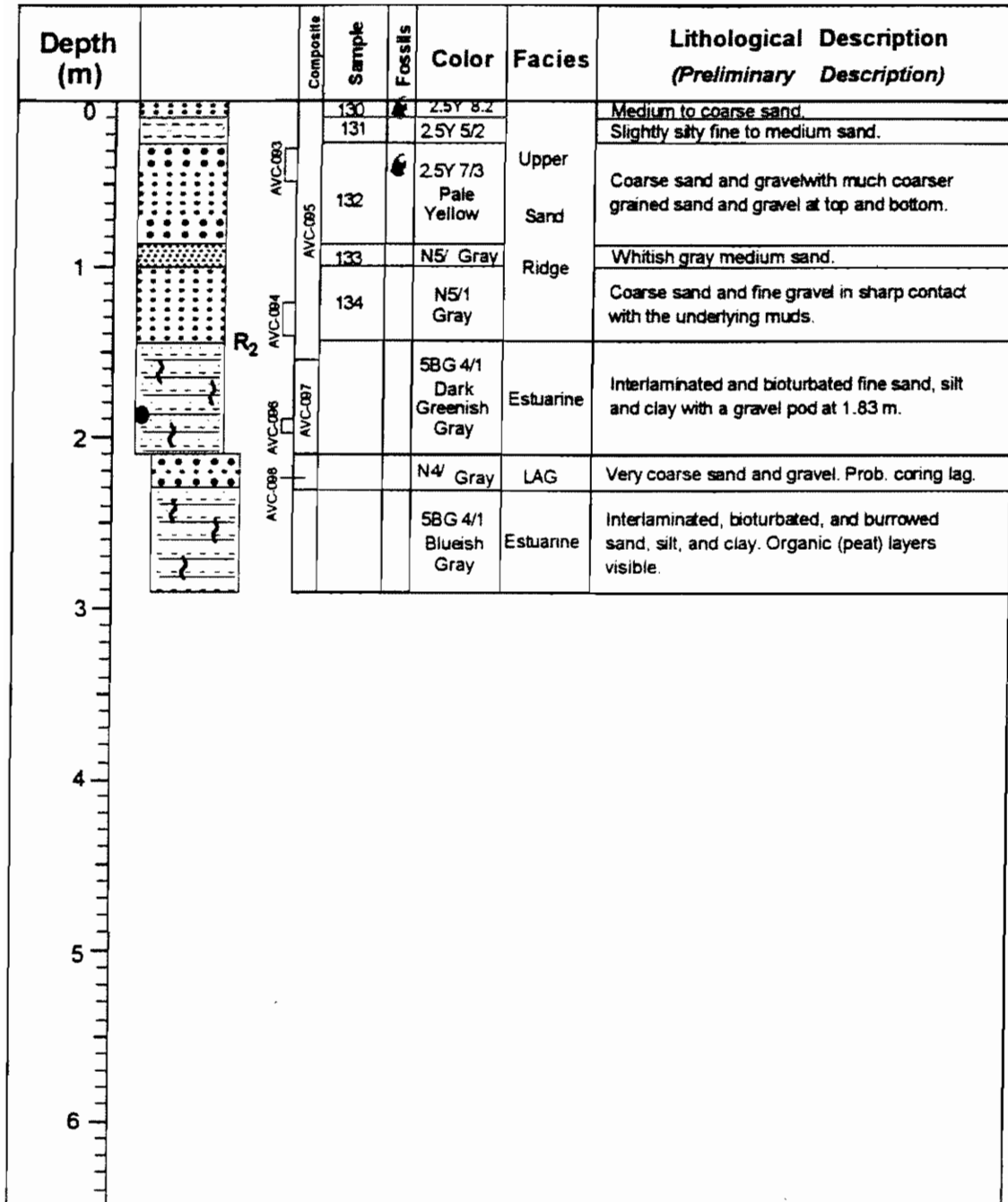
Recovery Date: 9-7-94

Describers: Peter C Smith & Matthew Goss

Core measured to 7.35 meters depth from
initial start depth due to clay expansion.

AVC-092 removed from 7.2m to 7.35 m.

CORE: AV-13



Recovery Date: 9-7-94

Latitude: 39° 09' 54.00"

Longitude: 74° 35' 14.91"

Water Depth: 47 feet (14.3 m)

Describers: Peter C. Smith & Matthew Goss

CORE: AV-14

Depth (m)		Composite	Sample	Fossils	Color	Facies	Lithological Description (Preliminary Description)	
0		AVC-100	135	☛	N4/ Dark Gray	Shelf Sand	Slightly muddy fine to medium sand.	
					5Y 2.5/1		Slightly sandy mud; high clay content.	
1		AVC-101	136		N4/ Dark Gray	Near Shore/ Estuarine	Coarse sand with clay interlamina- tions, fining downward to muddy fine sand.	
			137					
			138					
			139					
2						5G 4/1 (b)	Near Shore/ Estuarine	Medium to fine muddy sand with mud interlamina- tions. Generally fines downward.
				140	Dark Greenish Gray			
3								
4		AVC-102						
5		AVC-103						
6								

Recovery Date: 9-7-94

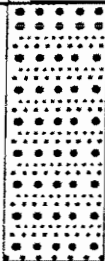
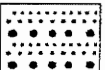
Latitude: 39° 09' 10.42"

Longitude: 74° 36' 51.86"

Water Depth: 48 feet (14.6 m)

Describers: Peter C Smith & Matthew Goss

CORE: AV-15

Depth (m)		Composite	Sample	Fossils	Color	Facies	Lithological Description (Preliminary Description)
0					N25/ Black	Fluvial Channel (Pleistocene)	Coarse sand and gravel lag deposit (black) at the upper surface, grading down to interbedded gravely coarse sand and slightly muddy (white mud) medium sand.
1		AVC-019			N3/ Very Dark Gray		
		AVC-020	033		5Y 7/1 Light Gray		
3					N7/ N8/	Fluvial Channel (Pleistocene)	Interbedded gravely coarse sand and medium sand.
4							
5							
6							

Recovery Date: 9-7-94

Latitude: 39° 07' 32.35"

Longitude: 74° 34' 27.15"

Water Depth: 69 feet (21.0 m)

Describers: Peter C. Smith & Matthew Goss

CORE: AV-16

Depth (m)		Composite	Sample	Fossils	Color	Facies	Lithological Description (Preliminary Description)
0		AVC-112	155		2.5Y 8/2 Pale Yellow	Upper Sand Ridge	Medium to coarse sand and gravel; indistinctly bedded, containing abundant shell hash.
1			156		↓		
			157		2.5Y 8/1 White		
			158		↓		
			159		N5/ Gray		
2		AVC-113	160		↓		
			161		N4/ ↓		
			162		5Y 8/1 White		
3		AVC-114	163		↓	Upper Sand Ridge	Medium to coarse sand and gravel; indistinctly bedded, containing abundant shell hash.
			164		5Y 5/1		
4		AVC-115	165		↓	Nearshore/ Estuarine	Interbedded fine sand and mud; burrowed. Sediment is bedded but exhibits an overall gradational contact with the overlying sediment.
			166		N6/ ↓		
5		AVC-116	167		N4/ ↓	Nearshore/ Estuarine	Interbedded fine sand and mud; burrowed.
			168		N8/ White		
			169		N6/ Gray		
6	AVC-117						

Recovery Date: 9-2-94

Latitude: 39° 02' 21.14"

Longitude: 74° 41' 47.81"

Water Depth: 30.5 feet (9.3 m)

Describers: Peter C. Smith & Matthew Goss

CORE: AV-17

Depth (m)		Composite	Sample	Fossils	Color	Facies	Lithological Description (Preliminary Description)
0			045		5Y 7/2	Shell Sand	Shell containing buff medium sand.
		AVC-035	046		2.5Y 7/1 to 5Y 4/1 Grays	Nearshore Tidal Channel	Interbedded medium and fine sand with mud laminae and shells. Coarsest sand and gravel is at the base. Sediment does not form a sharp contact with the underlying sediment.
1		AVC-036	047 048				
		AVC-037	049		2.5YR 2.5/2 V. Dusky Red	Estuarine Marsh	Medium to coarse sand and some gravel at the top but quickly fining downward to fine sand, silt and clay laminae, bioturbated and burrowed, but no shell material. Upper 0.5 m contains reddish brown lignite, with the highest concentration at the contact with the overlying sediment.
2			050	5Y 4/1			
			051	5Y 2.5/1 Black			
		AVC-038	052		5Y 6/1 Gray	Fluvial Channel (Pleistocene)	Coarse sand, gravel and pebble (lag) deposit in the upper 10 cm. Interbedded medium and coarse sand and gravel. No lignite or shell.
3			053-a			Estuarine Marsh	Same description as estuarine marsh above. Lignite bearing clay at 3.55 m.
		AVC-039	054-a		5GY 7/1		
		AVC-040	055		5Y 6/1 Gray	Fluvial Channel (Pleistocene)	Same description as fluvial channel above.
4		AVC-041	056		5GY 7/1 Light Gray		
5		AVC-042	056				
6							

Recovery Date: 9-2-94

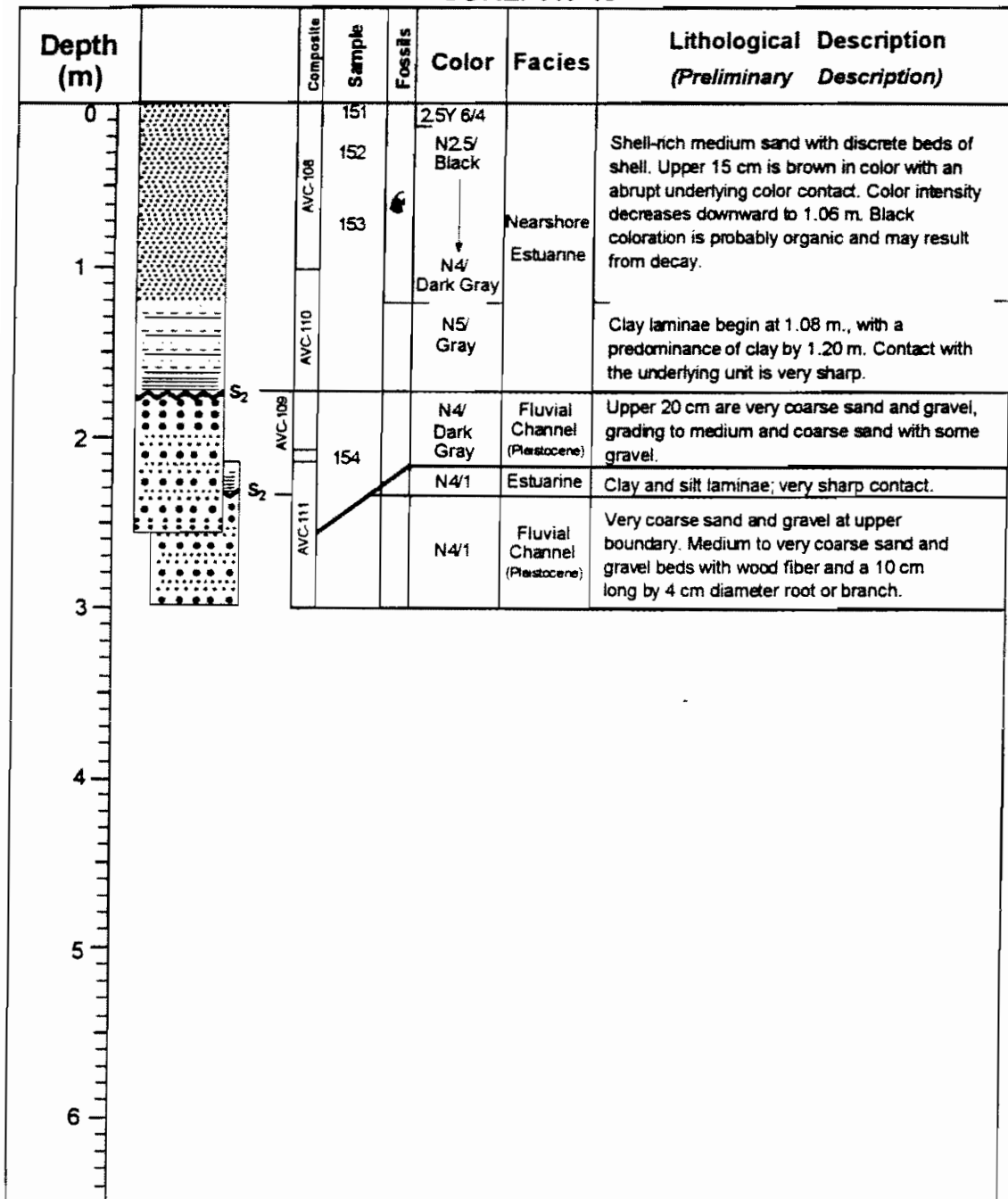
Latitude: 39° 01' 56.75"

Longitude: 74° 41' 11.42"

Water Depth: 41 feet (12.5 m)

Describers: Peter C. Smith & Matthew Goss

CORE: AV-18



Recovery Date. 9-1-94

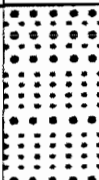

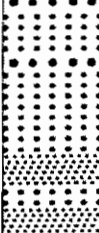







Latitude. 39° 00' 18.16"

Longitude: 74° 41' 16.76"

Water Depth. 52 feet (15.8 m)

Describers: Peter C. Smith & Matthew Goss

CORE: AV-19

Depth (m)		Composite	Sample	Fossils	Color	Facies	Lithological Description (Preliminary Description)	
0		AVC-104	141		2.5 Y 7/3 Pale Yellow	Upper Sand Ridge	Medium to coarse sand and gravel, clean, only poor quality remnant bedding remaining. Fines downward.	
1			142					
			143					
2		AVC-105	144		2.5Y 5/1 Gray			
			145		5Y 8/2 Pale Yellow	Upper Sand Ridge	Clean medium sand. Fines downward.	
3			146					
		AVC-106 (c)	149 (c)		5Y 7/2 Light Gray	Upper Sand Ridge	Clean medium sand with a little gravel. Becomes slightly more coarse toward the base.	
			147 (c)					
4			148 (c)					N6/ Gray
			150					N5/ Gray
		AVC-107						
5								
6								

Recovery Date: 9-1-94

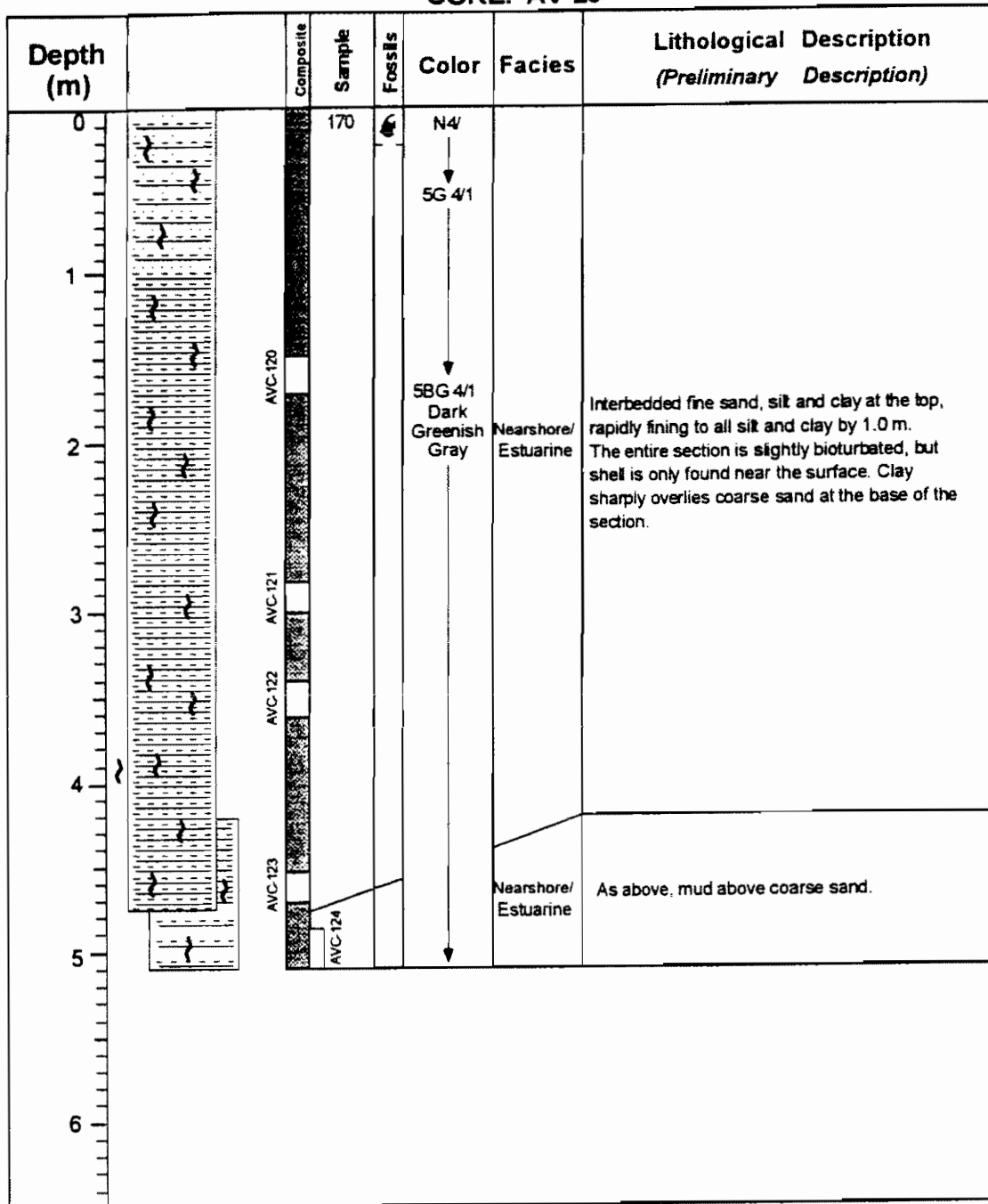
Latitude 38° 58' 34.53"

Longitude 74° 38' 39.15"

Water Depth 33 feet (10.1 m)

Describers: Peter C. Smith & Matthew Goss

CORE: AV-20



Recovery Date: 9-1-94

Latitude: 39° 00' 50.61"

Longitude: 74° 37' 26.57"

Water Depth: 52 feet (15.8 m)

Describers: Peter C. Smith & Matthew Goss

APPENDIX B

Navigation and Isopach Data

Avalon Shoal Area
Avalon, New Jersey

Notes to Appendix B

Grid coordinates are reported in the New Jersey State Plane System. Measurements are reported in meters. Fix numbers correspond to measured locations taken every 5 minutes from the on-board GPS navigation system.

Original seismic lines with fix positions are maintained by Rutgers University, Department of Geological Science, and the New Jersey Geological Survey.

Study Area Seismic Depth and Isopach Data

Line	Fix No.	NJSP E (ft)	NJSP N (ft)	Depth (m)	Depth to S2 (m)	Isopach (m)
T1-3.5E	583	135922	14602	-12	-22	10
T1-3.5E	584	136064	14753	-12	-23	11
T1-3.5E	585	136553	15275	-12	-22	11
T1-3.5E	586	136847	15808	-12	-24	12
T1-3.5E	587	137262	16032	-12	-22	10
T1-3.5E	588	137635	16515	-12	-22	10
T1-3.5E	589	138040	16950	-12	-21	10
T1-3.5E	590	138508	17483	-13	-22	9
T1-3.5E	591	138805	17852	-13	-22	9
T1-3.5E	592	139232	18254	-14	-22	8
T1-3.5E	593	139612	18716	-14	-22	8
T1-3.5E	594	140015	19158	-16	-23	6
T1-3.5E	595	140424	19629	-13	-21	8
T1-3.5E	596	140826	20087	-14	-22	8
T1-3.5E	597	141231	20548	-13	-22	9
T1-3.5E	598	141635	21018	-13	-22	9
T1-3.5E	599	142032	21471	-15	-21	6
T1-3.5E	600	142435	21931	-16	-21	5
T1-3.5E	601	142824	22371	-10	-19	9
T1-3.5E	602	143222	22833	-11	-20	9
T1-3.5E	603	143791	23498	-12	-21	9
T1-3.5E	604	143990	23750	-12	-22	9
T1-3.5E	605	144386	24137	-13	-22	9
T1-3.5E	606	144767	24572	-12	-21	9
T1-3.5E	607	145150	24988	-14	-22	8
T1-3.5E	608	145605	25519	-16	-22	6
T1-3.5E	609	145915	25855	-18	-24	7
T1-3.5E	610	146325	26325	-20	-24	4
T1-3.5E	611	146667	26721	-20	-23	4
T1-3.5E	612	147046	27161	-20	-23	4
T1-3.5E	613	147477	27647	-20	-25	5
T1-3.5E	614	147828	28048	-18	-23	5
T1-3.5E	615	148215	28449	-20	-22	2
T1-3.5E	616	148603	28935	-20	-23	2
T1-3.5E	617	148989	29398	-18	-22	4
T1-3.5E	618	149153	29678	-19	-22	3
T1-3.5E	619	149779	30308	-21	-22	1
T1-3.5E	620	150186	30780	-21	-	-
T1-3.5E	621	150580	31231	-22	-	-
T1-3.5E	622	150968	31683	-21	-	-
T1-3.5E	623	151389	32147	-20	-22	3
T1-3.5E	624	151824	32636	-21	-23	1
T1-3.5E	625	152189	33066	-21	-22	2
T1-3.5E	626	152597	33537	-21	-24	2
T1-3.5E	627	153008	33982	-21	-22	1
T1-3.5E	628	153407	34476	-20	-23	3

Study Area Seismic Depth and Isopach Data

Line	Fix No.	NJSP E (ft)	NJSP N (ft)	Depth (m)	Depth to S2 (m)	Isopach (m)
TI-3.5E	629	153812	34851	-21	-24	3
TI-3.5E	630	154223	35425	-20	-23	3
TI-3.5E	631	154644	35888	-20	-23	3
TI-3.5E	632	155044	36368	-22	-	-
TI-3.5E	633	155481	36854	-21	-	-
TI-3.5E	634	155884	37337	-21	-	-
TI-3.5E	635	156319	37790	-20	-	-
TI-3.5E	636	156719	38282	-20	-	-
TI-3.5E	637	157165	38753	-20	-	-
TI-00W	567	136668	24863	-12	-17	5
TI-00W	568	136403	24654	-13	-17	5
TI-00W	569	136254	24401	-13	-17	4
TI-00W	570	136140	24286	-13	-17	4
TI-08W	571	135941	24004	-13	-18	5
TI-00W	572	135708	23722	-12	-17	5
TI-00W	573	135342	23405	-12	-17	5
TI-00W	574	135153	23159	-13	-19	6
TI-00W	575	134948	22853	-12	-17	5
TI-00W	576	134715	22564	-12	-18	5
TI-00W	577	134452	22300	-12	-18	6
TI-0.8W	132	148672	41171	-16	-17	2
TI-0.8W	133	148282	40827	-16	-19	3
TI-0.8W	134	147956	40319	-17	-20	4
TI-0.8W	135	147557	39856	-18	-20	2
TI-0.8W	136	147108	39431	-18	-21	3
TI-0.8W	137	146757	38947	-18	-21	3
TI-0.8W	138	146337	38508	-18	-21	3
TI-0.8W	139	145980	38020	-20	-22	2
TI-0.8W	140	145543	37576	-18	-22	4
TI-0.8W	141	145212	37062	-16	-21	5
TI-0.8W	142	144729	36646	-13	-19	6
TI-0.8W	143	144352	36140	-13	-18	5
TI-0.8W	144	143975	35634	-14	-19	5
TI-0.8W	145	143568	35163	-12	-19	7
TI-0.8W	146	143157	34691	-11	-17	6
TI-0.8W	147	142733	34229	-12	-17	5
TI-0.8W	148	142319	33742	-10	-17	7
TI-0.8W	149	141893	33279	-10	-17	7
TI-0.8W	150	141486	32794	-7	-14	7
TI-0.8W	151	141058	32331	-7	-15	7
TI-0.8W	152	140631	31845	-11	-16	5
TI-0.8W	153	140213	31351	-17	-	-
TI-0.8W	154	139812	30844	-15	-	-
TI-0.8W	155	139402	30350	-15	-	-
TI-0.8W	156	138967	29874	-16	-	-
TI-0.8W	157	138509	29386	-17	-	-

Study Area Seismic Depth and Isopach Data

Line	Fix No.	NJSP E (ft)	NJSP N (ft)	Depth (m)	Depth to S2 (m)	Isopach (m)
TI-0.8W	158	138320	29172	-16	-	-
TI-1.0N	502	129111	23183	-10	-	-
TI-1.0N	503	126577	22697	-12	-	-
TI-1.0N	504	129852	22370	-13	-	-
TI-1.0N	505	130372	22026	-15	-	-
TI-1.0N	506	130749	21631	-14	-17	3
TI-1.0N	507	131188	21296	-12	-16	4
TI-1.0N	508	131571	20964	-12	-16	4
TI-1.0N	509	131955	20611	-14	-16	3
TI-1.0N	510	132339	20264	-12	-16	4
TI-1.0N	511	132753	19948	-12	-16	4
TI-1.0N	512	133146	19608	-11	-16	5
TI-1.0N	513	133520	19281	-14	-15	1
TI-1.0N	514	133945	18931	-16	-	-
TI-1.0N	515	134313	18566	-15	-	-
TI-1.0N	516	135005	17931	-15	-	-
TI-1.0N	517	135276	17741	-15	-16	1
TI-1.0N	518	135554	17578	-14	-15	1
TI-1.0N	519	135889	17203	-13	-16	3
TI-1.0N	520	136305	16880	-13	-16	3
TI-1.0N	521	136725	16552	-14	-16	2
TI-1.0N	522	137155	16176	-12	-16	4
TI-1.0N	523	137505	15873	-11	-16	5
TI-1.0N	524	137894	15532	-9	-14	5
TI-1.0N	525	138275	15192	-7	-12	5
TI-1.0N	526	138672	14861	-10	-13	3
TI-1.0N	527	139062	14517	-12	-14	2
TI-1.0N	528	139300	14309	-12	-14	2
TI-1.3W	379	129623	20801	-14	-	-
TI-1.3W	378	130041	21065	-15	-	-
TI-1.3W	377	130469	21571	-15	-	-
TI-1.3W	376	130886	22138	-15	-	-
TI-1.3W	375	131361	22632	-16	-	-
TI-1.3W	374	131829	23041	-15	-	-
TI-1.3W	373	132263	23655	-15	-	-
TI-1.3W	372	132727	24105	-15	-	-
TI-1.3W	371	133121	24567	-16	-	-
TI-1.3W	370	133553	25068	-16	-	-
TI-1.3W	369	134480	26124	-16	-	-
TI-1.3W	368	134917	26606	-16	-	-
TI-1.3W	367	135309	27185	-16	-	-
TI-1.3W	366	135783	27628	-16	-	-
TI-1.3W	365	136200	28100	-16	-	-
TI-1.3W	364	136533	28476	-14	-	-
TI-1.3W	162	137036	29044	-15	-	-
TI-1.3W	163	137456	29519	-15	-	-

Study Area Seismic Depth and Isopach Data

Line	Fix No.	NJSP E (ft)	NJSP N (ft)	Depth (m)	Depth to S2 (m)	Isopach (m)
TI-1.3W	164	137651	29739	-16	-	-
TI-1.3W	165	137652	29792	-14	-	-
TI-1.3W	166	138066	30259	-16	-	-
TI-1.3W	167	138422	30871	-15	-	-
TI-1.3W	168	138807	31048	-15	-	-
TI-1.3W	169	139132	31498	-15	-16	1
TI-1.3W	170	139518	31881	-13	-17	5
TI-1.3W	171	139881	32289	-13	-17	3
TI-1.3W	172	140201	32733	-14	-16	2
TI-1.3W	173	140597	33073	-16	-17	2
TI-1.3W	174	140935	33512	-14	-17	3
TI-1.3W	175	141280	33962	-13	-17	4
TI-1.3W	176	141661	34367	-14	-18	4
TI-1.3W	177	142057	34780	-16	-18	2
TI-1.3W	178	142410	35241	-16	-18	2
TI-1.3W	179	142814	35654	-18	-18	0
TI-1.3W	180	143190	36111	-18	-	-
TI-1.3W	181	143579	36545	-19	-	-
TI-1.3W	182	143977	36960	-21	-	-
TI-1.3W	183	144347	37469	-20	-	-
TI-1.3W	184	144734	37910	-19	-	-
TI-1.3W	185	145120	38375	-18	-	-
TI-1.3W	186	145522	38823	-17	-	-
TI-1.3W	187	145997	39281	-17	-	-
TI-1.3W	188	146289	39703	-16	-	-
TI-1.3W	189	146665	40163	-16	-	-
TI-1.3W	190	147028	40633	-16	-	-
TI-1.3W	191	147393	41100	-18	-	-
TI-1.3W	192	147730	41572	-18	-	-
TI-1.3W	193	147998	41802	-16	-	-
TI-1.8E	708	143397	27753	-16	-18	2
TI-1.8E	709	143690	28066	-16	-19	2
TI-1.8E	710	143780	28152	-17	-19	2
TI-1.8E	711	144015	28431	-11	-19	8
TI-1.8E	712	144389	28924	-13	-20	6
TI-1.8E	713	145098	29612	-13	-20	7
TI-1.8E	714	145506	30109	-14	-20	6
TI-1.8E	715	145943	30576	-14	-20	5
TI-1.8E	716	146414	30966	-14	-21	6
TI-1.8E	717	146807	31530	-13	-20	7
TI-1.8E	718	147295	32080	-13	-21	8
TI-1.8E	719	147685	32514	-15	-21	6
TI-1.8E	720	148139	33017	-18	-21	3
TI-1.8E	721	148304	33198	-20	-22	2
TI-1.8E	722	148485	33390	-21	-21	1
TI-1.9W	99	137077	30626	-16	-16	0

Study Area Seismic Depth and Isopach Data

Line	Fix No.	NJSP E (ft)	NJSP N (ft)	Depth (m)	Depth to S2 (m)	Isopach (m)
TI-1.9W	100	137429	31005	-16	-16	2
TI-1.9W	101	137785	31422	-15	-17	2
TI-1.9W	102	138114	31840	-14	-16	3
TI-1.9W	103	138438	32242	-8	-15	7
TI-1.9W	104	138788	32619	-8	-15	7
TI-1.9W	105	139120	32973	-9	-15	6
TI-1.9W	106	139497	33323	-10	-15	5
TI-1.9W	107	139811	33739	-11	-16	5
TI-1.9W	108	140128	34159	-12	-17	5
TI-1.9W	109	140487	34537	-12	-17	5
TI-1.9W	110	140787	34941	-12	-16	4
TI-1.9W	111	141214	35334	-12	-16	4
TI-1.9W	112	141547	35729	-13	-16	4
TI-1.9W	113	141866	36143	-12	-17	5
TI-1.9W	114	142239	36608	-14	-18	4
TI-1.9W	115	142554	37011	-17	-	-
TI-1.9W	116	142972	37459	-18	-	-
TI-1.9W	117	143289	37907	-16	-	-
TI-1.9W	118	143638	38307	-14	-17	3
TI-1.9W	119	144010	38741	-15	-17	2
TI-1.9W	120	144373	39178	-14	-17	3
TI-1.9W	121	144772	39562	-15	-16	1
TI-1.9W	122	145154	39987	-13	-16	3
TI-1.9W	123	145496	10439	-16	-17	0
TI-1.9W	124	145958	40881	-15	-	-
TI-1.9W	125	146272	41285	-15	-17	2
TI-1.9W	126	146621	41705	-15	-16	2
TI-1.9W	127	146968	42142	-12	-15	2
TI-2N	534	141476	15658	-15	-23	7
TI-2N	535	141035	16111	-14	-21	7
TI-2N	536	140515	16491	-13	-21	8
TI-2N	537	140003	16877	-12	-20	9
TI-2N	538	139471	17329	-12	-21	9
TI-2N	539	139015	17699	-13	-22	8
TI-2N	540	138535	18140	-15	-22	8
TI-2N	541	138108	18525	-14	-20	7
TI-2N	542	137641	18900	-15	-21	6
TI-2N	543	137181	19282	-12	-20	8
TI-2N	544	136741	19663	-12	-19	6
TI-2N	545	136301	20082	-13	-20	6
TI-2N	546	135836	20444	-12	-18	7
TI-2N	547	135381	20809	-13	-18	5
TI-2N	548	134946	21191	-14	-19	5
TI-2N	549	134506	21564	-14	-17	4
TI-2N	550	134070	21946	-12	-18	6
TI-2N	551	133635	22329	-16	-17	1

Study Area Seismic Depth and Isopach Data

Line	Fix No.	NJSP E (ft)	NJSP N (ft)	Depth (m)	Depth to S2 (m)	Isopach (m)
T1-2N	552	133196	22897	-9	-15	6
T1-2N	553	132781	23078	-12	-16	4
T1-2N	554	132328	23451	-15	-	-
T1-2N	555	131890	23828	-14	-	-
T1-2N	556	131431	24230	-14	-	-
T1-2N	557	131035	24577	-13	-	-
T1-2N	558	130694	24862	-12	-	-
T1-3.0N	469	131400	28839	-8	-19	11
T1-3.0N	470	131538	26738	-9	-18	9
T1-3.0N	471	131943	26428	-13	-18	5
T1-3.0N	472	132274	26077	-14	-16	2
T1-3.0N	473	132872	25764	-15	-	-
T1-3.0N	474	133053	25430	-16	-	-
T1-3.0N	475	133427	25084	-16	-	-
T1-3.0N	476	133830	24751	-14	-16	3
T1-3.0N	477	134234	24413	-10	-15	5
T1-3.0N	478	134571	24068	-9	-15	6
T1-3.0N	479	134967	23734	-12	-17	5
T1-3.0N	480	135350	23408	-13	-18	5
T1-3.0N	481	135741	23062	-11	-17	6
T1-3.0N	482	136143	22739	-13	-17	4
T1-3.0N	483	136522	22395	-13	-18	5
T1-3.0N	484	136924	22056	-13	-19	6
T1-3.0N	485	137320	21713	-13	-20	7
T1-3.0N	486	137706	21369	-14	-20	6
T1-3.0N	487	138096	21055	-12	-19	7
T1-3.0N	488	138471	20722	-12	-20	8
T1-3.0N	489	138862	20383	-14	-20	6
T1-3.0N	490	139257	20051	-18	-22	4
T1-3.0N	491	139657	19717	-16	-21	5
T1-3.0N	492	140049	19377	-15	-20	5
T1-3.0N	493	140437	19033	-16	-21	5
T1-3.0N	494	140840	18691	-16	-21	5
T1-3.0N	495	141244	18364	-15	-20	6
T1-3.0N	496	141630	18023	-16	-21	5
T1-3.0N	497	142010	17675	-17	-21	4
T1-3.0N	498	142401	17347	-17	-20	3
T1-4.0N	440	143932	18689	-18	-22	3
T1-4.0N	441	142947	19614	-18	-23	5
T1-4.0N	442	142410	19941	-16	-21	5
T1-4.0N	443	141906	20349	-15	-20	5
T1-4.0N	444	141428	20753	-14	-20	7
T1-4.0N	445	140938	21158	-15	-20	5
T1-4.0N	448	140437	21542	-19	-21	3
T1-4.0N	447	139981	21980	-21	-21	0
T1-4.0N	448	139502	22364	-18	-22	3

Study Area Seismic Depth and Isopach Data

Line	Fix No.	NJSP E (ft)	NJSP N (ft)	Depth (m)	Depth to S2 (m)	Isopach (m)
TI-4.0N	448	139026	22775	-19	-21	2
TI-4.0N	450	138545	23159	-18	-21	3
TI-4.0N	451	138052	23517	-16	-21	5
TI-4.0N	452	137611	23933	-15	-21	6
TI-4.0N	453	136985	24487	-13	-19	5
TI-4.0N	454	136673	24706	-12	-19	6
TI-4.0N	455	136237	25099	-15	-20	4
TI-4.0N	456	135772	25445	-13	-17	4
TI-4.0N	457	135329	25836	-12	-18	5
TI-4.0N	458	134866	26186	-16	-19	3
TI-4.0N	459	134429	26556	-16	-20	3
TI-4.0N	460	133992	26915	-15	-18	3
TI-4.0N	461	133500	27300	-18	-21	3
TI-4.0N	462	133093	27622	-14	-17	4
TI-4.0N	463	132677	28020	-12	-16	4
TI-4.0N	464	132489	28165	-9	-14	5
TI-5.8E	280	149193	22613	-21	-	-
TI-5.8E	281	148357	22935	-22	-	-
TI-5.8E	282	148605	23423	-21	-	-
TI-5.8E	283	148835	23939	-21	-	-
TI-5.8E	284	150068	24313	-20	-	-
TI-8.0N	237	137241	32945	-12	-12	0
TI-8.0N	238	137610	32572	-16	-16	0
TI-8.0N	239	138137	32179	-7	-13	6
TI-8.0N	240	138323	32082	-7	-13	7
TI-8.0N	241	138453	31868	-10	-14	4
TI-8.0N	242	138530	31761	-14	-17	3
TI-8.0N	243	139002	31343	-14	-17	3
TI-8.0N	244	139322	31243	-15	-18	4
TI-8.0N	245	139504	31059	-14	-17	3
TI-8.0N	246	139939	30607	-14	-20	5
TI-8.0N	247	140380	30207	-15	-20	4
TI-8.0N	248	140873	29871	-16	-20	4
TI-8.0N	249	141319	29485	-17	-20	3
TI-8.0N	251	141750	28932	-15	-18	3
TI-8.0N	252	142095	28638	-16	-19	3
TI-8.0N	254	142544	28339	-16	-19	3
TI-8.0N	255	142962	27954	-14	-19	5
TI-8.0N	256	143370	27552	-16	-20	4
TI-8.0N	257	143815	27252	-17	-19	2
TI-8.0N	258	144238	26881	-17	-21	4
TI-8.0N	259	144634	26491	-16	-20	3
TI-8.0N	260	144997	26174	-16	-21	5
TI-8.0N	261	145443	25774	-16	-20	5
TI-8.0N	262	145839	25391	-15	-21	6
TI-8.0N	263	146244	25048	-14	-20	6

Study Area Seismic Depth and Isopach Data

Line	Fix No.	NJSP E (ft)	NJSP N (ft)	Depth (m)	Depth to S2 (m)	Isopach (m)
TI-8.0N	264	146658	24703	-17	-21	4
TI-8.0N	265	147052	24357	-17	-22	5
TI-8.0N	266	147545	23967	-20	-23	2
TI-8.0N	267	147905	23588	-17	-21	4
TI-8.0N	268	148216	23336	-18	-23	5
TI-8.0N	269	148612	23005	-18	-21	3
TI-8.0N	270	148985	22653	-19	-21	2
TI-8.0N	271	149385	22345	-19	-22	2
TI-8.0N	272	149739	22008	-18	-23	5
TI-8.0N	273	150131	21694	-16	-23	6
TI-8.0N	274	150484	21351	-19	-23	4
TI-8.0N	275	150709	21177	-18	-23	5
TI-8.5N	77	139585	34651	-18	-	-
TI-8.5N	78	139772	34533	-18	-	-
TI-8.5N	79	140197	34148	-18	-	-
TI-8.5N	80	140633	33784	-18	-	-
TI-8.5N	81	141085	33435	-17	-	-
TI-8.5N	82	141483	33023	-13	-17	4
TI-8.5N	83	141926	32558	-11	-17	6
TI-8.5N	84	142359	32307	-9	-16	7
TI-8.5N	85	142789	31963	-16	-	-
TI-8.5N	86	143182	31575	-15	-	-
TI-8.5N	87	143594	31194	-13	-16	3
TI-8.5N	88	143122	30730	-14	-17	3
TI-8.5N	89	142892	30588	-13	-16	3
TI-9N	7	137377	35304	-13	-13	0
TI-9N	8	137847	34903	-12	-12	0
TI-9N	9	137914	34818	-14	-14	0
TI-9N	10	138240	34557	-14	-14	0
TI-9N	11	138640	34196	-15	-15	0
TI-9N	12	139031	33848	-16	-16	0
TI-9N	13	139444	33497	-12	-16	5
TI-9N	14	139860	33183	-9	-15	6
TI-9N	15	140251	32839	-15	-17	2
TI-9N	16	140647	32522	-12	-16	5
TI-9N	17	141045	32199	-9	-16	7
TI-9N	18	141392	31823	-16	-18	2
TI-9N	19	141805	31512	-19	-19	0
TI-9N	20	142187	31190	-20	-20	0
TI-9N	21	142575	30856	-18	-20	2
TI-9N	22	142968	30528	-17	-19	2
TI-9N	23	143309	30141	-17	-19	2
TI-9N	24	143727	29853	-16	-20	4
TI-9N	25	144122	29524	-16	-21	5
TI-9N	26	144520	29208	-15	-19	4
TI-9N	27	144893	28884	-11	-20	8

Study Area Seismic Depth and Isopach Data

Line	Fix No.	NJSP E (ft)	NJSP N (ft)	Depth (m)	Depth to S2 (m)	Isopach (m)
TI-9N	28	145295	28589	-17	-20	3
TI-9N	29	145645	28237	-22	-	-
TI-9N	30	146051	27946	-22	-	-
TI-9N	31	146840	17288	-21	-	-
TI-10N	323	138588	36743	-13	-15	2
TI-10N	324	138923	36475	-13	-15	2
TI-10N	325	138397	36146	-10	-14	4
TI-10N	326	138820	35761	-12	-15	2
TI-10N	328	140645	34892	-11	-14	3
TI-10N	329	141080	34827	-12	-16	4
TI-10N	330	141473	34247	-13	-16	3
TI-10N	331	141901	33915	-14	-16	2
TI-10N	332	142323	33587	-10	-15	5
TI-10N	333	142752	33269	-12	-	-
TI-10N	334	143131	32906	-19	-	-
TI-10N	335	143751	32319	-18	-	-
TI-10N	336	143924	32204	-18	-	-
TI-10N	337	144274	31831	-16	-	-
TI-10N	338	144618	31458	-16	-	-
TI-10N	339	145086	31077	-17	-	-
TI-10N	340	145371	30815	-17	-	-
TI-10N	341	145648	30565	-16	-19	3
TI-10N	342	145723	30489	-14	-19	5
TI-10N	343	146141	30270	-12	-17	5
TI-10N	344	146506	30010	-13	-17	4
TI-10N	345	147057	29489	-18	-19	1
TI-10N	346	147198	29366	-19	-	-
TI-10N	347	147855	28828	-21	-	-
TI-10N	348	148183	28542	-19	-	-
TI-10N	349	148503	28264	-20	-	-
TI-10N	350	148890	27938	-20	-	-
TI-10N	351	149162	27735	-22	-	-
TI-10N	352	149464	27470	-19	-20	2
TI-10N	353	149754	27196	-17	-20	3
TI-10N	354	150071	26928	-19	-20	1
TI-10N	355	150376	26672	-21	-	-
TI-10N	356	150681	26411	-20	-	-
TI-10N	357	150980	26164	-20	-	-
TI-10N	358	151347	25857	-23	-	-
TI-11N	286	152637	26775	-19	-24	5
TI-11N	287	152238	27181	-23	-	-
TI-11N	288	151773	27657	-22	-	-
TI-11N	289	151283	28093	-19	-22	3
TI-11N	290	150757	28480	-20	-22	2
TI-11N	291	150335	28972	-22	-22	0
TI-11N	292	149833	29375	-20	-22	2

Study Area Seismic Depth and Isopach Data

Line	Fix No.	NJSP E (ft)	NJSP N (ft)	Depth (m)	Depth to S2 (m)	Isopach (m)
TI-11N	293	148363	29824	-18	-22	4
TI-11N	294	148871	30240	-19	-22	2
TI-11N	295	148427	30736	-17	-21	4
TI-11N	296	147949	31164	-20	-22	2
TI-11N	297	147481	31528	-16	-21	6
TI-11N	298	147018	32072	-14	-20	6
TI-11N	299	146834	32253	-17	-20	4
TI-11N	300	146569	32539	-19	-20	1
TI-11N	301	146046	32929	-19	-21	2
TI-11N	302	145558	33355	-15	-20	5
TI-11N	303	145408	33534	-15	-21	6
TI-11N	304	145093	33751	-20	-21	2
TI-11N	305	144859	34214	-19	-21	2
TI-11N	306	144187	34645	-16	-20	4
TI-11N	307	144044	34848	-15	-20	5
TI-11N	308	143736	35066	-13	-19	6
TI-11N	309	143281	35490	-18	-19	2
TI-11N	310	142822	35696	-17	-18	1
TI-11N	311	142357	36347	-15	-19	5
TI-11N	312	141930	36805	-15	-19	4
TI-11N	313	141472	37207	-16	-19	3
TI-11N	314	141027	37613	-11	-16	5
TI-11N	315	140450	38185	-16	-16	0
TI-12N	639	141452	39349	-16	-17	2
TI-12N	640	141735	39143	-13	-15	2
TI-12N	641	142022	38934	-14	-16	2
TI-12N	642	142460	38615	-12	-17	5
TI-12N	643	142916	38283	-12	-16	3
TI-12N	644	143314	37953	-16	-17	1
TI-12N	645	143751	37503	-16	-18	2
TI-12N	646	144188	37153	-20	-	-
TI-12N	647	144626	36760	-13	-19	5
TI-12N	648	145062	36343	-15	-19	4
TI-12N	649	145427	36009	-18	-18	1
TI-12N	650	145857	35593	-20	-20	0
TI-12N	651	146314	35233	-18	-20	2
TI-12N	652	146728	34831	-15	-20	5
TI-12N	653	147156	34584	-17	-20	3
TI-12N	654	147609	34222	-18	-20	2
TI-12N	655	148082	33759	-16	-21	5
TI-12N	656	148422	33491	-19	-23	4
TI-12N	657	148875	33134	-20	-22	3
TI-12N	658	149318	32785	-20	-22	3
TI-12N	659	149702	32414	-20	-	-
TI-12N	660	150138	32075	-20	-	-
TI-12N	661	150569	31727	-20	-	-

Study Area Seismic Depth and Isopach Data

Line	Fix No.	NJSP E (ft)	NJSP N (ft)	Depth (m)	Depth to S2 (m)	Isopach (m)
TI-12N	662	150985	31352	-20	-21	2
TI-12N	663	151420	30985	-22	-22	0
TI-12N	664	151821	30628	-20	-22	2
TI-12N	665	152227	30262	-17	-21	4
TI-12N	666	152682	29944	-16	-21	5
TI-12N	667	153099	29576	-17	-21	4
TI-12N	668	153545	29264	-19	-21	2
TI-12N	669	153845	29054	-19	-23	3
TI-13N	680	155596	29886	-21	-23	2
TI-13N	681	155095	30269	-20	-24	3
TI-13N	682	154531	30631	-22	-23	1
TI-13N	683	154270	30762	-21	-24	2
TI-13N	684	153284	31268	-19	-22	3
TI-13N	685	152681	31776	-22	-	-
TI-13N	686	152229	32158	-22	-	-
TI-13N	687	151821	32597	-21	-	-
TI-13N	688	151342	32976	-22	-	-
TI-13N	689	150831	33358	-20	-	-
TI-13N	690	150183	33985	-22	-	-
TI-13N	691	148874	34237	-21	-	-
TI-13N	692	148277	34804	-14	-20	6
TI-13N	693	148908	35063	-12	-19	7
TI-13N	694	148395	35462	-18	-20	1
TI-13N	695	147925	35906	-21	-21	0
TI-13N	696	147425	36346	-21	-21	0
TI-13N	697	146931	36779	-20	-20	0
TI-13N	698	146418	37208	-21	-21	0
TI-13N	699	145892	37635	-20	-20	0
TI-13N	700	145399	38071	-20	-20	0
TI-13N	701	144873	38507	-16	-20	3
TI-13N	702	144377	38951	-15	-19	5
TI-13N	703	143861	39379	-11	-18	7
TI-13N	704	143332	39766	-18	-18	0
TI-13N	705	143243	39868	-17	-17	0
TI-13N	706	143049	40043	-15	-19	4
TI-14N	201	144136	42018	-13	-17	4
TI-14N	202	144662	41715	-14	-19	5
TI-14N	203	145119	41366	-15	-19	4
TI-14N	204	145559	40981	-17	-20	3
TI-14N	205	146011	40596	-15	-20	5
TI-14N	206	146445	40211	-15	-21	6
TI-14N	207	146864	39836	-17	-22	4
TI-14N	208	147329	39469	-20	-22	2
TI-14N	209	147776	39084	-17	-23	6
TI-14N	210	148203	38725	-18	-23	5
TI-14N	211	148630	38347	-22	-24	2

Study Area Seismic Depth and Isopach Data

Line	Fix No.	NJSP E (ft)	NJSP N (ft)	Depth (m)	Depth to S2 (m)	Isopach (m)
TI-14N	212	149074	37964	-23	-24	1
TI-14N	213	149486	37588	-20	-23	3
TI-14N	214	149932	37224	-20	-22	2
TI-14N	215	150392	36868	-20	-23	2
TI-14N	216	150825	36487	-17	-20	3
TI-14N	217	151283	36075	-21	-21	0
TI-14N	218	151737	35700	-20	-20	0
TI-14N	219	152220	35258	-21	-22	1
TI-14N	220	152681	34913	-20	-21	2
TI-14N	221	153164	34568	-20	-23	2
TI-14N	222	153647	34223	-22	-	-
TI-14N	223	154130	33878	-22	-	-
TI-14N	224	154613	33533	-23	-	-
TI-14N	225	155096	33188	-23	-	-
TI-14N	226	155579	32843	-24	-	-
TI-14N	227	156062	32498	-23	-23	0
TI-14N	228	156545	32153	-21	-24	2
TI-14N	229	157028	31808	-24	-	-
TI-14N	230	157511	31463	-23	-	-

- Data Unresolvable.
Depth data converted from seismic two way travel time.

APPENDIX C

Summary Sediment Statistics

Avalon Shoal Area
Avalon, New Jersey

Summary Sediment Statistics
Avazon, NJ

AVS	Core #	% Grav	% Sand	% Mud	Facies	Mean	SD	Skw	Kur
1	AV-02	22.23	77.73	0.04	Sand Ridge	-0.30	1.47	-0.63	2.41
2	AV-02	44.80	54.98	0.21	Sand Ridge	-0.87	1.85	-0.37	0.84
3	AV-02	43.41	54.81	1.98	Sand Ridge	-1.02	1.53	0.40	0.78
4	AV-02				Sand Ridge				
5	AV-02				Sand Ridge				
6	AV-02	31.97	64.88	3.17	Sand Ridge	-0.12	1.88	-0.24	0.83
7	AV-02	25.28	74.89	0.05	Sand Ridge	-0.80	1.55	-0.33	0.89
8	AV-02				Sand Ridge				
9	AV-02				Channel				
10	AV-02				Channel				
11	AV-02				Channel				
12	AV-02	2.89	94.21	2.90	Channel	1.82	1.12	-0.44	2.13
13	AV-06				Estuarine				
14	AV-03a	0.29	98.71	Trace	Sand Ridge	1.28	0.49	-0.17	1.03
15	AV-03a	10.91	89.09	Trace	Sand Ridge	0.57	1.08	-0.42	1.52
16	AV-03a	0.25	98.37	0.38	Sand Ridge	1.48	0.47	-0.24	1.37
17	AV-03a				Sand Ridge				
18	AV-03b	0.27	99.72	0.01	Sand Ridge	1.15	0.55	0.00	0.93
19	AV-03b	1.37	98.57	0.06	Sand Ridge	1.08	0.64	-0.24	0.95
20	AV-03b	0.04	99.48	0.48	Sand Ridge	1.30	0.57	-0.44	1.20
21	AV-08a	5.32	92.35	2.33	Channel	1.01	1.29	-0.32	1.08
22	AV-08a	0.17	99.73	0.10	Channel	1.42	0.58	-0.18	1.28
23	AV-08a	2.98	88.59	28.43	Estuarine	3.87	2.66	0.21	1.97
24	AV-08a	1.03	84.20	14.77	Pleistocene	1.88	2.39	0.80	2.10
25	AV-08a	0.00	95.73	4.27	Pleistocene	1.88	0.52	0.28	1.99
26	AV-08b				Pleistocene				
27	AV-08b				Pleistocene				
28	AV-08b				Pleistocene				
29	AV-08b				Pleistocene				
30	AV-08c				Pleistocene				
31	AV-08c	0.00	89.46	10.54	Pleistocene	2.11	1.71	0.49	3.28
32	AV-08c				Pleistocene				
33	AV-15a	12.46	82.03	5.51	Pleistocene	0.49	1.81	0.19	1.24
34	AV-09a	0.62	94.03	5.35	Sand Ridge	2.35	1.04	-0.12	2.90
35	AV-09a	0.57	92.91	6.52	Estuarine	2.47	0.97	0.09	3.09
36	AV-09a				Estuarine				
37	AV-09a	0.13	92.95	6.92	Estuarine	2.88	0.79	0.40	2.78
38	AV-09a	16.35	80.24	3.41	Channel	-0.22	0.99	0.28	1.32
39	AV-09a	4.99	89.93	5.08	Channel	0.87	1.18	0.12	1.82
40	AV-09b				Channel				
41	AV-09b	1.33	93.98	4.69	Channel	0.96	0.86	0.38	2.08
42	AV-09b	35.30	96.57	8.13	Pleistocene	-0.28	2.48	0.57	3.38
43	AV-09b				Pleistocene				
44	AV-09b				Pleistocene				
45	AV-17a	0.62	99.25	0.13	Sand Ridge	1.58	0.74	-0.39	1.89
46	AV-17a				Estuarine				
47	AV-17a				Estuarine				
48	AV-17a				Estuarine				
49	AV-17a				Estuarine				
50	AV-17a				Estuarine				
51	AV-17a				Estuarine				
52	AV-17a				Pleistocene				
53	AV-17a				Pleistocene				
54	AV-17a				Pleistocene				
55	AV-17a				Pleistocene				
56	AV-17a				Pleistocene				
57	AV-04a	4.81	95.24	0.15	Sand Ridge	1.08	0.80	-0.18	1.31
58	AV-04a				Sand Ridge				
59	AV-04a	17.70	80.48	1.84	Sand Ridge	0.52	1.43	-0.20	0.98
60	AV-04a				Channel				
61	AV-04a	3.39	89.79	6.82	Channel	2.45	1.29	0.08	3.60
62	AV-04a				Channel				

**Summary Sediment Statistics
Avalon, NJ**

AVS	Core #	% Grav	% Sand	% Mud	Facies	Mean	SD	Skw	Kur
63	AV-04a	1.37	97.09	1.54	Channel	1.63	0.85	-0.22	1.12
64	AV-04a	33.55	61.84	4.61	Pleistocene	-0.33	1.86	0.20	1.21
65	AV-04a				Pleistocene				
66	AV-05a				Estuarine				
67	AV-05a				Estuarine				
68	AV-06a	6.58	93.28	0.18	Channel	0.80	1.02	-0.18	0.91
69	AV-05a	1.06	98.45	0.49	Channel	1.59	0.82	-0.36	1.85
70	AV-05a	0.24	97.52	2.24	Channel	1.88	0.86	-0.19	1.35
71	AV-05a				Channel				
72	AV-05a	1.83	96.28	1.89	Channel	1.96	0.70	-0.32	1.21
73	AV-05a				Channel				
74	AV-05a	0.41	98.85	0.94	Channel	1.39	0.52	-0.29	1.45
75	AV-05a				Channel				
76	AV-07a	21.18	78.78	0.04	Sand Ridge	-0.07	1.56	-0.31	1.01
77	AV-05a				Estuarine				
78	AV-05a	0.00	74.07	25.93	Estuarine	3.42	1.88	0.74	1.18
79	AV-05a				Estuarine				
80	AV-07a	3.65	96.09	0.06	Sand Ridge	0.98	0.88	-0.33	0.86
81	AV-07a	5.64	94.32	0.04	Sand Ridge	0.94	0.93	-0.38	1.14
82	AV-07a	5.72	94.25	0.03	Sand Ridge	1.16	0.89	-0.45	1.28
83	AV-07a	8.58	91.40	0.04	Sand Ridge	0.94	1.10	-0.43	1.35
84	AV-07a	11.99	87.84	0.17	Sand Ridge	0.78	1.23	-0.44	1.27
85	AV-07a	2.65	97.29	0.06	Sand Ridge	1.03	0.75	-0.13	0.89
86	AV-07b	3.34	96.66	0.00	Sand Ridge	1.05	0.71	-0.26	0.83
87	AV-07b	2.42	97.39	0.19	Sand Ridge	1.10	0.79	-0.27	1.00
88	AV-07b	0.95	97.44	1.61	Sand Ridge	1.20	0.78	-0.31	1.09
89	AV-07b	1.21	97.54	1.25	Sand Ridge	1.08	0.77	-0.21	0.67
90	AV-07c	1.86	98.09	0.05	Sand Ridge	1.14	0.75	-0.29	0.92
91	AV-07c	0.50	99.36	0.14	Sand Ridge	1.26	0.74	-0.37	0.91
92	AV-07c	3.13	96.35	0.52	Sand Ridge	1.20	0.91	-0.32	0.92
93	AV-07c	3.29	95.96	0.75	Sand Ridge	1.16	0.88	-0.19	0.96
94	AV-07c	7.33	91.56	0.81	Sand Ridge	0.72	1.07	-0.12	1.05
95	AV-07c	6.02	93.45	0.53	Sand Ridge	0.82	1.00	-0.22	0.92
96	AV-08a	2.75	97.22	0.03	Sand Ridge	1.44	0.61	-0.37	1.54
97	AV-08a	0.59	96.04	3.37	Sand Ridge				
98	AV-08a	8.39	91.23	0.38	Sand Ridge	0.93	1.09	-0.47	1.28
99	AV-08b				Sand Ridge				
100	AV-08b	2.19	97.57	0.24	Sand Ridge	1.40	0.85	-0.34	1.29
101	AV-08b				Sand Ridge				
102	AV-08b	0.38	96.22	3.40	Sand Ridge	1.83	0.58	-0.13	1.31
103	AV-08b	0.59	96.04	3.37	Sand Ridge	1.79	0.43	0.22	1.60
104	AV-10a				Sand Ridge				
105	AV-10a	29.96	72.90	0.14	Sand Ridge	-0.22	1.21	0.10	0.85
106	AV-10a	37.05	62.44	0.51	Sand Ridge	-0.18	1.86	-0.25	0.68
107	AV-10a	36.48	62.55	0.97	Sand Ridge	-0.18	1.52	-0.03	0.78
108	AV-10b				Channel				
109	AV-10b	8.86	86.10	7.24	Pleistocene	0.80	1.74	0.18	3.38
110	AV-10b	0.96	43.55	55.49	Estuarine	5.42	4.16	0.28	0.80
111	AV-10b	1.36	82.52	6.12	Pleistocene	1.06	1.34	0.30	2.36
112	AV-10b	21.87	72.79	5.54	Pleistocene	0.36	1.68	-0.06	1.37
113	AV-11a				Estuarine				
114	AV-11a				Estuarine				
115	AV-11a	0.71	97.37	1.82	Channel	1.74	0.78	-0.16	1.05
116	AV-11a	4.36	79.05	16.59	Estuarine	2.67	2.04	0.08	2.90
117	AV-11a	2.11	97.42	0.47	Pleistocene	1.31	0.63	-0.18	1.29
118	AV-11a				Pleistocene				
119	AV-11a				Pleistocene				
120	AV-11b	0.82	89.60	9.58	Pleistocene				
121	AV-11b	41.10	56.60	2.30	Pleistocene	-0.64	1.82	0.08	0.65
122	AV-11c	10.50	87.58	1.92	Pleistocene	1.05	1.33	-0.48	1.13
123	AV-11c	16.84	80.79	2.37	Pleistocene	0.81	1.66	-0.50	1.16
124	AV-12a				Estuarine				

Summary Sediment Statistics
Avalon, NJ

AVS	Core #	% Grav	% Sand	% Mud	Facies	Mean	SD	Skw	Kur
125	AV-12a				Estuarine				
126	AV-12a	1.00	82.11	38.89	Estuarine	3.85	3.15	0.52	0.90
127	AV-12a	0.82	88.80	9.58	Estuarine	1.38	1.84	0.38	3.47
128	AV-12a	2.05	90.08	7.87	Pleistocene	1.34	1.45	0.20	2.21
129	AV-12b				Pleistocene				
130	AV-13a				Sand Ridge				
131	AV-13a	12.78	84.84	2.38	Sand Ridge	0.30	1.24	0.05	0.90
132	AV-13a				Sand Ridge				
133	AV-13a				Sand Ridge				
134	AV-13a	3.05	95.12	0.80	Sand Ridge	0.77	0.96	0.08	1.00
135	AV-14a	0.05	90.38	9.57	Estuarine	3.19	0.96	0.37	3.81
136	AV-14a	1.48	95.09	3.42	Estuarine	1.38	1.02	0.00	1.04
137	AV-14a				Estuarine				
138	AV-14a	0.13	84.29	15.58	Estuarine	2.45	1.87	0.48	3.18
139	AV-14a	0.21	89.83	29.96	Estuarine	3.89	2.18	0.74	1.18
140	AV-14a				Estuarine				
141	AV-19a				Sand Ridge				
142	AV-19a	3.92	95.98	0.12	Sand Ridge	1.08	0.91	-0.29	0.98
143	AV-19a	4.49	95.22	0.29	Sand Ridge	1.10	0.95	-0.33	0.98
144	AV-19a				Sand Ridge				
145	AV-19b	1.08	95.84	0.08	Sand Ridge	1.23	0.91	-0.13	0.74
146	AV-19b	1.93	97.49	-0.58	Sand Ridge	1.21	0.82	-0.22	1.08
147	AV-19b	0.46	99.20	0.34	Sand Ridge	1.41	0.88	-0.41	1.04
148	AV-19b	0.60	97.83	1.77	Sand Ridge	1.45	0.67	-0.21	1.02
149	AV-19c				Sand Ridge				
150	AV-19c				Sand Ridge				
151	AV-18a	0.59	95.89	0.52	Sand Ridge	1.97	0.41	-0.17	1.35
152	AV-18a				Sand Ridge				
153	AV-18a				Sand Ridge				
154	AV-18a				Pleistocene				
155	AV-18a	2.85	97.28	0.07	Sand Ridge	1.48	0.87	-0.41	1.08
156	AV-18a	7.59	92.01	0.40	Sand Ridge	0.52	1.05	-0.05	1.13
157	AV-18a	1.90	97.91	0.19	Sand Ridge	1.58	0.75	-0.35	1.09
158	AV-18a	6.29	91.92	1.79	Sand Ridge	1.02	1.19	-0.18	0.93
159	AV-18a	3.34	96.29	0.37	Sand Ridge	1.50	0.91	-0.39	1.04
160	AV-18a				Sand Ridge				
161	AV-18a				Sand Ridge				
162	AV-18a				Sand Ridge				
163	AV-18b				Sand Ridge				
164	AV-18b				Sand Ridge				
165	AV-18b	0.06	91.30	8.64	Estuarine	2.77	1.27	0.37	3.09
166	AV-18b	0.00	90.51	9.49	Estuarine	2.53	1.10	0.41	4.13
167	AV-18c				Estuarine				
168	AV-18c	0.10	90.05	9.85	Estuarine	2.58	1.11	0.48	4.19
169	AV-18c	0.04	90.49	9.47	Estuarine	2.43	1.34	0.17	3.17
170	AV-20a				Estuarine				
C-021	AV-01	10.71	89.13	0.16	Sand Ridge	0.11	1.02	0.45	0.89
C-022	AV-01	42.57	95.82	0.81	Sand Ridge	-0.49	1.27	0.20	0.84
C-023	AV-01	39.28	99.82	0.92	Sand Ridge	-0.57	1.08	0.37	1.28
C-024	AV-01	24.76	74.75	0.49	Sand Ridge	-0.42	0.92	0.32	1.89
C-025	AV-01	22.38	75.99	1.83	Sand Ridge	0.12	1.35	0.24	0.90
C-026	AV-01	4.33	94.88	0.79	Sand Ridge	1.26	1.26	-0.30	0.70